Device-to-Device Communication and Multihop Transmission for Future Cellular Networks

Ahmed Mohammed Amate

A thesis submitted to the University of Hertfordshire in partial fulfilment of the requirements for the degree of Doctor of philosophy

November 2014

ABSTRACT

The next generation wireless networks i.e. 5G aim to provide multi-Gbps data traffic, in order to satisfy the increasing demand for high-definition video, among other high data rate services, as well as the exponential growth in mobile subscribers. To achieve this dramatic increase in data rates, current research is focused on improving the capacity of current 4G network standards, based on Long Term Evolution (LTE), before radical changes are exploited which could include acquiring additional/new spectrum. The LTE network has a reuse factor of one; hence neighbouring cells/sectors use the same spectrum, therefore making the cell edge users vulnerable to inter-cell interference. In addition, wireless transmission is commonly hindered by fading and pathloss.

In this direction, this thesis focuses on improving the performance of cell edge users in LTE and LTE-Advanced (LTE-A) networks by initially implementing a new Coordinated Multi-Point (CoMP) algorithm to mitigate cell edge user interference. Subsequently Device-to-Device (D2D) communication is investigated as the enabling technology for maximising Resource Block (RB) utilisation in current 4G and emerging 5G networks. It is demonstrated that the application, as an extension to the above, of novel power control algorithms, to reduce the required D2D TX power, and multihop transmission for relaying D2D traffic, can further enhance network performance. To be able to develop the aforementioned technologies and evaluate the performance of new algorithms in emerging network scenarios, a beyond-the-state-of-the-art LTE system-level simulator (SLS) was implemented. The new simulator includes Multiple-Input Multiple-Output (MIMO) antenna functionalities, comprehensive channel models (such as Wireless World initiative New Radio II i.e. WINNER II) and adaptive modulation

and coding schemes to accurately emulate the LTE and LTE-A network standards. Additionally, a novel interference modelling scheme using the 'wrap around' technique was proposed and implemented that maintained the topology of flat surfaced maps, allowing for use with cell planning tools while obtaining accurate and timely results in the SLS compared to the few existing platforms.

For the proposed CoMP algorithm, the adaptive beamforming technique was employed to reduce interference on the cell edge UEs by applying Coordinated Scheduling (CoSH) between cooperating cells. Simulation results show up to 2-fold improvement in terms of throughput, and also shows SINR gain for the cell edge UEs in the cooperating cells. Furthermore, D2D communication underlaying the LTE network (and future generation of wireless networks) was investigated. The technology exploits the proximity of users in a network to achieve higher data rates with maximum RB utilisation (as the technology reuses the cellular RB simultaneously), while taking some load off the Evolved Node B (eNB) i.e. by direct communication between User Equipment (UE). Simulation results show that the proximity and transmission power of D2D transmission yields high performance gains for a D2D receiver, which was demonstrated to be better than that of cellular UEs with better channel conditions or in close proximity to the eNB in the network. The impact of interference from the simultaneous transmission however impedes the achievable data rates of cellular UEs in the network, especially at the cell edge. Thus, a power control algorithm was proposed to mitigate the impact of interference in the hybrid network (network consisting of both cellular and D2D UEs). It was implemented by setting a minimum SINR threshold so that the cellular UEs achieve a minimum performance, and equally a maximum SINR threshold to establish fairness for the D2D transmission as well. Simulation results show

an increase in the cell edge throughput and notable improvement in the overall SINR distribution of UEs in the hybrid network. Additionally, multihop transmission for D2D UEs was investigated in the hybrid network: traditionally, the scheme is implemented to relay cellular traffic in a homogenous network. Contrary to most current studies where D2D UEs are employed to relay cellular traffic, the use of idle nodes to relay D2D traffic was implemented uniquely in this thesis. Simulation results show improvement in D2D receiver throughput with multihop transmission, which was significantly better than that of the same UEs performance with equivalent distance between the D2D pair when using single hop transmission.

ACKNOWLEDGEMENTS

My sincere gratitude goes to my principal supervisor Dr. Pandelis Kourtessis for his relentless guidance and continuous motivation, and also to my second supervisor Prof. John M. Senior for his professionalism and support during the course of my research. I would also like to thank Dr. Milos Milosavljevic and Dr Stratis Sofianos who were not only excellent mentors during my research but are also good friends. My appreciation goes to my friends, colleagues in the Optical Network research group, and also the Radio and Mobile Communication group who have provided a friendly atmosphere during my time of study. I will like to acknowledge the Petroleum Trust Development Fund (PTDF) for funding my expenses for most of my research period.

I cannot express enough gratitude to my parents, siblings and family friends for the love, affection and support of all sorts they have given me all my life and especially during my programme. I will like to thank my lovely wife and children for giving me the extra motivation and support I needed in achieving my goals. And last but not the least; I will like to thank Almighty Allah for providing me with the grace, tolerance and the ability to see through my programme and for my life achievements in general.

TABLE OF CONTENTS

Chapter 3:

LIST OF FIGURES

LIST OF TABLES

.

GLOSSARY

1G	First generation
2G	Second generation
3G	Third generation
3GPP	3rd Generation partnership project
4G	Fourth generation
5G	Fifth generation
AWGN	Additive white Gaussian noise
BBU	Baseband unit
BLER	Block error rate
BS	Base station
CAPEX	Capital expenditure
CDF	Cumulative distribution function
CDMA	Code division multiple access
CLSM	Closed loop spatial multiplexing
CoBF	Coordinated beamforming
CoMP	Coordinated multipoint
CoSH	Coordinated scheduling
CP	Cyclic prefix
CR	Cognitive radio
CRAN	Cloud/Centralised radio access network
CSI	Channel state information
CQI	Channel quality index
D2D	Device-to-Device

.

DL	Downlink
eNB	Evolved node b
EDGE	Enhanced data rate for GSM evolution
EU	European-union
EPC	Evolved packet core
FDD	Frequency division duplex
GPRS	General packet radio services
GPS	Global positioning system
GSM	Global system for mobile
HDTV	High-definition television
HetNet	Heterogeneous network
HSPA	High speed packet access
IMT-A	International mobile telecommunications-Advance
IP	Internet protocol
ISD	Inter-site distance
ISM	Industrial, scientific and medical
ITU	International telecommunication union
JP	Joint processing
kbps	kilobits per second
LTE	Long term evolution
LPM	Link performance model
LQM	Link quality model
LTE-A	Long term evolution-Advanced
MAC	Medium access control
Mbps	Megabits per second

MCS	Modulation and coding scheme
MHz	Mega Hertz
MH	Multihop
MIMO	Multiple-input multiple-output
OFDM	Orthogonal frequency-division multiplexing
OFDMA	Orthogonal frequency-division multiple access
OLSM	Open loop spatial multiplexing
PF	Proportional fair
OPEX	Operational expenditure
PAPR	Peak to average power ratio
QoS	Quality of service
RB	Resource block
RAN	Radio access network
RAT	Radio access technology
ROI	Region of interest
RNC	Radio network controller
RR	Round robin
RS	Reference signal
RX	Receiver
SE	Spectral efficiency
SH	Single hop
SISO	Single-input single-output
SLS	System-level simulator
SMS	Short message service
SIC	Self-interference cancellation

.

SINR	Signal to interference noise ratio
SNR	Signal to noise ratio
SC-FDMA	Single carrier frequency-division multiple access
TDD	Time division duplex
TTI	Transmission time interval
TB	Transport block
TxD	Transmit diversity
TX	Transmitter
UE	User equipment
UL	Uplink
UMTS	Universal terrestrial mobile system
VeNBs	Virtual eNBs
WA	Wrap around
WiFi	Wireless fidelity
WiMAX	Worldwide interoperability for microwave access
WINNER	Wireless world initiative new radio
WLAN	Wireless local area network
WMAN	Wireless metropolitan area network
WPAN	Wireless personal area network
WWAN	Wireless wide area network

DECLARATION

The following papers are either under review or already published, and parts of the materials are included in this thesis:

- A. Amate, S. Sofianos, M. Milosavljevic, P. Kourtessis, and J. M. Senior, "An efficient inter-site interference model for 4G wireless networks," in 2013 IEEE International Conference on Communications (ICC) , 2013, pp. 5355-5359.
- A. Amate, M. Milosavljevic, P. Kourtessis, M. Robinson, J. M. Senior, “SDN based millimeter wave Radio over Fiber (RoF) network” 2015 SPIE photonics WEST, the laser, photonics, Biomedical Optics Conference.
- A. Amate, M. Milosavljevic, P. Kourtessis, and J. M. Senior, “Interference mitigation using power control in LTE-A networks overlaying D2D communication” submitted to IEEE transaction on communication.

Chapter 1

Introduction

1.1 Mobile communication

The growth of wireless networks in general as complementary to the wireline alternatives (e.g. optical networks [1]) has continuously amplified: mainly due to the cost-effective terminals, increasing data rates and ubiquity provided by the wireless networks [1]. This has led to constant advances in mobile communication from the initial provision of analogue voice services to the present state-of-the-art technologies, which are expected to support future 3-play services with multi-channel HDTV, 3D TV, and other high capacity services that generate overwhelming traffic [2]. These services include multi-player online gaming, cloud computing, remote application hosting, social networking and home management services (i.e. video surveillance). Figure 1-1 illustrates an estimate of active mobile subscribers worldwide from 2011 to 2014 [3].

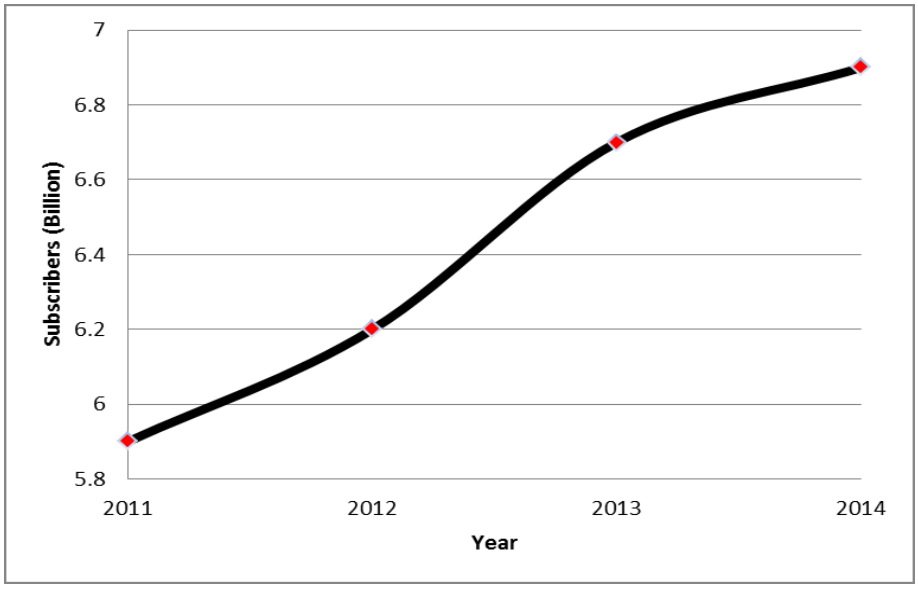

Figure 1-1 Estimation of active mobile subscribers from 2011 to 2014 [3]

The International Telecommunications Union (ITU) provided the statistic in May 2014, showing the increasing number of active mobile subscribers worldwide till present. It shows almost 7 Billion mobile subscribers in 2014, equivalent to about 95 percent of the world population. In more detail, it indicates up to 5.9 Billion active subscribers in 2011, with an estimated growth of over a billion users worldwide through to 2014. Consequently, there has been increasing demand for provision of broadband on the go to offer bandwidth-demanding services such as HD real-time multimedia and other high data rate services as earlier mentioned by the growing subscribers of the networks [4, 5]. A study presented by Ericsson in Figure 1-2 [6] shows a projection of mobile data traffic for voice and data, through 2016, which was based on measurements from live networks of the company over several years up to 2011. The forecast in the graph shows over 10-fold increase in the projected period, with more requirements on mobile data usage (using smart phones and tablets) compared to voice services: over 4500 Petabytes (10^{15} bytes) of mobile data utilisation with PCs/tablets by 2016. This type of prognostications has compelled the need for continuous research in developing capable infrastructure for providing the required services to the ever-increasing subscribers to the network.

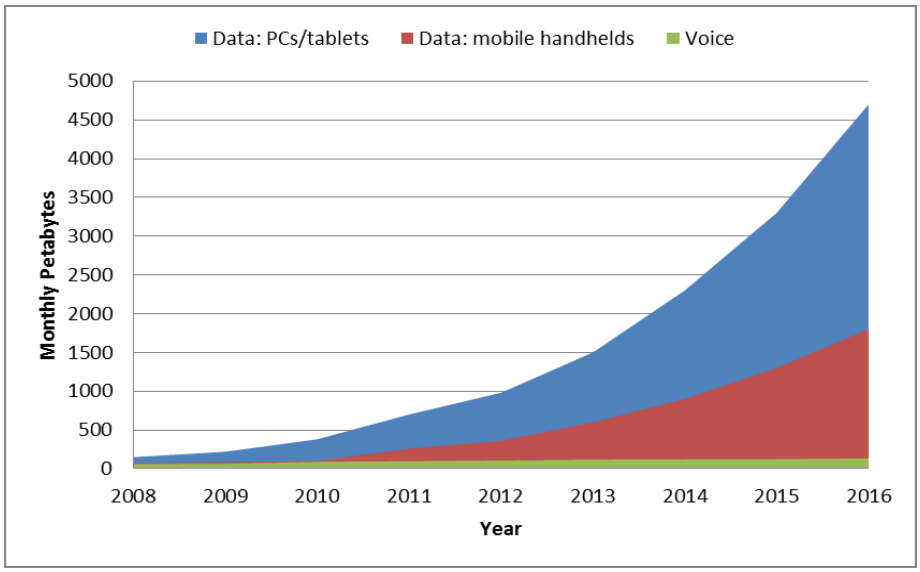

Figure 1-2 Projection of mobile data traffic from 2008 to 2016 [6]

Mobile communication has evolved through various generations of wireless network standards with improvements in coverage area, data rate provision etc. to the current 4G networks. The 3GPP [7] and Institute of Electrical and Electronics Engineers (IEEE) [8] have been actively involved in developing and/or advancing the network technologies for the cellular and broadband access networks respectively. Examples of some prevalent technologies by these organisations include the Long Term Evolution (LTE) [9] and IEEE 802.11 standards (also referred to as WiFi) [10]. The 3GPPs LTE network is presently dominating the Wireless Wide Area Network (WWAN) market over competing 4G technologies with exponential increase in the network's deployment worldwide since the last quarter of 2009 [9]. While 4G networks deployment is ongoing, active research is conducted alongside to determine solutions for the next generation of cellular networks (i.e. 5G). The research initiatives are spearheaded by the European Union (EU) through the recently finished FP7 and current Horizon-2020 research frameworks, with relevant projects including METIS-2020, 5GNOW, COMBO, MiWaves, and MiWEBA [11-16]. These projects are also in collaboration with major telecoms companies such as Alcatel Lucent, Ericsson, and Huawei. Some key measures commonly considered in the aforementioned projects include improved network architectures and protocols, and complimentary/add-on technologies to the existing networks, in order to achieve the data rates requirement of the increasing subscribers for the current and future networks such as LTE-Adanced networks.

1.1.1 Network performance and limitations of the 4G LTE network

The initial release of the LTE standard was presented commercially as a 4G network along with other similar technologies [17]. The LTE network was however more auspicious as it has a flat architecture, leading to lower latency, better throughput, and

high-quality user experience even with the initial release (release 8): with theoretical throughput of up to 300 Mbps and 75 Mbps for the Downlink (DL) and Uplink (UL) respectively for LTE release 9 [18]. The network is implemented using current technologies such Orthogonal Frequency-Division Multiple Access (OFDMA, for the DL) [19] and Multiple-Input Multiple-Output (MIMO) [20] in order to achieve the specified data rates improvement. Additionally, the UL is based on the Single-Carrier Frequency Division Multiplexing Access (SC-FDMA) scheme [21]. Hence there is more energy efficiency from the User Equipment (UE) processing power requirement perspective, as the SC-FDMA transmission scheme has a low peak to average power ratio (PAPR).

The network is deployed with a universal reuse factor (frequency reuse of 1), which increases the efficiency in the spectrum utilisation of the network. Despite the advantage of the universal reuse factor, it however causes high inter-cell interference, since all the cells use the same spectrum, especially for users at the cell edge. Consequently, 3GPP introduced Coordinated Multipoint (CoMP) scheme [22] to improve the spectral efficiency for cell edge users in the initial and future releases of the LTE network standards. The scheme involves coordination between network entities such as base stations, referred to Evolved Node B (eNB) in LTE networks, and UEs of different cells/sites in order to achieve this improvement [22]. The initial release however fell short on the ITU's definition of International Mobile Telecommunications-Advanced (IMT-A), to provide up to 1 Gbps throughput as the ultimate goal for 4G networks. This was then fulfilled in the latest release (i.e. release 10) referred to as LTE-Advanced (LTE-A) [23] as a true 4G network. The LTE-A is specified to provide up to 1 Gbps throughput DL and 500 Mbps UL theoretically with an aggregate of 100 MHz radio channels. Furthermore, the current release is

backward compatible with the initial releases (LTE releases 8 and 9) and previous 3G networks, hence provides seamless/cheaper migration to the network [23].

One of the main performance limitations of the 4G LTE network is in the cell edge performance degradation. Another example of these limitations is the capabilities of the transceiver terminals relative to the specified requirement to achieve LTE performance, e.g. multiple antenna user terminals. The cell edge performance degradation is caused mainly due to the tight reuse factor of the network, and limitations of the wireless propagation medium itself. One example of such limitation is 'multi-path fading', where obstacles in the surrounding environment (which vary from hills, buildings, etc.) attenuate the propagated signal, hence, leading to flawed detection of the received signal [24]. Another major issue with the wireless communication in general is the scarcity of radio spectrum (which is finite and expensive) and inefficiency in the spectrum usage. These factors amongst other challenges limit the wireless networks (such as LTE) from providing the increasing high data rate requirement and QoS. Thus with the growing demand for mobile communication and cost effectiveness of implementing and maintaining the wireless networks, significant research is channelled towards mitigating the network discrepancies and making efficient use of the limited spectrum to provide sufficient data for the high bandwidth service requirement.

1.2 Worldwide deployment of LTE networks

The stride of LTE network deployment is remarkably growing, as mobile operators invest to keep up with peer competition and growth in mobile data traffic demand. The LTE network is arguably one of the fastest growing mobile networks being deployed yet. This is demonstrated in a recent Global mobile Suppliers Association

(GSA) report (a well renowned association with members such as Qualcomm, Ericsson, Huawei amongst others) [25], indicating over 90 LTE networks commercially launched during 2012. The report further forecasts over 200 new LTE networks to be lunched in more than 83 countries by the end of 2013 as illustrated in Figure 1-3. This clearly shows the increasing popularity of LTE networks compared to other competing standards.

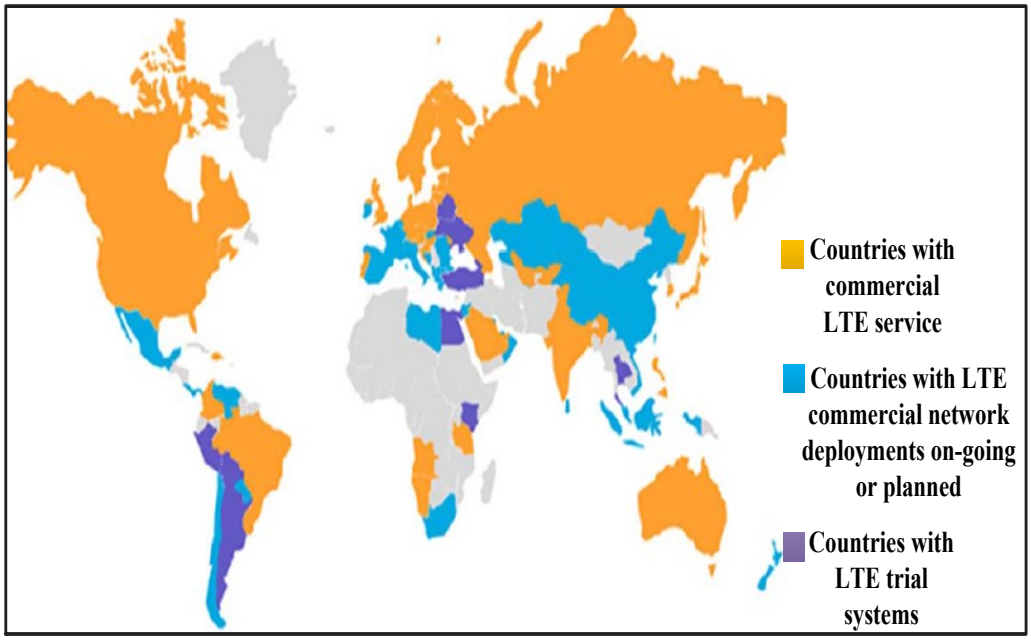

Figure 1-3 LTE deployment plans and strategies between 2012-2015 [26]

Even though the first LTE network in the world to be turned on was in Europe (by TeliaSonera in Sweden), the growth of LTE networks is however slower in that region of the world (i.e. Europe) [27]. The networks are more successful in the United States (US) and Asian markets. The slow pace in the deployment is associated with regulation delays, wide/dense spread of High Speed Packet Access (HSPA) networks, and wide availability of fixed networks in the region [27]. This is however perceived to change in the near future as higher demand for data and availability of LTE smart phones continue to increase in the region. As the deployment of the initial releases (release 8 and 9) of LTE networks are quickly spreading around the world, advances

are already on the way for the deployment of the most recent release (i.e. LTE-A). According to the claims in [28], Russian operator (YOTA networks) and Huawei technology company recently announced the launch of the world's first LTE-A commercial network. Huawei claimed to have modified the single Radio Access Network (RAN) of the LTE Evolved Packet Core (EPC), providing solutions which include carrier aggregation to provide up to 300 Mbps DL peak rates so far, which was reported to be dependent on the capacity of the radio channel [28].

1.3 Advances to 5G network implementation

While the 4G networks haven't been fully deployed yet (as discussed in the previous section), there are already a lot of advancements towards the specification of 5G wireless networks. One prominent project in this field is the aforementioned METIS-2020 [11]. Ericsson spearheads this particular project with members including telecommunication manufacturers, network operators amongst many in the sector, to establish a path for the future of mobile communication. A driving force for the project is a forecast showing dramatic growth for smartphone subscriptions from 1.2 billion in 2012 to 4.5 billion by 2018. This means an equally astounding increase in mobile data traffic, which was seen to have doubled between the first quarter of 2012 and 2013. This tremendous rise in subscribers is expected to rise over ten times by the end of 2018 from 2012 [11].

Some key candidate factors that could determine the achievement of the supposed 5G network requirement include better utilisation of spectrum and deployment of more low powered base stations (BS) to make small cells in addition to changing the system design principle (if necessary) [29]. There is also a lot of emphasis on the development of existing technologies to improve capacity. Some of the concepts that

have been highlighted include massive machine-to-machine communication, and ultra-dense networks amongst many [30]. In that view, the aspect that is common with current situation is the need to improve spectrum utilisation by implementing emerging Heterogeneous Networks (HetNet) [31] and Cognitive radio (CR) [32].

1.3.1 Projected technologies and architectures to enhance spectrum utilisation for future networks

3GPP has been working on various aspects in the framework of LTE-A to further improve the user experience of the 4G networks and make better use of the available spectrum, considering the spectrum bottleneck with wireless network transmission. One method adopted to serve this purpose is by implementing the networks based on a heterogeneous topology: i.e. achieving a HetNet by integrating macrocells with Pico cells, Femto cells etc. [31]. The concept of the HetNet was initially adopted at the last phase of the 3G networks, and then fully applied in the 4G networks. The concept is also popular in research towards 5G wireless networks as earlier stated. An illustration of the macro cell expansion to HetNets is shown in Figure 1-4.

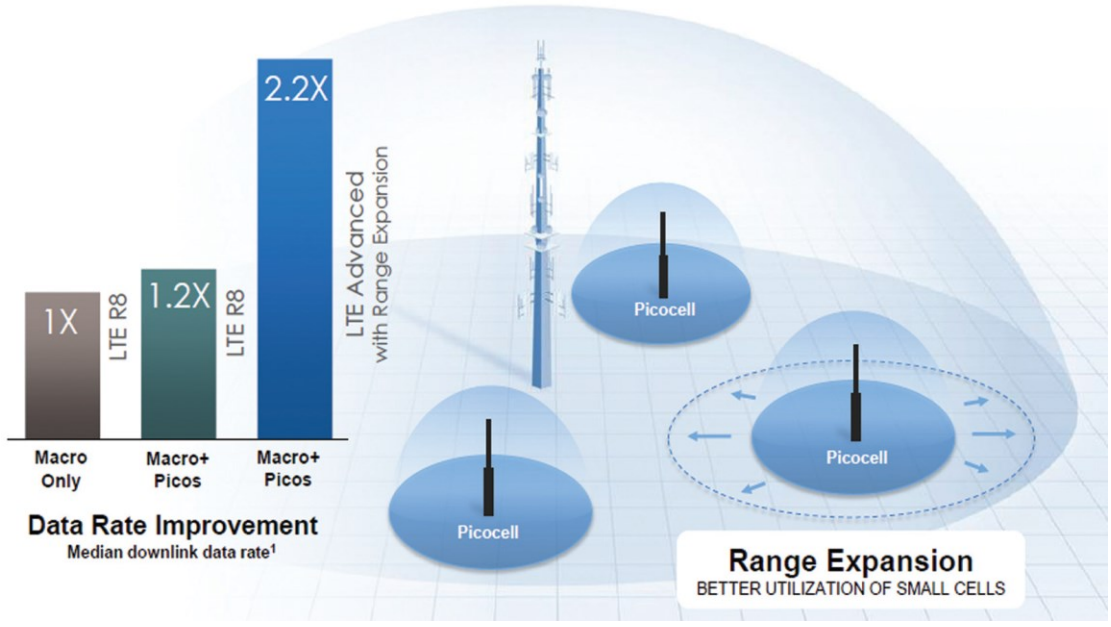

Figure 1-4 Range expansion with heterogeneous cellular implementation [31]

The HetNets provide flexible and low cost deployment by adding low powered small cells (such as Femto cells), to eliminate the coverage holes in the macro cells at the most required regions within the network (such as shopping malls, large offices etc.). Additionally, the HetNet implementation focuses on improving Spectral Efficiency (SE) of the network per unit area, and also seeks to provide uniform broadband experience for the users anywhere in the network in a cost effective manner. This cuts down on Operational Expenditure (OPEX) in term of the power budget for the network operators [33].

CR is a technology that enables secondary users (unlicensed users of a spectrum) to sense/find and utilise the spectrum when it is not in use by the primary users (licensed users) with interference control for transmission between the respective users [32]. It differs from technologies like Bluetooth and ZigBee [34] which are constrained mainly to the 2.4 GHz Industrial, Scientific and Medical (ISM) band, and vulnerable to interference from the primary users transmission in the spectrum. The technology (i.e. CR) was proposed as a solution to the spectrum bottleneck for wireless communication so as to eliminate the white spaces (unused frequencies), hence, making better use of the spectrum. Spectrum measurements that were conducted in some parts of the world indicate massive underutilisation of allocated frequency bands. The spectrum underutilisation is particularly evident in the TV band, unlike the cellular band which is saturated with increasing active subscribers [35]. An example is statistics from [35, 36], which shows only about 11% usage of the frequency band between 30 to 300 MHz in the respective regions, mainly from the TV band. Thus, CR is being considered in the aforementioned literature as a promising solution to temporarily allocate the unused spectrum (allocated for TV band and also the cellular spectrum) as a solution to maximise the general use of the spectrum. Furthermore, the

concept of enabling direct link between consumer devices is now introduced to reduce the load on the base stations by conveying local services between the devices referred to as Device-to-Device (D2D) communication [37]. D2D technology is highly anticipated to maximise the resource utilisation in the cellular band, in addition to projected solutions such as CR as earlier discussed. Unlike CR however, D2D communication is carried out simultaneously between the primary and secondary users even when there are no white spaces in the spectrum [38]. While the HetNets implementation requires fixed access point for the small cell networks, D2D communication provides an instantaneous network communication without the need to install fixed infrastructure and with even lower transmission power required. The technology is underlaying the cellular network, and reuses the cellular resources to improve spectrum efficiency of the network. The technology is envisioned for implementation in the LTE-A network, and equally a strong candidate technology for the 5G networks. It does however come with some technical challenges that require solutions before its full implementation in the later aspects of the 4G networks and the subsequent 5G networks. These include interference management between the primary and secondary (i.e. D2D UEs) constituent of the network and resource management amongst others.

1.4 Research motivation

Sufficient research is required as reference point for vendors, network operators, and service providers to improve and develop their individual services. Researchers on the other hand should continue to provide algorithms and solutions to assist in achieving this objective. This normally requires first of all a comprehensive simulation platform for researchers to implement algorithms in a timely manner. This would immensely reduce cost in implementing the services by initially establishing the functionality of

the developments before field trials or deployments. Hence, the need for providing enhancements to existing methods/platforms or providing completely new methods of simulating the wireless communication networks cannot be over emphasised.

As stated earlier, the LTE and LTE-A networks are implemented using 4G technologies such as OFDMA and SC-FDMA to increase the data rates of the network and reduce the power requirement of UEs respectively. To further extend the network capacity, the LTE standards are implemented with a universal reuse factor, hence allowing all cells to make maximum use of the available bandwidth. Despite the advantages of the universal reuse factor, it leads to degradation in the performance of cell edge UEs as they incur inter-cell interference. This is in addition to fading and pathloss commonly experienced in wireless communication. Thus, recent research focuses on developing inter-cell interference coordination algorithms to improve the cell edge performance of UEs in the LTE network.

Current research is also focusing on emerging architectures such as HetNets, along with technologies such as CR and D2D communication. In HetNets, small cell networks are put in place to enhance the signal transmission at most required regions with low powered infrastructures (i.e. BSs). While CR identifies and allocates the licensed spectrum to unlicensed users (when not in use by the licensed users), D2D communication is proposed as an integral part of the cellular network to eliminate the white spaces in the network and use the spectrum simultaneously between the licensed and unlicensed users. These technologies are being considered as promising add-ons to the 4G networks and the forthcoming 5G networks implementation. D2D communication like the small cells lowers the load of the base station by reducing cellular traffic with even lower transmission power and mobile transmission

compared to the small cells. One common problem with the HetNet is the issue of interference signal power offered to the different users in the network (i.e. between the different sub-cells and macrocell). In the case of D2D communication, the resource of the cellular network is reused for D2D transmission, which could then negatively affect the spectrum efficiency of the network. Thus, increasing research is ongoing to efficiently implement the constituents of the network with minimal hazard (by mitigating interference) from the multiple transmissions in the network, hence, the motivation of this research.

In these directions, this thesis is focused on investigating add-on technologies to improve the recent 4G networks and ratify their suitability as candidate technologies for the future 5G network implementations. Specifically, inter-site coordination and D2D communication underlaying the LTE network with multihop transmission are investigated. To achieve this, a comprehensive LTE-A System-Level Simulator (SLS) was firstly implemented and enhanced to incorporate the technologies considered efficiently.

1.5 Research contribution

The major contributions of this thesis are highlighted as follows:

- ✓ A comprehensive review was carried out to identify the limitations of standardised wireless access technologies for the provision of gigabit/s data traffic. This includes firstly a detailed evolution of wireless networks from the first generation to the current fourth generation implementation of the networks. It also includes a review of the currently deployed 4G LTE network in terms of physical layer implementation and medium access, and current

initiatives in the direction of multi-gigabit data traffic implementation for the future wireless networks.

- ✓ A comprehensive LTE system-level simulator was implemented to evaluate the performance of the 4G networks. The detail of the simulation environments and channel models were presented. The transmission mode's diversity techniques and scheduling algorithms of the LTE network were first of all evaluated to identify the most efficient parameters for subsequent research investigation.
- ✓ An inter-cell interference modelling method using 'wrap around' was proposed. The method entails inclusion of virtual eNBs in the model to eliminate the border effect in simulation platforms and accurately relocate the users to their transiting cells. These allow processes like handover between cells or sectors to be studied properly. The performance of the cell edge users was then illustrated, and a CoMP algorithm was proposed, which was shown to improve the performance of users in the network by reducing the effect of interference power on the cell edge users.
- ✓ D2D communication was then implemented in the simulator, with details of the system modelling and all acceptable assumptions encompassed discussed. The model was used to illustrate spectrum utilisation efficiency and proximity gain with D2D communication included in the LTE network for users further away from the eNB, or with relatively poor channel condition. A power control algorithm was then proposed which entails the adjustment of D2D transmitter power depending on the SINR feedback of the cellular UEs in its existing cell. This was implemented to maintain a good performance between the cellular and D2D users in the network even with the simultaneous sharing of resources between the network entities.

- ✓ Multihop transmission for D2D traffic was then investigated. This differed from the current use of the scheme to increase cell capacity and improve cellular user experience. In this case, D2D communication was implemented using up to 2 hops to communicate between the D2D users. This has shown further improvement in the achievable cell throughput compared to single-hop D2D communication in the networks.

1.6 Thesis outline

Chapter 2 critically reviews the wireless networks, highlighting the specifications and evolution of the state of the art, and advances to the future 5G networks. Subsequently Chapter 3 describes the system-level simulator model implemented for this research investigation. Chapter 4 presents a proposed method for interference modelling of 4G networks such as the LTE. It includes several simulation results showing cell edge user performance enhancement by implementing a proposed CoMP algorithm. This is followed by Chapter 5, which evaluates the performance gain of D2D communication as an integral part of cellular networks. It includes a power control algorithm to mitigate the interference between the cellular and D2D users. It also includes an implementation of multihop communication for D2D traffic. Simulation results in the chapter demonstrate the proximity gain of D2D communication, and performance gain with the power control algorithm implemented. Finally, Chapter 6 summarises the studies conducted throughout this research thesis followed by a detailed discussion on future directions that the research could be further carried on towards.

Chapter 2

Towards Providing Multi-Gigabits Data Rate Traffic for Future Cellular Networks

2.1 Introduction

In this chapter, a detailed evaluation of cellular networks development is presented. It starts with an overview of cellular network evolution from 1G to the current 4G network standards. Considering the prevalence of LTE standard as a predominant 4G network (as discussed in the preceding chapter), this research, and hence this chapter, focuses mainly on the LTE network standard. Thus, a thorough description of the implementation, architectural development and advances towards implementing the most current release (release 10, i.e. LTE-A) relevant to this research is discussed in this chapter. This includes eNB signaling, resource grid structure, and channel bandwidths amongst other features of the LTE network standard.

Furthermore, developments towards efficient radio resource utilisation i.e. cellular Resource Blocks (RBs) is then discussed, conferring the significance of including technologies such as Cognitive Radio (CR) and Device-to-Device (D2D) communication in the developing 4G networks, and subsequently for the future 5G multi gigabit data traffic networks. The chapter then concludes by discussing leading research organisations with the initiative of achieving the aforementioned targets, highlighting developments of some promising architectures and protocols proposed in current research literature.

2.2 Evolution of cellular networks to the current 4G standards

The cellular networks have evolved through various standards and generations, improving in vital aspects such as coverage area, mobility, data rates and QoS. An overview of the cellular networks evolution and their data rate capabilities are summarised in Figure 2-1 [39, 40]. As shown in the figure, the cellular network standards have evolved tremendously from offering data rates as low as ~2.4 kbps in the 1G era, to peak rates of up to 1 Gbps in the current 4G networks. The future generation of the networks i.e. 5G is envisioned to offer multi-gigabits data rates and is projected for deployment by the year 2020. The 1G cellular standards consisted of analogue based systems and was able to offer significant services such as handover and roaming. A major limitation of the 1G network standards however was their inability to interoperate between the cellular networks in different countries/regions. This is in addition to the limited services offered by the network, as it was restricted to voice services.

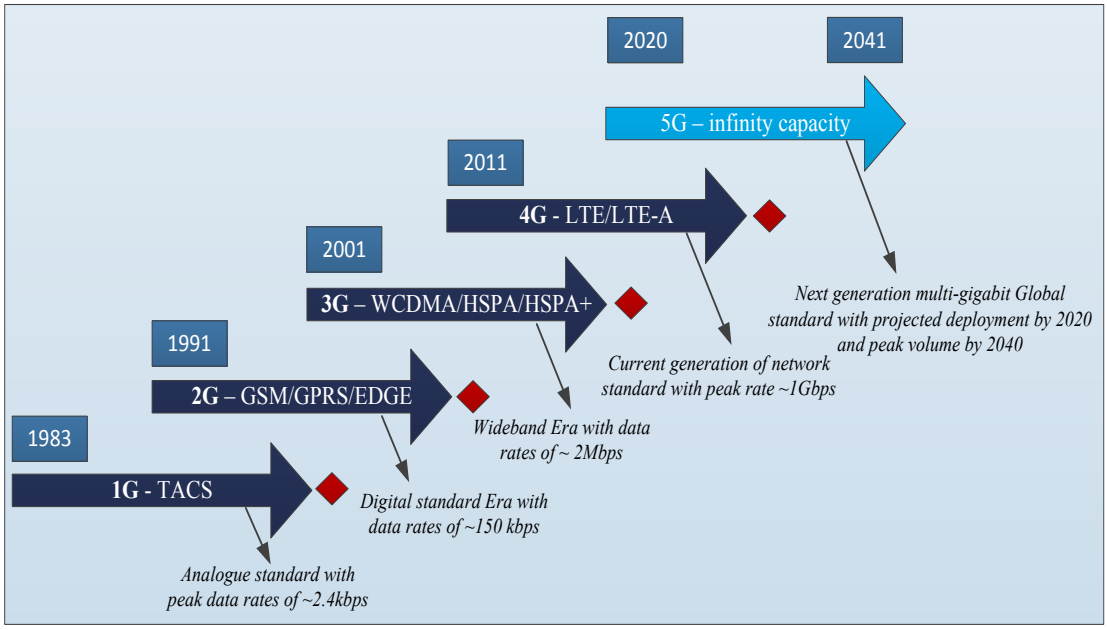

Figure 2-1 Overview of cellular network generations and data growth [39, 40]

Following the implementation of the 1G network, the second generation (2G) of mobile systems was then introduced, which initiated the implementation of complete digital capabilities to the cellular systems. The 2G networks were enhanced mainly in terms of spectrum efficiency, data services and advanced roaming; with additional low bit rate data services (such as short message services i.e. SMS) compared to the 1G networks. Most prominently however, the network was enhanced to eliminate the interoperability issue in the preceding generation with the deployment of Global System for Mobile (GSM) Communication [41], offering a unified standard (initially deployed in Europe and subsequently to the US and Asia). This enabled seamless services to be introduced with international roaming to support multiple users in the network.

As data sending services became increasingly popular in the air interface, General Packet Radio Services (GPRS) [42] was introduced in the network to implement a packet switched domain in addition to the circuit switched domain, which was then referred to as the 2.5G network. This also changed the subscriber charging method in the networks from connection time, to a charging method based on the amount of data sent. The introduction of a packet core network enabled wireless access to the Internet, achieving up to 150 kbps in peak channel conditions. Subsequently, the Enhanced Data rate for GSM Evolution (EDGE) [43], was implemented, which yielded increase in data rates, providing up to 384 kbps (in optimum conditions) and up to 2 Mbps with its coexistence with 3G Wideband CDMA (WCDMA) as shown in Figure 2-1. In the EDGE network however, the packet transfers were partly similar to circuit switch calls, hence compromising on the complete packet switching function of the network, and furthermore lacks a global standard for developing the networks.

Following the deployment of the 2.5 G networks, the ITU defined IMT-2000 demands for a global network design, irrespective of technology's platform, which was complied by 3G networks in Universal Terrestrial Mobile System (UTMS)/CDMA-2000 standards [44]. The network includes components such as base station/node B, and Radio Network Controllers (RNC) in addition to the WCDMA switching centre and serving GPRS support node/ gateway GPRS support node of the previous generation. This offered the network providers the capacity to offer a good range of services (such as video calls, and broadband wireless data) to their subscribers with a larger network capacity and better SE. The additional features of the 3G network includes High Speed Packet Access (HSPA) [45], which delivers up to 14 Mbps on the DL and 5.8 Mbps UL. The 3G networks deployment was again spearheaded in Asia, and shortly followed by Europe, and then the US by 2002. The network was equally launched in Africa using WCDMA standard by 2006. Despite the widespread of the standard, limiting factors such as spectrum license fees and site equipment hindered the pace in upgrading from the 2G/2.5G networks in most countries. Some examples are countries like Indonesia and China, who have delayed adopting the 3G networks (up until 2009 in china) due to spectrum licensing setbacks.

Due to the dramatic growth in subscribers and user demand in the wireless network, research was then triggered for the manifestation of the 4G networks with a lot of emphases on data rates and QoS. This was mainly due to the increasing demand for mobility of users requiring broadband services to compliment the wired networks. The cost effectiveness of the wireless terminals (relative to wired terminals) has also influenced the increasing popularity of the networks. The 4G era was aimed at achieving all IP architecture, so as to establish a common platform for all the existing

technologies and match with the expectations of the many services to be provided. The fundamental difference of the network's architecture with GSM/3G is distribution of RNC and BSC functionalities to the base stations and a set of serving gateways, thus, establishing a cheaper and simpler/ flat architecture. The continuous development and evolution of the 3G cellular networks to the 4G era have also witnessed remarkable improvement in broadband access technologies in the WMAN/WLAN as illustrated in Figure 2-2. As shown in the figure, the WiMAX (i.e. IEEE 802.16 standards) and WiFi (i.e. IEEE 802.11 standards) are dominant broadband access technologies, which have also evolved to the 4G era with increased data rates using OFDMA and MIMO technologies (similar to the cellular standards). The most current versions of these standards are 802.16m [46] and 802.11ac [47] for WiMAX and WiFi respectively. Although these technologies are out of the scope of this thesis, they are however mentioned as they equally represent the 4G wireless networks development and some current research are even focusing on the coexistence of 4G LTE networks with the WiFi access technology [48].

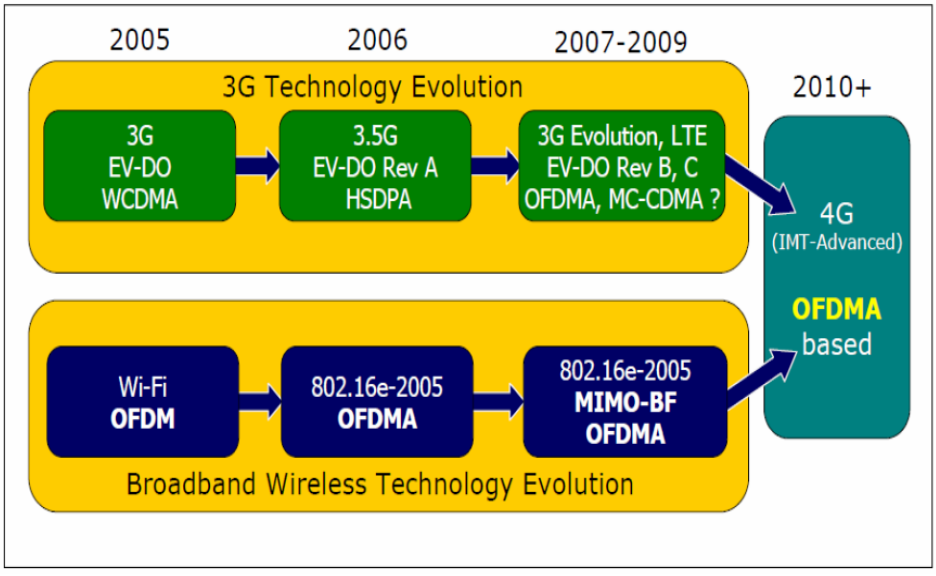

Figure 2-2 Evolution of broadband wireless technologies with 3G networks [49]

The IMT-A was set to make a global platform available, which would be used to develop generations of interactive mobile services offering higher speed data access, enhanced roaming services, and broadband multimedia amongst other services. Some of the agreements on the requirement of IMT-A are as follows [45];

- Backward compatibility and interoperability with previous standards.
- Peak data rate of 1 Gbps for DL and 500 Mbps UL
- Maintain connection with up to 350 km/h mobility.
- Achieve up to 15 and 6.75 bps/Hz SE for DL and UL respectively.
- Support for scalable bandwidth and spectrum aggregation with more than 40 MHz transmission bandwidths in DL and UL respectively.
- Cell edge SE of 0.06 bps/Hz and 0.03 bps/Hz for DL and UL respectively.

2.3 The 4G LTE network architecture

The LTE network standard is developed under the auspices of 3GPP as an evolution towards higher capacity and improved architecture of the 3G cellular standards such as UMTS and HSPA. The network standard was finalised in 2007 (for the initial release i.e. LTE release 8), which was at that time referred to as a 4G network, together with some wireless network technologies such as mobile mobile-WiMAX and HSPA+ [50]. The following release (i.e. release 9) trailed shortly after, with minor enhancements from the initial release, mainly in terms of data rates (peak rates of 300 Mbps DL). While the following subsections provide a general overview of the LTE network architecture, it however concentrates on highlighting theory and technologies that are relevant to algorithms and performance evaluations carried out in this research. These include the resource grid structure, signaling protocols, and technologies such as CoMP.

2.3.1 Network implementation of the 4G LTE standard

The network has a flat all-IP architecture specifically designed to achieve lower latencies (less than 5 ms in the RAN), thus achieving well reduced Capital Expenditure (CAPEX) and Operational Expenditure (OPEX) [9]. A comprehensive illustration of the LTE network architecture is shown in Figure 2-3. The Evolved packet core (EPC) consists of the protocol data network gateway (P-GW), serving gate-way (S-GW), and the mobility management entity (MME). The P-GW connects the EPC to the external IP networks, the S-GW conveys IP data traffic between UE and external network, and the MME coordinates the signalling for the Evolved UMTS terrestrial RAN (E-UTRAN) access [9].

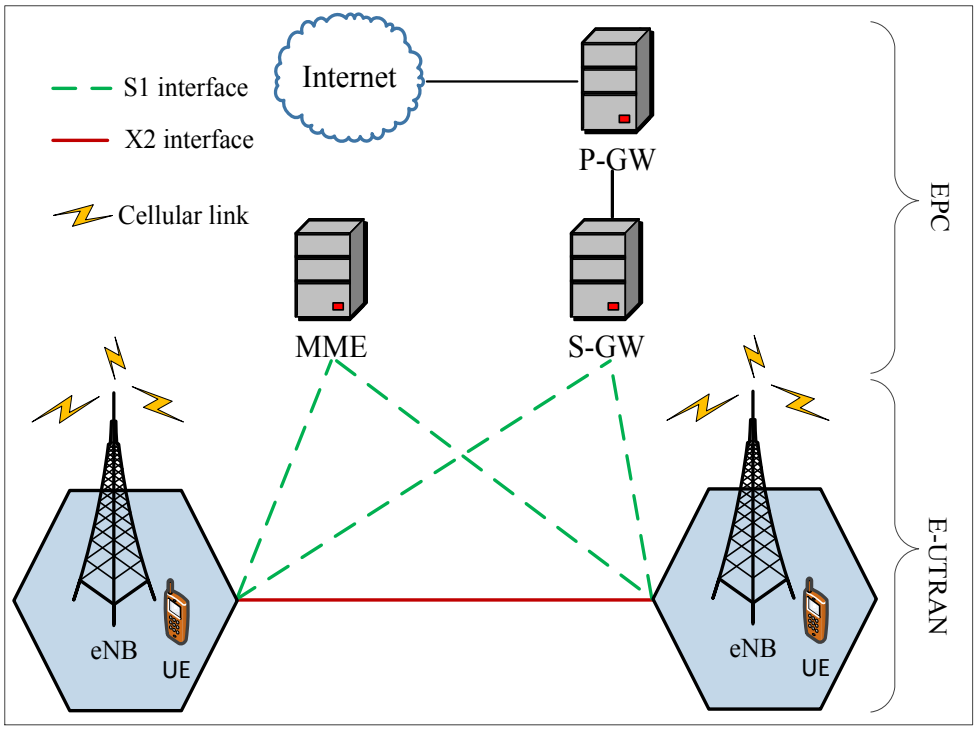

Figure 2-3 A comprehensive LTE network architecture

The LTE network provides peak rate of about 100 Mbps and 50 Mbps DL and UL respectively with the initial release (release 8), using a scalable transmission bandwidth (ranging from 1.25 MHz to 20 MHz). The DL is implemented using

OFDMA, while the UL with SC-FDMA, which in turn improves the SE and improves battery life of the UE respectively [9]. The SC-FDMA uses single carrier modulation with frequency domain equalisation, hence requires similar complexity to the OFDMA systems [21]. However, SC-FDMA has a significant advantage compared to conventional OFDMA in terms of lower peak to average power ratio (PAPR) due to the single-carrier transmission, which therefore reduces UE power requirement for UL transmission as earlier stated. The physical signal is generated in layer 1 of the LTE frame structure, and is used to perform functions such as cell identification, radio channel estimation, and UE/system synchronisation with the network in the DL [51]. Both DL and UL use the pilot signals to tackle the error issues in data reception, thus ensuring reliable and efficient demodulation at the receiver (especially for higher order modulation). Out of the two frame structure types of the LTE (TDD and FDD), the FDD is optimised to coexist with the 3.84Mb/s UMTS system, hence commonly considered in most literature. It contains 10 sub-frames with a total of 10ms (each sub-frame having two slots of 0.5ms), and has similar frame structure for DL and UL (with different channels and signal positions respectively) [51]. Figure 2-4 presents a diagram of the LTE frame structures (both TDD and FDD).

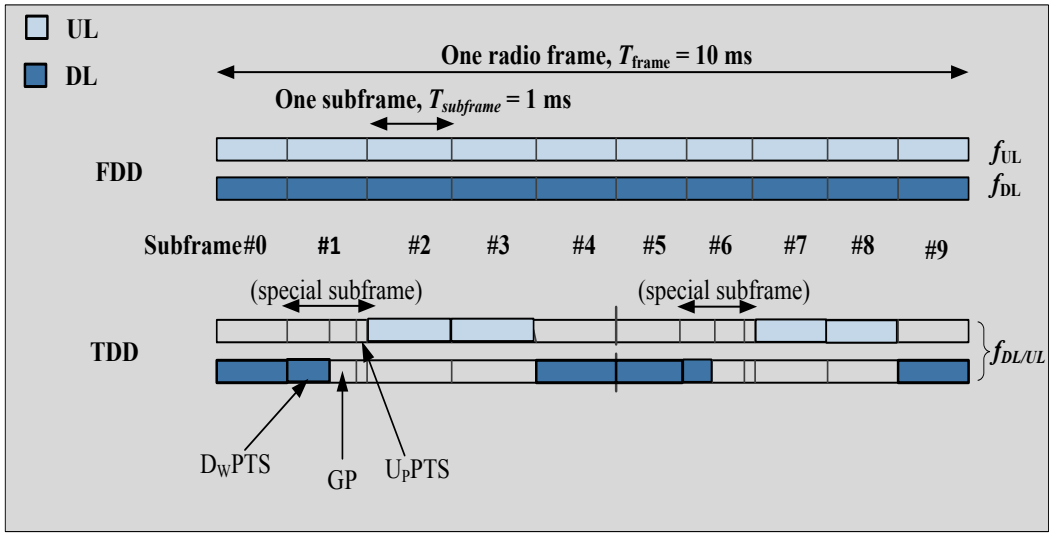

Figure 2-4 TDD and FDD frame structures of the LTE network [9]

The network has a simple protocol structure at the Radio link control (RLC), Medium access control (MAC) and physical layers. Some of the functions performed by RLC and MAC layers include retransmission and data multiplexing, whereas the physical layer offer information transfer to the higher layers, and transmits turbo-coded data via QPSK, 16-QAM, or 64-QAM, then followed by OFDM modulation [9]. The subcarrier spacing of the LTE is 15 KHz (with two CP lengths), in both the UL and DL. One of the most outstanding characteristics of the LTE is its ability to utilise both the TDD and FDD frame structures. Hence LTE achieves an efficient QoS using both HARQ and selective repeat ARQ for occasional retransmissions, and also has an efficient use of its radio resources by using channel dependent scheduling in the time/frequency domain to exploit rapid channel quality variations.

The bandwidth allocated to a UE (i.e. DL) in an LTE network is in the form of a resource block (RB), which is a constituent of a resource grid (shown in Figure 2-5). The resource grid comprises of 12 subcarriers and a number of OFDM symbols which differs for different CP length and system bandwidth.

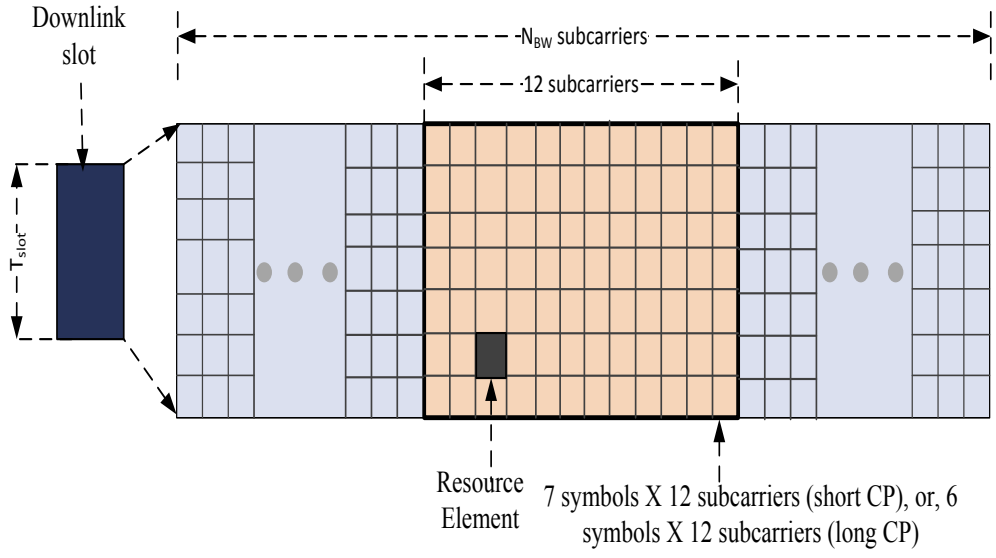

Figure 2-5 Resource grid structure of the LTE network [51]

The smallest time-frequency unit used for DL transmission is referred to as a resource element (one symbol on one subcarrier). The RB is a group of 12 subcarriers joining in frequency and one slot in time. A UE can be allocated more than a single RB based on its data rate requirement [51]. The total number of available RBs depends on the overall transmission bandwidth of the system, ranging from 1.25 to 20 MHz as shown in Table 2-1. Taking a 20 MHz bandwidth as an example from the table, a total of 100 RBs is available for data transmission for the whole UEs in the cell.

Table 2-1 Number of available RBs for different LTE bandwidths (DL) [51]

Bandwidth (MHz)	1.25	2.5	5.0	10.0	15.0	20.0
Subcarrier bandwidth (kHz)	15					
Resource block bandwidth (kHz)	180					
Number of available RBs	6	12	25	50	75	100

2.4 Enhancements in the LTE-Advanced networks

Shortly after finalising the initial releases of the LTE network, LTE-A (release 10) specifications were then approved by ITU as a true 4G network, having met the IMT-A requirements as mentioned in preceding section from [39]. The LTE-A network even shows slightly better capabilities in some aspects of the network performance compared to the IMT-A requirements as shown in Table 2-2. These include peak and cell edge SE for both DL and UL as shown in the table. This is however associated with the higher channel bandwidth (up to 100 MHz) specified for the LTE-A standard compared to the 40 MHz requirement of IMT-A. The proposal included major improvements on top of the initial release with full backward compatibility. These

primarily include enhanced antenna techniques (up to 8 X 8 and 4 X 4 MIMO for DL and UL respectively), and higher order modulation (up to 64 QAM modulation schemes). These influenced the significant improvement in data rates of the LTE-A network, with peak rate of up to 1 Gbps DL and around 500 Mbps UL compared to the initial release i.e. release 8 [52]. Additionally, a summary of SE targets defined for different antenna configurations are shown in Table 2-3. It should be noted that the SE targets in the table are specifically for a 10 MHz bandwidth channel in a multi-cell macro cellular environment [52].

Table 2-2 IMT-A requirement and LTE-A projected capability [53]

Item	**IMT-A requirement**	**LTE-A capability**
Peak data rate DL (Gbps)	1	1
Peak data rate UL (Gbps)	1	0.5
Spectrum allocation (MHz)	Up to 40	Up to 100
Latency user plane (ms)	10	50
Latency control plane (ms)	100	50
Peak SE DL (bps/Hz)	15	30
Peak SE UL (bps/Hz)	6.75	15
Average SE DL (bps/Hz)	2.2	2.6
Average SE UL (bps/Hz)	1.4	2.0
Cell edge SE DL (bps/Hz)	0.06	0.09
Cell edge SE UL (bps/Hz)	0.03	0.07

With the high achievable data rates specified for LTE networks, a major limiting factor is due to the interference from neighbouring cells/sectors on the UEs at the cell

edge of the universal reuse network (i.e. reuse factor of 1): inter-cell interference (from different cells/sectors) significantly affect the cell edge UEs SE. This in addition to signal attenuation (due to the distance of the UEs from the eNB and fading), especially in macro cells essentially affects the overall SE of the networks. Thus, the CoMP technology (which involves coordination between different cells) was specified for LTE-A so as to proffer solution to the inter-cell interference issue and increase the cell edge data rates/SE of UEs in the network.

Table 2-3 SE comparison for LTE release 8 with LTE-A targets [52]

Link	**Antenna configuration**	**LTE Release 8** [bps/Hz]	**LTE-A** [bps/Hz]
Uplink	1x2	0.8	1.2
	2x4	N.A	2.0
Downlink	2x2	1.6	2.4
	4x2	1.7	2.6
	4x4	2.7	3.7

2.4.1 Coordinated multipoint

CoMP transmission/reception is considered a key element in achieving the specified requirement of the LTE-A network. The technology spiked up a lot of research in both DL and UL implementations so as to improve the achievable data rates/SE of the network [54, 55]. Recently, field implementations have demonstrated the capacity enhancement of the coordination scheme as shown in [28]. While the UL CoMP is mainly vendor specific, the specification of DL CoMP schemes have been detailed by 3GPP [52]. These schemes are namely: Joint processing (JP) and coordinated scheduling/beamforming (CoSh/CoBF) [56, 57]. The X2 interface is a major element

in facilitating the CoMP technology in LTE networks. It is specified as a virtual interface initiated in the event of hand-over and CoMP process, thus enabling a temporary communication between the eNB of communicating cells [58]. A model classifying the elements of the CoMP schemes is shown in Figure 2-6.

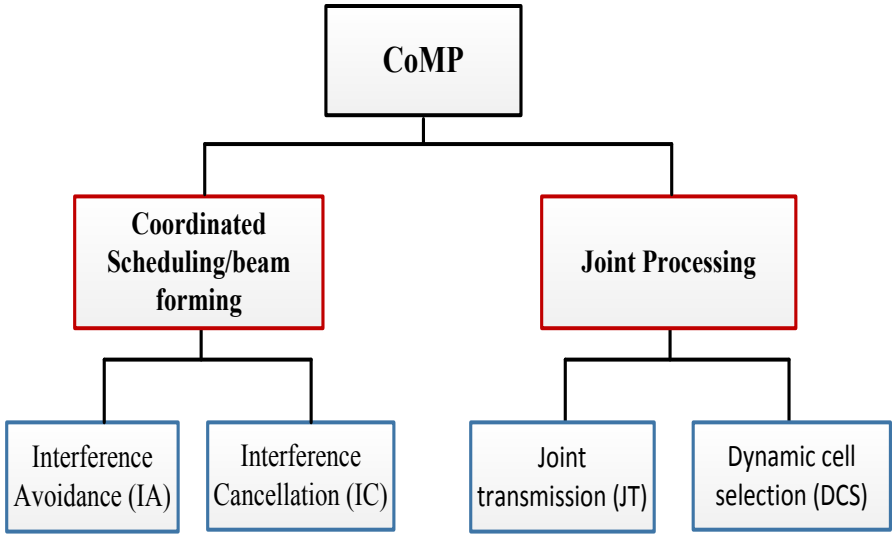

Figure 2-6 Classification of the CoMP schemes [54]

For the JP scheme, RBs intended for a single UE is transmitted from different coordinating cells (i.e. the non-serving and serving cells), referred to as Joint transmission (JT). Another technique for the JP scheme is referred to as Dynamic cell selection (DCS), where the RB allocated to a UE is transmitted from a single cell (among the coordinating cells), which is selected based on the channel condition by the central BS controller. In the CoBF/CoSH schemes, the RBs to a cell edge UE are always transmitted from a single cell. This is done by the cooperating cells coordinating their scheduling (i.e. when to allocate the UEs RB), or applying beamforming (signal processing to direct signal transmission) techniques [59] to mitigate interference on the cell edge UEs. While the CoMP scheme is broadly classified into CoBF and JP techniques, various algorithms have been proposed in research literatures to implement these techniques. In this direction, a CoBF algorithm

based on UE location is proposed in this research, where system-level simulation results showing performance improvement of implementing the algorithm is presented and discussed in Chapter 4 of this thesis.

2.5 Efficient spectrum utilisation with maximum use of cellular resources in future networks

One significant limitation in wireless network implementation in general is the scarcity of the finite spectrum, especially radio frequency ranging from 3 kHz to 300 GHz as shown in Figure 2-7. The congested frequency is being utilised for WiFi, 3G, and Bluetooth standards (amongst others) as illustrated in the figure. The increasing requirement of wireless broadband services has equally intensified the congestion of the spectrum. This has compelled strict regulations in individual regions around the world on how to effectively allocate and manage the limited spectrum to ensure efficient wireless communication.

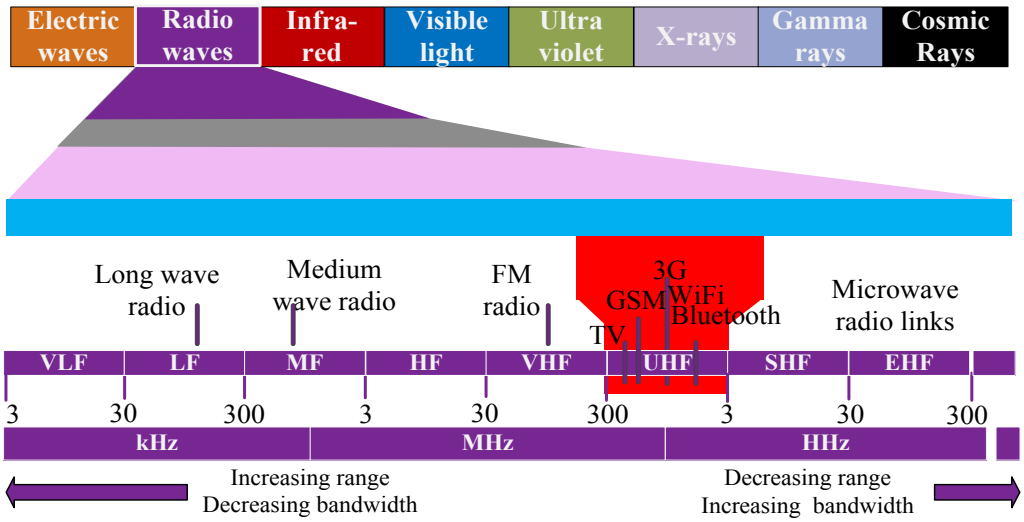

Figure 2-7 Illustration of the radio frequency spectrum

Astonishingly however, research statistics have shown that the major problem is not only in the scarcity of the spectrum itself, but with the underutilisation of the allocated

spectrums within the congestion zone as (shaded spectrum region in Figure 2-7). While the cellular spectrum is saturated with active users, the TV band has been identified to have significant redundancy in spectrum usage (as it is allocated a static spectrum that is seldom used). An example is a study conducted in some populated countries (Malaysia and China), which shows that only about 11% of the TV spectrum was actively utilised at the time of acquiring the statistics in the regions [35, 36]. The outcomes of such studies have sparked increasing research in finding solutions to making efficient use of the spectrum. This could be a significant factor for timely and cost-effective implementation of future wireless networks, since acquiring new spectrum is not only expensive but has been shown to hinder the timely migration to new technologies as discussed earlier. Thus to resolve the spectrum congestion and white spaces (unused spectrum) for the cellular and TV bands, inherent technologies such as D2D communication and CR are highly considered in current research initiatives to facilitate maximum usage of the spectrum. Thus D2D communication underlaying the cellular networks is projected to ensure effective reuse of the cellular resources (i.e. RBs), while CR is employed to eliminate spectrum holes by sensing/identify unused spectrum and temporarily allocating it to active unlicensed users when required. Additionally, the existing concept of Multihop (MH) transmission scheme is emphasised to enable cellular coverage extension and also to establish a common link between small cells and micro cells in the trending Heterogeneous Network (HetNet) implementation. The aforementioned technologies are discussed with further details in the following subsections;

2.5.1 Cognitive radio

CR [32, 60] senses the spectrum for a wide range of frequency bands, and then utilises the instantaneous white spaces/spectrum holes (i.e. the unused licensed

spectrum) for transmission, commonly referred to as opportunistic transmission. It is one of the technologies envisioned to proffer solution to the spectrum underutilisation discussed earlier in this section. The technology immensely suits the strict policies of fixed long-term spectrum allocation for the wireless communications. Wireless standards such as ZigBee and WiFi have been a success in the WLANs over the years, utilising the unlicensed spectrum (mainly in the 2.4 GHz spectrum band), which is also currently becoming crowded [34]. Some key aspects of the technology include spectrum sensing (i.e. identifying white spaces) [61], and interference management between the primary (licensed) users and secondary (unlicensed) users [62]. Although this technology is out of the scope of this thesis, it is however generally summarised in this subsection as it has been demonstrated as a key candidate for further enhancing the investigated technology in this thesis (as described in the future work in Chapter 6) to improve resource utilisation in the cellular networks. Hence what follows is a brief overview of the technology with some solutions proposed in current research as a form of reference.

In 2004, the IEEE formed a working group (802.22) so as to develop a standard Wireless Regional Area Network (WRAN) system to operate on unused VHF/UHF bands (originally allocated for TV broadcasting services) [61]. The aim of the WRAN system is to periodically sense the presence of primary users around the region so as to provide opportunistic access to rural areas. Some factors that have been identified to drastically affect the efficiency of spectrum sensing are the SNR of the primary users and fading of the wireless channels. The SNR of the primary users received at the secondary users might be too low (which has been shown to significantly decrease the quality of detection), and fading can cause the received signal power fluctuate

dramatically [63]. In [61], a spectrum sensing method was proposed based on the eigenvalues of the covariance matrix signals received at the secondary users. The ratio of the maximum or average eigenvalue to the minimum eigenvalue was used to detect the signals. In [63], a comparative study was shown, to evaluate the performance of different spectrum sensing methods, namely Energy detection (ED) method, Cyclostationary (CS) method, and the Roy largest root test (i.e. RLRT, based on the aforementioned Eigenvalue method) method. The ED method compares the energy of the received signal to the level of the noise while the CS method uses cyclic correlation function to differentiate noise from signals (since noise is not correlated).

In the case of interference management, the transmission between the primary and secondary users greatly affects the performance of the network in general. In [62], the effect of aggregated interference from multiple secondary users transmission on the primary users was analysed in a CR system. The literature first of all implemented a process to smartly study the interference in the system (referred to as Q-learning in the literature) with partial and full channel information. The method was shown to have maintained the aggregated interference (from DL and UL transmissions) to a desired value due to the information obtained from the observation. A common method of managing this issue is by including a power control method so as to reduce the interference power between the primary and secondary users in a CR system [64]. The literature [64] targeted finding a suitable power allocation of the secondary users such that the effect on the primary users QoS is maintained above a set threshold. A significant approach implemented was to detect and remove infeasible secondary users QoS constraints from the secondary user power allocation. It was shown to considerably improve the performance of the secondary users in the CR network.

2.5.2 Device-to-Device communication

D2D communication underlaying the cellular network is currently considered as a promising add-on technology to the LTE-A and future 5G cellular networks [38, 65, 66]. Unlike the traditional D2D communication technologies such as Bluetooth which functions in the unlicensed ISM bands (instead of the cellular spectrum), D2D communication utilising the cellular spectrum has recently been considered: with potential of better QoS as it occurs in the controlled cellular spectrum. It is studied as a key technology that improves utilisation of cellular spectrum resources with low power/energy requirement. D2D communication promises three types of gains: the proximity of UEs would achieve high data rate using low power transmission, improvement in the hop gain as D2D communication uses a either DL or UL for complete transmission, and also make efficient use of the reuse 1 network (i.e. reuse gain, as it reuses the cellular resources in the same cell/sector) [65]. Figure 2-8 depicts a simple network assisted D2D communication scenario.

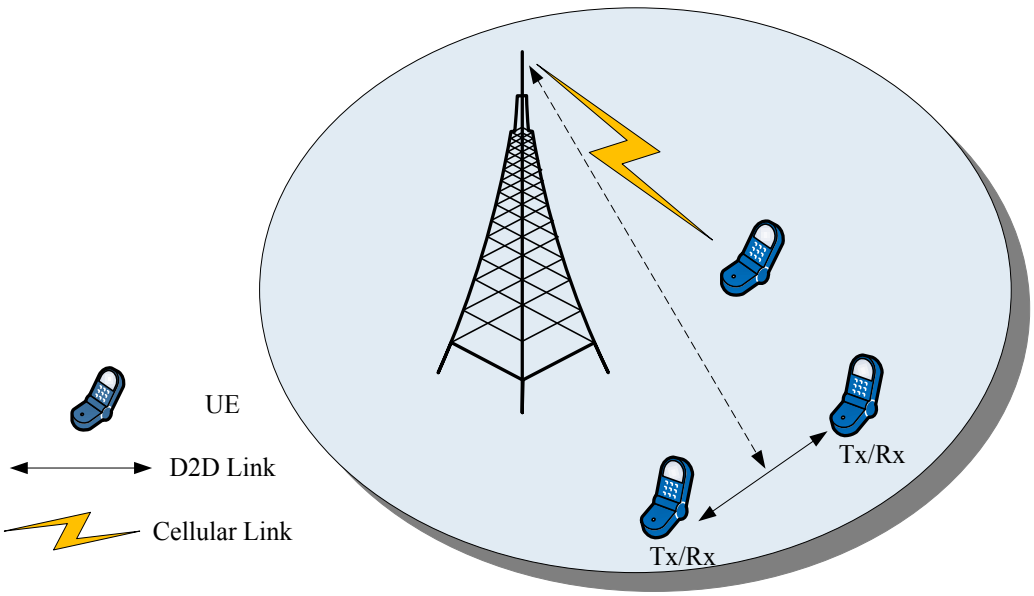

Figure 2-8 Illustration of network assisted D2D communication in a single cell

The eNB transports the cellular traffic, where the D2D transmission is conveyed using the D2D link with partial involvement of the eNB for handling control information signalling, and session setup. Some key design questions raised in the implementation of the D2D technology include resource allocation, and interference mitigation in the integrated networks (network with cellular and D2D UEs) amongst others. The location of D2D UEs within a cell/sector plays a significant role in attaining the proximity gain of D2D communication. As an example using the figure below, the D2D UEs receive less interference when they are further away from the eNB while reusing the downlink resources. This is because the signal from the eNB (during downlink transmission) will be weaker at the D2D receiver compared to the D2D transmitter signal in this circumstance (i.e. further distance from the eNB) [67]. Hence the D2D UEs are preferably located at the cell edge when reusing the downlink cellular RBs.

Generally, the resource allocation scheme for cellular networks which include D2D communication are classified into three: the cellular mode (all resources are allocated to cellular UEs), non-orthogonal sharing mode (the D2D UEs reuse the whole cellular resources), and orthogonal sharing mode (the whole cellular resources are divided to the cellular and D2D UEs in each cell/sector) [68]. Several contributions have been provided in literature to identify efficient resource allocation in the integrated network. In [68], a greedy policy resource allocation scheme was implemented using a proportional subcarrier algorithm: where the UEs with the minimum normalised transmit rate were allowed to select the best subcarrier every time. In [69], a resource allocation method was proposed using fractional frequency reuse: where the frequency of a single cell is divided into 4 frequency bands (assigned to different

regions in the cell). Thus, the D2D UEs in the scheme select a frequency band to use depending on the region of the cell that they occupy. In [70], the D2D transmitter derives the transmission power and number of RBs required for its transmission (for each D2D pair) and then sends a request for transmission to the eNB. The eNB then allocates the grant (power level and number of RBs) to the D2D links.

Resource allocation is one way of achieving interference management in the integrated network, specifically when the resources are being shared orthogonally between the cellular and D2D UEs as explained earlier. However, the ultimate achievement would be to reuse the cellular resources non-orthogonally whilst mitigating the impact of the interference in the network. A common method studied for performance improvement of networks with different constituents/entities is the use of power control [71]. This usually involves the adjustment of the D2D transmitter power and/or the eNB transmitter power, or adopting some antenna functionalities (such as beamforming) to achieve the objective. In [72], two methods were employed to apply power control in the network. In the first instance, the UE power is minimised while ensuring a target SINR (fixed SINR) for each stream, while in the second instance, variable SINR target was defined (having a maximum and minimum target) which was inversely proportional to the UE power. Hence, the SINR target for each stream is minimum with maximum UE power, and maximum with minimum UE power. In [73], transmit and receive beams are formed based on the channel state information (CSI) through traditional D2D links. Thus, WPAN such as WiFi and Bluetooth technologies are used to convey the CSI to reduce the overhead on the entities in the network in this proposal. Following the general overview of the D2D technology in this subsection, the issue of interference between the simultaneous

transmission of cellular and D2D traffic has been identified as a key challenge in realising the hybrid network. Thus, specific algorithms proposed for interference mitigation in the network will be further presented in Chapter 5 to compare and contrast implementation methods and performance results with the algorithm proposed in this research work.

2.5.3 Multihop communication in cellular networks

Multihop (MH) communication entails using relay stations (fixed or ad hoc) as intermediate nodes between BS/eNBs (i.e. source) and their corresponding mobile hosts/destination (i.e. UEs in this context) [74]. In this network architecture, the destination nodes with good channel quality communicate directly with the source nodes, while those with poorer channel condition (e.g. cell edge UEs) communicate via a single hop or multiple hops of relay nodes. Some studies have however shown performance drop with increasing hops/relays [75]. MH transmission has been shown to generally improve achievable data rates, extend cellular coverage, and also increase the energy efficiency of the network (as the relay nodes are either fixed low-cost/low-power nodes or idle users) [76, 77]. Figure 2-9 illustrates an overview of MH communication (limited to a maximum of 2 hops for simplicity in the figure) between a pair of source/destination node, where the nodes can communicate directly with each other or via any of the $R_{i\to n}$ relay nodes. It should be noted that the detailed processes and implementation of MH transmission itself is not in the scope of this research (as the scheme has been existing in traditional cellular networks), but rather, the performance gain of adopting the transmission scheme for relaying D2D traffic is studied. Hence this subsection provides a brief theoretical overview of the scheme, which will be followed by numerous simulation results (with the MH scheme) in the context of this research in Chapter 5 of the thesis.

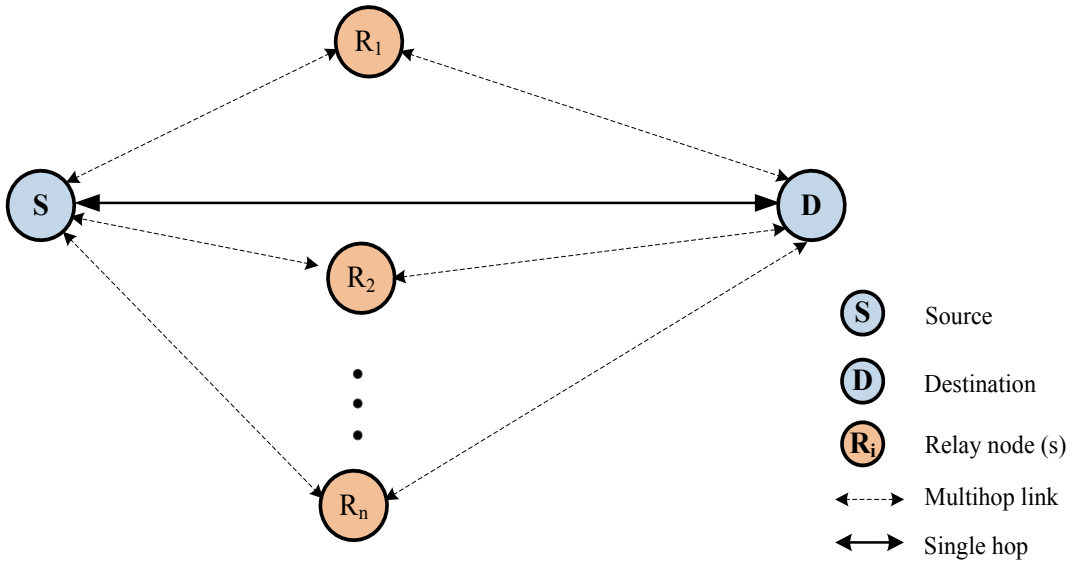

Figure 2-9 A general description of MH communication with two-hop relay between source and destination nodes

Despite the numerous advantages of implementing MH transmission in cellular networks, it does require some key aspects to be effectively implemented in order to achieve the required gain. These include relay selection/set up, and interference management between relay nodes and traditional cellular entities (i.e. BS and UEs) [78]. Relaying itself is broadly classified into Amplify-and-Forward (AF), and Decode-and-Forward (DF) relay schemes [79]. As the names imply, the signal from the source node is simply amplified and forwarded to the destination node in AF, while the signal is decoded and re-encoded by the relay node before forwarding to the destination node in DF. Both schemes have their trade-offs: the DF scheme can avoid interference and noise propagation, however, it requires accurate decoding and encoding of the relayed data, which increases the complexity and is therefore suited for dedicated/fixed relay stations. The AF scheme on the other hand is vulnerable to noise and interference propagation, however, it is highly less complex than the DF alternative and thus suitable for low powered/low-complexity devices [79]. Amongst

other methods of relay selection/set-up, a common method often referred to is the use of pilot signals (exchanged between source and potential relay nodes) to estimate the channel quality between the source and destination node via the potential relays [80]. This information (which is fed back to the source node) is then used to determine the required number of hop(s) and ideal relay(s) to achieve the required gain of MH transmission.

Another key aspect in adopting MH transmission as mentioned earlier is the issue of interference management in a MH network. This is not limited to the interference between the relay nodes and the BS/eNBs and UEs alone, but also extends to interference between the different relay nodes themselves [81]. A simple method adopted to reduce interference between source and relay node is by implementing a half-duplex transmission, i.e., the source and relay nodes transmit pilot/data signals in consecutive time slots [82]. Some research initiatives proposed to mitigate the interference issue in MH communication include resource portioning/scheduling, and power control [83]. In this literature, the dominant interference is reduced by separating the resources utilised by the nodes, or by simply varying the transmission power level of the interfering nodes [83]. Some current research initiatives have analysed using the spectrum sensing capabilities of CR to select optimum relays (in the case of multiple relay nodes) in a MH network to mitigate interference [84].

2.6 Architectural developments and research initiatives for multi-gigabit data rates in future networks

With the wide and fast deployment of the wireless networks, a major criticism of the network deployment has always been the low data rate provision when compared to

the wire line alternative (due to propagation limitations discussed in the previous chapter). The standardisation of the 4G networks such as LTE-A has however propelled the provision of Gbps data traffic in the wireless network. This is an enormous achievement in the mobile communication industry as the deployment and maintenance cost of the network remains relatively cheaper for the network operators, thus resulting to the deliverance of more mobile services to subscribers at lower cost. With the forecasted exponential increase of these users and services however, it is alleged that even the 4G networks will shortly require increased capacity.

Hence, some architectures and network designs are being proposed to efficiently use the current spectrum and new/future spectrum to offer multi-Gbps data rate traffic. Some prevalent projects with the aim of achieving this goal include METIS-2020, Horizon-2020 [13], and 5G-now [85]. The projects are mostly aimed at instigating and leading research with availability of sufficient funding in order to achieve multi Gbps 5G network by the year 2020 to 2040. Some initiatives proposed to achieve this objective include new technologies such as massive MIMO, virtualised antennas, machine-to-machine communication [86], and even advanced interference management techniques, since the networks have adopted tighter reuse factor to improve spectrum efficiency in recent standards [87].

One requirement for the next generation network in research literature is the enhancement of UE capabilities [88-91]. It has been implied that an effective way to achieve the dramatic increase in data rates is to first of all provide devices that can seamlessly access different Radio Access Technologies (RATs). Furthermore, the networks could be based on individual UE QoS (e.g. in terms of ease of connectivity

and improved energy efficiency). Emphasis have also been placed on the enabling of Cloud-RAN (CRAN) [92]. The CRAN forms a central base station with distributed antennas supporting different RAN protocols and dynamically adjusting its signal processing resources based on the varying traffic load within its coverage area. It could also be used as a convenient tool in networks such as LTE-A to easily carry out cooperative schemes such as CoMP. Additionally, integrated virtual radio networks are also supposed as a key requirement for developing 5G network architecture [88].

An enhancement of the cellular network architecture was suggested in [89], which lays emphasis on HetNet implementations. The literature also highlights the separation of indoor and outdoor transmission. This is based on statistics showing that mobile users are indoors 80% of the time, where penetration losses and transmission power requirement affects the performance of the network in general (as they are transmitting via BSs located in the outdoor). Thus introduction of Visible Light Communication (VLC) [93] in the spectrum between 400 to 490 THz (in the uncrowded spectrum) together with access network technologies like WiFi could be used solely for indoor transmission while the BSs are used for outdoor transmissions. The literature based its capacity improvement on the well-known Shannon theory [94] which shows the maximum capacity of the networks. In the context of the literature, the theory was modified to illustrate that the total system capacity is equivalent to the sum capacity of all sub-channels and HetNets as represented in Equation (2.1) [93].

$$C_{sum} \approx \sum_{HetNets} \sum_{Channels} B_i \log_2 \left(1 + \frac{P_i}{N_p} \right) \tag{2.1}$$

Where the bandwidth of the *i*th channel is B_i, P_i is the signal power of the *i*th channel, and N_p denotes the noise power. Therefore to increase C_{sum}, the key functionalities to

incorporate in the network include: increased network coverage (via HetNets), increased number of sub-channels (e.g. via massive MIMO [95]), increased bandwidth (via CR, VLC etc.), and also energy efficiency. The architecture of the proposed network is shown in Figure 2-10. Outdoor UEs can collaborate to form a virtual large antenna array, which could be added to the BS antenna arrays to realise a virtual massive MIMO link. An optical fibre link is then used to connect the distributed antennas in the cell.

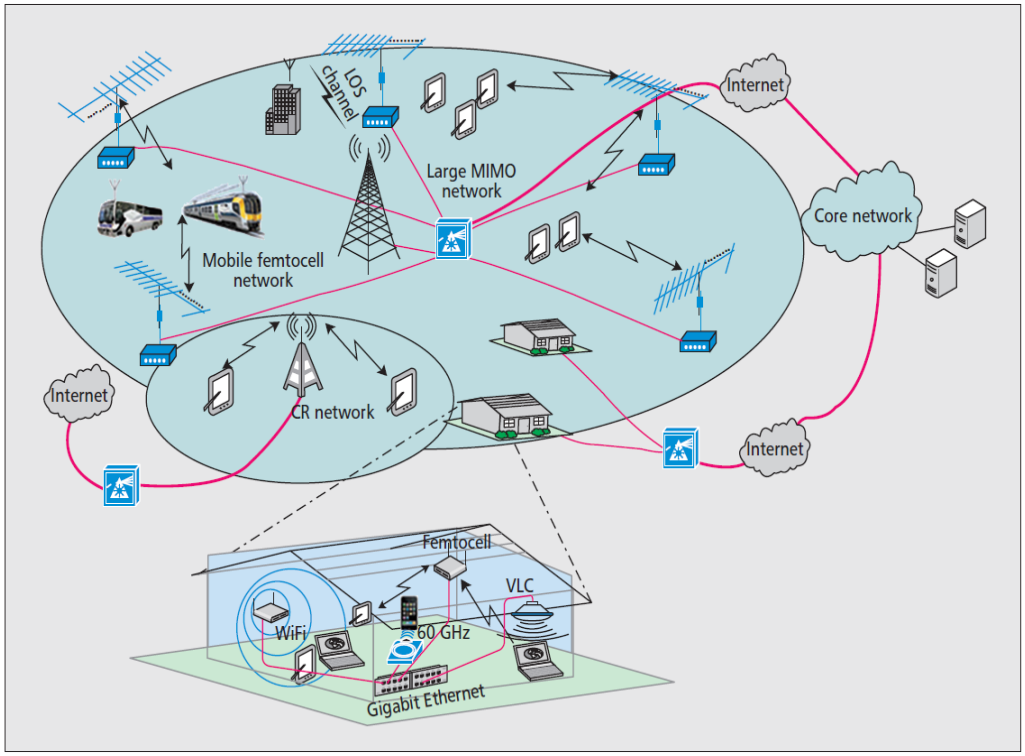

Figure 2-10 Consolidation of technologies for future 5G cellular architecture [89]

In [90], a proposed architecture was presented for 5G wireless networks. A new node referred to as a 'policy-router' was included in the core network of the architecture to enable the mobile terminal change the Radio Access Technology (RAT, such as LTE-A) based on certain conditions such as instantaneous QoS. An illustration of the architecture is shown in Figure 2-11. As stated earlier, the authors equally advocated that a key approach in the future generation of the network would be user-eccentric due to the increasing capabilities of the UEs. Thus, each of the RATs is an IP link to

the Internet (each having different interface in the UE). The Policy Router creates IP tunnels with the UE via each of the interfaces to different RATs (in the UE terminal). Based on the given policies, the change of the RAT (vertical handover) is accomplished via tunnel change by the Policy Router. Such change is based on the given policies regarding the QoS and user preferences, as well as performance measurement obtained by the UE with the newly defined procedure for that purpose (i.e. QoS Policy based Routing) in the literature [91].

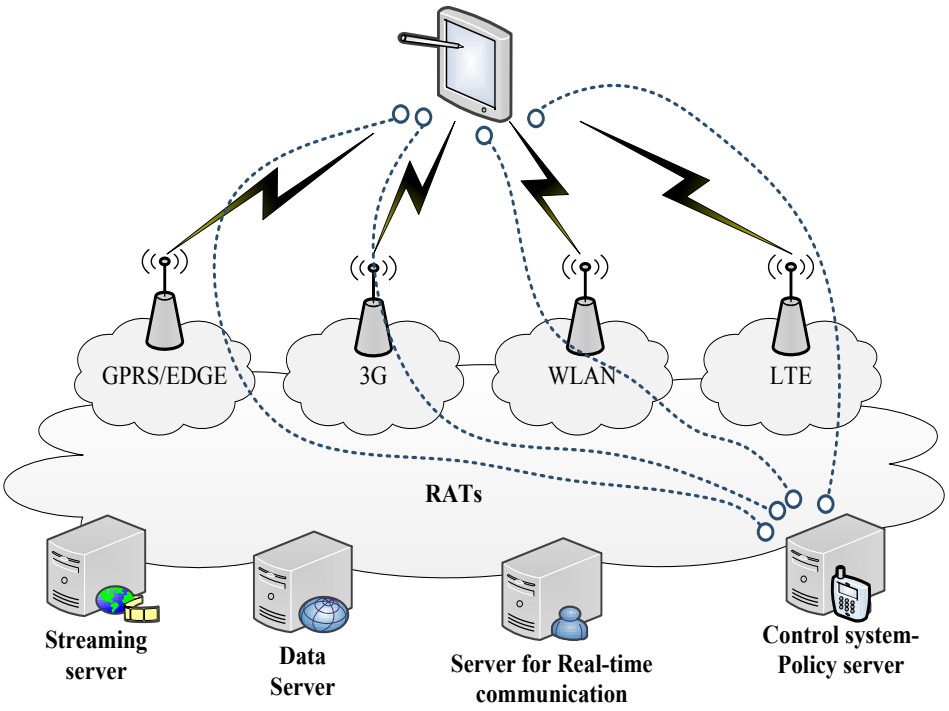

Figure 2-11 RAT selection by devices in future 5G networks [90]

Furthermore, Self-Interference Cancellation (SIC) [96] is equally explored as a requirement for future cellular networks, so as to support the demand for high throughput services and QoS constraint within the limited available spectrum. A SIC enabled network would then be able to implement full-duplex transmission, which is theoretically inferred to double spectral efficiency, since bidirectional communication can occur in the same channel/frequency band at the same time. In literature, the main schemes for achieving SIC are antenna cancellation, RF cancellation, and digital

cancellation [96]. Implementing SIC in future cellular networks would also offer the potential to sustain the dense deployment of HeTNeTs, which is highly projected as a key architectural enhancement for future network implementation[97]. It has also been proposed in some current literature as a viable means of implementing enhanced interference coordination and providing solution to relay interference in MH networks [97, 98]. In [97], a mixed signal SIC design was provided (shown in Figure 2-12)

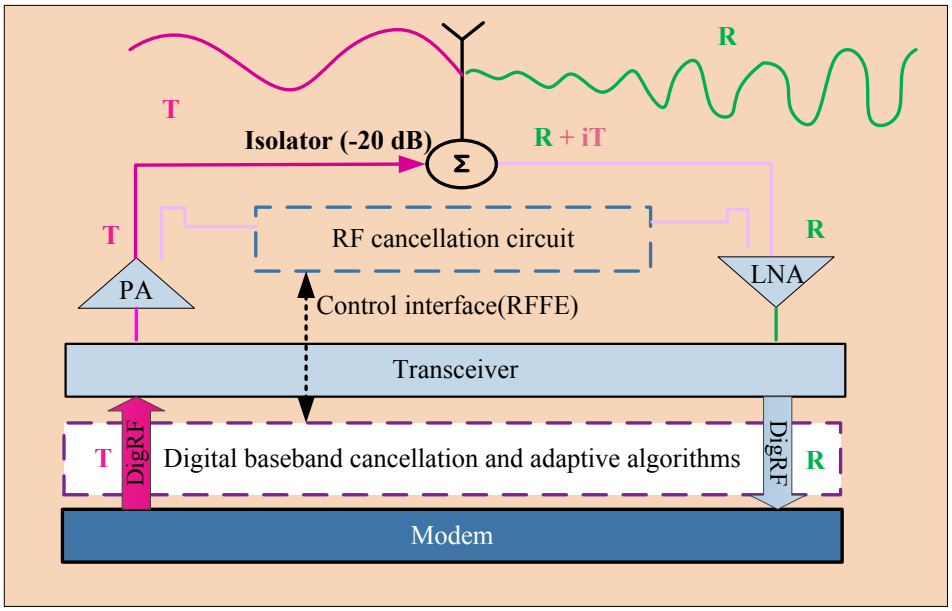

Figure 2-12 Self-interference cancellation architecture [97]

In the architecture, the receiver saturation is prevented by cancelling receiver noise in analogue RF before it reaches the low-noise amplifier (LNA), and the remaining digital interference is cancelled by modelling the non-linearity distortions with cancellation algorithms operating in the digital baseband between the transceivers [97].

2.7 Summary

In this chapter, the evolution of wireless networks to the current 4G networks was thoroughly discussed. It includes detailed limitations of the previous and even current networks in providing higher data rates (multi-Gigabits/s data traffic) as required for

future 5G networks. Additionally, technologies and advancements towards achieving the required data rates for the current 4G and beyond networks (i.e. 5G) were discussed.

In summary, while the 1G network introduced voice services, the 2G networks focused on increasing network capacity and coverage. Afterwards, 3G networks were dedicated to increasing data rates and speed with a global standard. The 4G network objectives are primarily to provide the mobile users with broadband multimedia services using very high data rates, higher mobility and better QoS. Preliminary 4G standards such as LTE release 8-9, and mobile WiMAX provided better system performance compared to the preceding generations of the wireless network standards. Key technologies in these prevailing networks include MIMO and OFDMA to achieve the high data rates. However, the networks were short in the performance requirement for 4G networks as specified by IMT-A. The LTE network however edged similar standards due to the lower latency, higher data rates, and most importantly backward compatibility to the preceding 3G networks (allowing easier and cost-effective migration). This has influenced the rapid deployment of the network around the world as illustrated in the earlier part of the thesis (Chapter 1). Nevertheless, having a universal reuse factor (reuse factor of 1), the network performance, especially at the cell edge, is limited due to inter-cell interference amongst other factors constraining wireless transmission.

Subsequently, LTE-A (release 10) standard was specified in 2009 and copiously fulfilled the requirements of a true 4G network as specified by IMT-A. The enhanced network included CoMP (inter-cell coordination schemes), higher order MIMO, and

carrier aggregation (up to 100 MHz bandwidth channels) amongst many features, with far superior data rate, leading to Gbps data rate transmission for wireless networks. Currently, the stride of investigating the implementation of 5G networks to provide multi-Gbps data rate is already in progress with organisations such as METIS-2020, and Horizon 2020 supporting research towards achieving this goal. These projects are being spearheaded by the EU, offering adequate funding to support research in achieving the networks by the year 2020. Measures envisioned to achieve the dramatic increase in the data rates include adding new spectrum, virtualised antenna architecture, SIC, and inclusion of new protocols in the networks amongst others. Additionally, emphases have been made in literature (discussed in this chapter) on the increased capabilities of the user interface. Smart phones will require additional functionalities to seamlessly access different RATs based on the QoS and other criteria.

The concept of adopting CRANs (central node connecting the RANs with fibre cables) was also discussed as a method of achieving centralisation between the RANs. Before the big step however, ongoing research is focused on integrating recent technologies to the current networks, which could enhance the utilisation of the spectrum as best as possible, and subsequently to extend these technologies to the future network. Some key technologies identified for this purpose include HetNet, CR and D2D communication underlaying the cellular networks. While all the mentioned technologies are equally promising for efficient use of the spectrum, this research is focused on CoMP and D2D communication underlaying cellular networks (specifically the predominant 4G LTE network). The obvious choice for focusing on CoMP is the due to the immense effect of the cell edge UE performance degradation

in the reuse 1 network to the achievable performance specified for LTE networks. A significant reason for focusing on the D2D communication technology is due to its ability to utilise the spectrum simultaneously with the cellular entities without waiting for opportunistic transmission (as is the case for CR). Additionally, it could have the potential of having less complicated interoperability protocol requirements between the numerous small cells and the macrocell in HetNets (which equally requires additional fixed infrastructures to serve as mini BSs in their respective cells). This could reduce CAPEX and OPEX as the cost of small cell base station is not required.

Thus, the next chapter of the thesis presents a comprehensive system-level design of a state-of-the-art 4G LTE simulator developed to carry out this research. These include appropriate channel modelling and evaluation of the preferred transmission methods in the simulator, which will further incorporate the technologies implemented to carry out further research investigations.

Chapter 3

System-Level Design and Evaluation of LTE Simulator Platform

3.1 Introduction

This chapter presents a detailed system-level design and implementation of a state-of-the-art Downlink (DL) LTE System-Level Simulator (SLS), which is further enhanced to incorporate CoMP functionalities, investigate D2D communication, and implement efficient interference modelling in this thesis. The simulator adheres to the 3GPP specification for the LTE/LTE-A network features and characteristics, which includes pathloss models, MIMO/antenna configurations, eNB/UE specifications, and the defined channel bandwidths amongst other features of the network standard. Additional simulator-specific features such as proper User Equipment (UE) positioning, and methods of retrieving performance metrics (such as UE throughput) have been enhanced to achieve accurate results in an efficient manner, so as to evaluate algorithms proposed in this thesis. Example of some common limitations in the few existing platforms include the random repositioning of UEs when out of a defined region on a flat surfaced map, and retrieval of UE metrics based on aggregating UE performance over a few Transmission Time Intervals (TTIs). Furthermore, theoretical overviews of the aforementioned features, such as channel modelling, are provided in this chapter to corroborate their use in the simulator. As part of verification of these features, simulation scenarios were devised, and results are presented to evaluate the different scheduling algorithms, transmission modes, and

also to demonstrate the cell edge UE performance of LTE networks with the developed SLS.

3.2 Link-level to system-level modelling

The concurrent simulation of the complete processes in a wireless system is not viable as it entails prohibiting computational complexity [99, 100]. In order to solve this problem, a common method is to separate the network tasks into link-level and system-level functionalities in different models [99-101]. The link-level model includes link functionalities such as receiver algorithms, feedback strategies, coding design etc. between an eNB and its serving UE (considering an LTE network). The system-level model includes a collection of network entities (i.e. it can contain several eNBs and UEs), where functionalities such as network planning, handover, and scheduling algorithms can be implemented. Thus, the traditional method for achieving a complete system-level performance is to abstract the link-level functionalities (i.e. the physical layer) with sufficient detail and high accuracy, and then perform link-level to system-level mapping (L2SM) [100, 101]. This allows simulation of the network in system-level, with measured performance of the link-level incorporated. Figure 3-1 depicts typical layers for implementing SLS models [101].

Although methods of implementing the SLSs vary, a common approach of achieving an efficient L2SM is by developing two major Models: the link quality model (LQM) and the Link Performance Model (LPM) [100, 102, 103]. To that extent, the SLS model for the purpose of this research is based on the framework in [103, 104]. An initial version (created in 2010) of a state-of-the-art DL LTE SLS model with fundamental functionalities (provided by the University of Vienna [105]) was

accessed and significantly enhanced to include inter-site/inter-cell coordination, D2D communication, Multihop (MH) transmission and wrap around interference modelling for the purpose of this research. The scope of this research is mainly focused on the DL performance of the LTE network i.e. the link from the eNB to the UE, and the allocation of resources (i.e. scheduling) in the LTE network. The Uplink (UL) processes are accounted for by adding a feedback delay to achieve a complete system-level process. The UL delay represents the period for HARQ processing and acknowledgment feedback by the UE after receiving control signal or RBs from the eNBs. The LQM abstracts the measurement for link adaptability and resource allocation with reduced complexity. It then outputs a metric (SINR in this case) quantifying the quality of the received signal after reception and equalisation. The metric is then mapped into the Block Error Rate (BLER) and throughput based on the code rate, modulation and coding schemes (MCS) at the LPM.

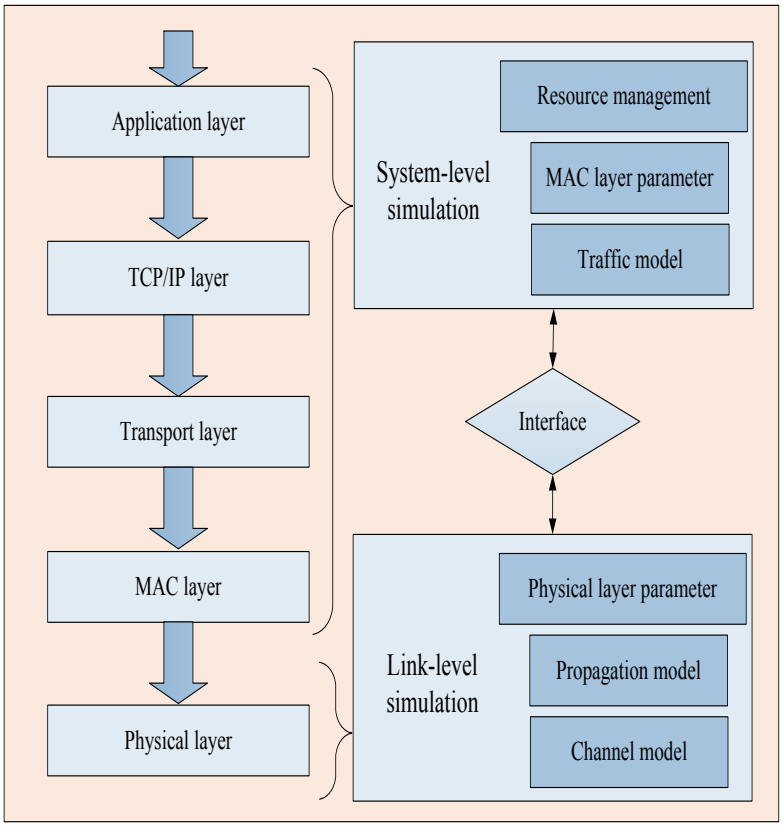

Figure 3-1 General layers for simulator modelling [101]

The detailed description of the L2SM in the framework is shown in Figure 3-2 [103]. Different blocks/functionalities are been fed to the LQM in order to obtain the SINR metric for the system-level link. An instance is the macroscopic pathloss that is determined by the position an individual UE occupies relative to its serving eNB and interfering eNBs, which is then used to model the propagation pathloss with the antenna gain. Another instance is the shadow fading, i.e. obstacles between the path of an eNB and attached UEs, which is typically modelled by a log-normal distribution of mean zero and standard deviation (σ = 10) in SLS platforms [104]. The aforementioned position dependent variables are created on a map referred to as Region of Interest (ROI), where all the physical properties/entities of the network are confined (such as eNB antennas).

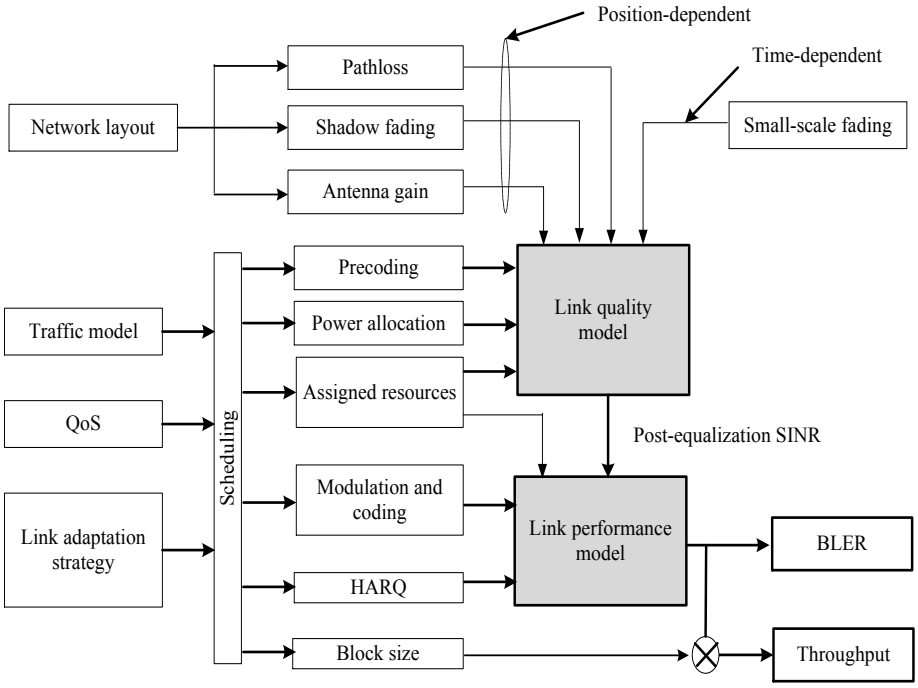

Figure 3-2 Link-system level modelling of the LTE network SLS [103]

Assuming an LTE system with N_{TX} transmit antennas and N_{RX} receive antennas, the signal received at the r^{th} antenna (y_r) can be expressed in the time domain as:

$$y_r = \sum_{t=1}^{N_{TX}} (h_{t,r} * x_t) + n_r, \tag{3.1}$$

where the signal (x_t) from the t^{th} transmit antenna is convolved with the channel impulse response between the t^{th} transmit to the r^{th} receive antenna ($h_{t,r}$), combined with AWGN (n_r) [103]. Thus, stacking the ($h_{t,r}$) values into a $N_{RX} \times N_{TX}$ matrix, Equation (3.2) represents the received symbol vector ($\mathbf{y}$) of length N_{RX} for a single link, $\mathbf{H}$ represents the channel matrix, $\mathbf{x}$ represents the transmitted symbol vector, and $\mathbf{n}$ represents the noise (i.e. AWGN). Expanding from the single link signal to consider multiple eNBs, the received signal for individual UEs after the L2SM is then represented in Equation (3.3)

$$\mathbf{y} = \mathbf{Hx} + \mathbf{n}, \tag{3.2}$$

$$\mathbf{y_0} = \mathbf{H_0 x_0} + \mathbf{n} + \sum_{i=1}^{N_{\text{int}}} \mathbf{H_i x_i} \tag{3.3}$$

where $\mathbf{y_0}$ is the received signal, and the sub-index $i = 0$ denotes the desired signal while $i = 1 \ldots \boldsymbol{N}_{int}$ is the signal from each of the eNBs [103]. From the variable $\boldsymbol{N}_{int}$, the subscript *int* stands for interference, which is from each of the N eNBs because they use the same set of frequency in all the cells.

Thereupon, the channel quality measured output by the LQM serves as input to the LPM as traditionally done in SLS platforms stated earlier [101]. Subsets of the subcarrier post-equalisation SINR represent the channel conditions on a per-spatial-layer basis. The RBs are set such that the UE are then scheduled (if scheduled): the total number of RBs depends on the channel bandwidth. The LPM model combines the output of the LQM with that of the applied modulation order and code rate and it

envisages the BLER of the received Transport Block (TB). The successful or failed reception of a TB is randomly decided via a "coin toss" corresponding to the BLER probability [103]. Figure 3-3 illustrates the SNR to BLER mapping used in the SLS to abstract the individual UE link. The UE SNR is mapped to the corresponding CQI and fed-back to the eNB. Figure 3-3 (a) shows the simulated SNR-CQI mapping with the SLS, while Figure 3-3 (b) illustrates a general CQI-SNR mapping model. The graph was simulated using the developed model in this chapter to conform that the SNR corresponding to the CQI values are similar to that of the benchmark model in [103]. The UE sends a CQI feedback to the eNB, indicating the data rate it can support. The measurement is carried out by the UE using the reference signal sent to it by its serving eNB. The UE determines the CQI to correspond to the highest MCS, so that the UE can decode the TB with error rate probability not exceeding 10% [106].

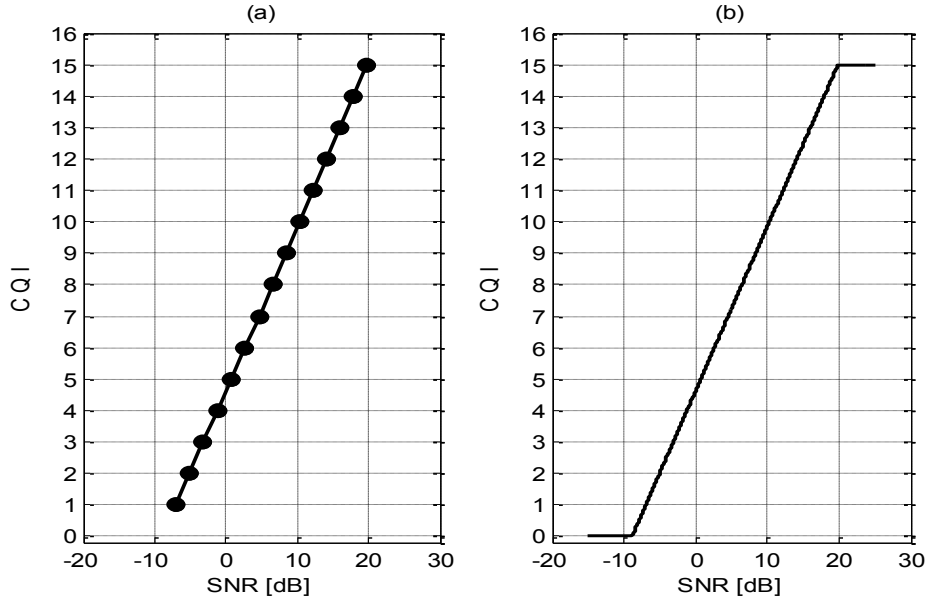

Figure 3-3 SNR to CQI mapping

A summary of the different CQIs and their corresponding coding rate and efficiency (data bits per symbol) is shown in Appendix A. Combined with the TB size, the throughput metric is then determined for the UEs to illustrate the system-level simulation performance [103].

3.2.1 Link quality measurement in SLS model

As discussed earlier, the key metric used to abstract the measured link quality in the SLS is the SINR. This is obtained by modelling the macroscopic pathloss, shadow fading, and the fast-fading as represented in Figure 3-2. As indicated in the figure, the latter is time variant while the rest are position dependent. A zero forcing [107] (ZF) receiver is modelled for the MIMO transmission modes in the SLS, to represent the time-and-frequency variant behaviour of the channel i.e. fast-fading. ZF is an existing technique used to retrieve desired signal stream at a receiver from the multiple streams simultaneously transmitted in a MIMO system by employing channel state information (CSI) [108] Thus the SINR calculation (in the LQM) for this SLS model is based on ZF on a per-subcarrier basis, thus incorporating the OFDM-based physical and MIMO processing of LTE into the design.

The macroscopic pathloss map models the propagation losses (due to distance) between the UE and its serving eNB, and also the antenna gain. An illustration of the map is shown in Figure 3-4. The graph represents pathloss of a single sector in a ROI. The sector has a directional antenna with an azimuth of 30 degrees as shown in the graph. It can be realised that the pathloss (in dB) is significantly lower closest to the eNB, particularly in the direction of the antenna gain (within the range of 80 to 100 dB pathloss).

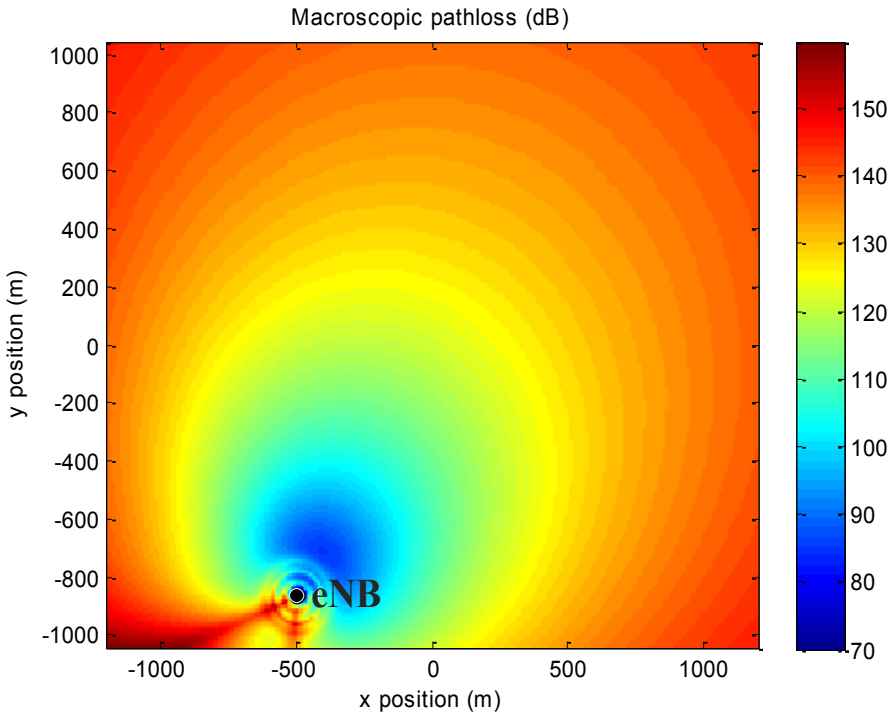

Figure 3-4 Macroscopic pathloss for an eNB with 30 degrees azimuth in a ROI

Another property modelled to obtain link quality in the SLS is the shadow fading. This is modelled to represent obstacles/obstruction in the propagation path between a UE and the eNB i.e. irregularities in the environment. The shadow fading is generally modelled as a zero-mean log-normal distribution with correlation of 0.5 between eNB sites [109]. For a cell layout representing an urban environment with multiple sectors per site (usually 3), a correlation factor of 1 is generally assumed since they occupy the same geographical location [103]. An illustration of the correlated shadow fading map of multiple sites (a total of 7 sites) in a ROI is presented in Figure 3-5. For each of the sites, a cluster of pixels constitute the geographical surface of the different sectors within the sites. It can be shown in the figure that the pixels vary in colour, indicating the shadow fading value (in dB) for each pixel as indicated by the chat

incorporated.

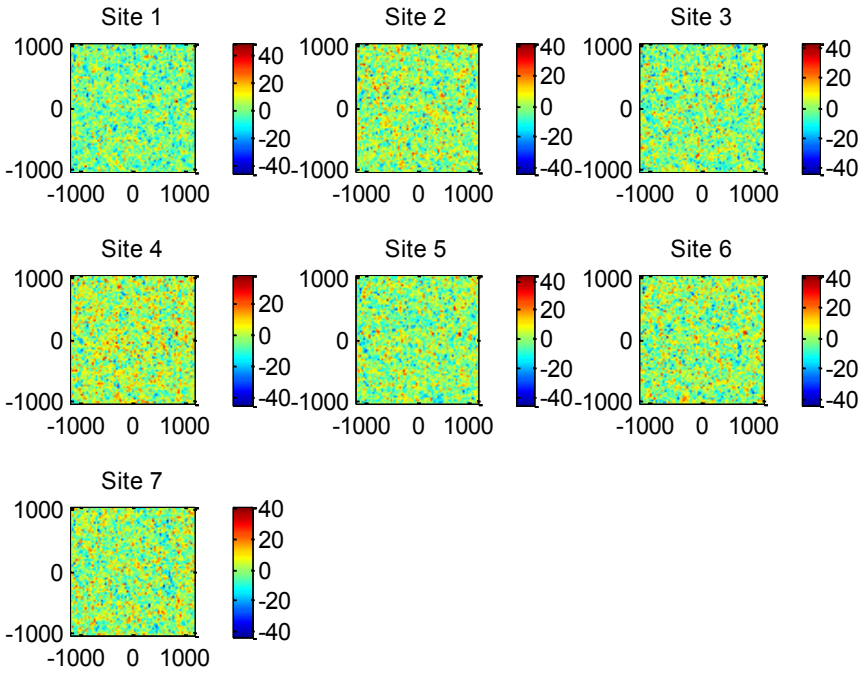

Figure 3-5 Correlated shadow fading map for multiple eNB sites

The SINR of the *j*th UE for the system-level can then be summarised as:

$$SINR_j = \frac{P_T}{\sum_{i=1}^{N_{\text{int}}} P_i + N} \tag{3.4}$$

where P_T is the desired signal power (from the *j*th UEs' transmitting eNB), and P_i is the sum of power from the surrounding/interfering eNBs (sub-index i = 1…N_{int} represents each of the interfering eNBs), and N represents noise.

3.3 Network architecture and channel modelling

The network layout used for SLS platforms are seldom modelled uniquely based on field measurements/surveys to emulate specific geographical features of certain cell

sites (such as cell size, actual cell edge etc.) [110]. Traditionally however, a common assumption is made by using hexagonal grids to represent the cell sites or sectors, differentiating the cellular scenarios (e.g. macro and micro cells) by the size and distance between the sites [111]: with accurate modelling of entities such as antenna heights, and gain pattern. Thus, the SLS topology for this research investigation depicts a typical macrocell system cell layout, where a hexagonal grid represents an eNB sector (uniquely indexed for clarity in Figure 3-6).

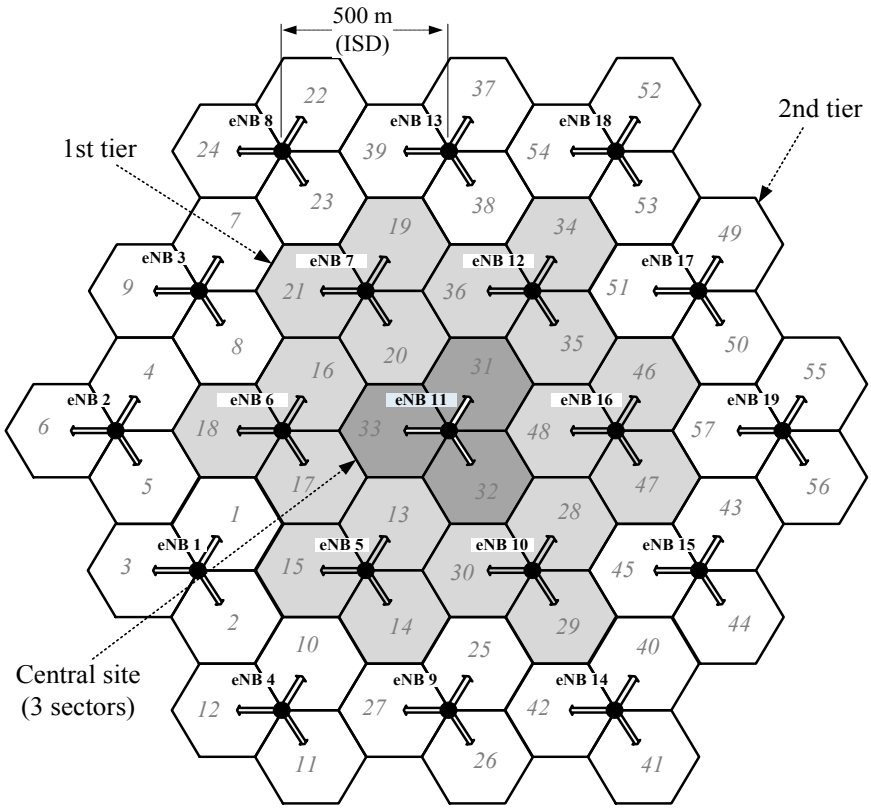

Figure 3-6 Cell layout of SLS representing typical macrocell with 500 m ISD

It consists of N number of eNB cell sites as shown in Figure 3-6 (where N = 19), separated by an inter-site distance (ISD) of 500 m: all modelled within the ROI to simulate the network. All the sites comprise of 3 sectors each (S_1, S_2, and S_3) i.e. a total of 57 sectors. The sectors are separated with 120 degrees directional antennas: where the azimuth (i.e. ground plane angle of a point relative to true North) of S_1 is 30 degrees, S_2 is 150 degrees, and S_3 is 270 degrees. A detailed description of the

azimuth angles in the different sectors of the SLS model is provided in Appendix A. The sectors have a fixed antenna pattern (i.e. horizontal), which is expressed as:

$$A(\theta) = -\min\left[12\left(\frac{\theta}{\theta_{3dB}}\right)^2, A_m\right] -180 \le \theta \le 180, \tag{3.5}$$

where $A(\theta)$ is the 2D radiation pattern A, which is dependent on azimuth θ, θ_{3dB} is the 3 dB beam-width (in degrees), and A_m is the maximum attenuation, with an antenna gain of 15 dB [111, 112]. The antenna gain pattern for the individual sectors in this SLS model is shown in Figure 3-7.

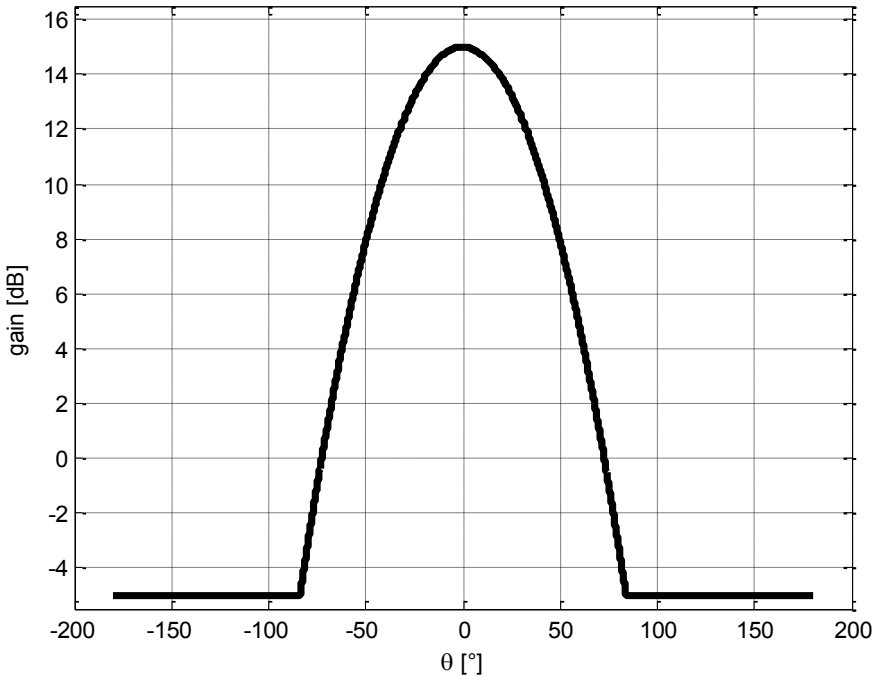

Figure 3-7 Antenna gain pattern for the individual sectors in SLS

Another important parameter considered in the model is the Minimum Coupling Loss (MCL) i.e. the minimum distance loss including antenna gains measured between connectors [112]. This describes the minimum signal loss between the cellular entities (such as eNB-to-UE, or UE-to-UE). Thus, the received signal between the cellular entities in both DL and UL can be expressed as:

$$P_r = P_t - max(PL - G_t - G_r, MCL) \tag{3.6}$$

where P_r represents the received signal power, P_t represents the transmitted signal power, G_r and G_t represent the receiver and transmitter antenna gain respectively, and PL represents the propagation pathloss (which will be discussed in detail in the following section).

3.3.1 SLS parameters and Simulation methodology

The general parameters for the SLS are summarised in Table 3-1. The UEs are distributed equally among all the sectors i.e. 10 UEs per sector. As the cell layout depicts a typical macrocell, shadow fading is caused by large features such as hills and buildings, usually modelled as log-normal distributed random variable with zero-mean [111]. It is a position dependent feature and a function of the UE location in the cell. Hence, it is modelled to be space correlated, as the fading experienced by UEs around the same vicinity would be interrelated. The SLS has the ability to simulate various LTE transmission modes with standard channel models (as will be discussed and evaluated in the following section).

As shown in the cell layout from Figure 3-6, the network can be simulated using one tier (with 21 sectors), or two tiers (with 57 sectors). For the one-tier simulation layout, performance of UEs in the central sectors is considered (i.e. 30 UEs, considering 10 UEs per sector) and the rest discarded, while for the 2-tier simulation layout, the performance of UEs in the 1st tier are considered (i.e. 210 UEs), while the rest are discarded. This is done to ensure all the UEs experience the same interference level, hence avoiding attaining optimistic performance result from the UEs at the border sectors (such as sectors 3, 6, and 12) in the cell layout. The UE performance such as throughput is logged after every TTI, which is then averaged to determine the UE

performance after several TTIs. The average throughput of the i^{th} UE in the SLS is determined by;

$$\text{Average Throughput}_{UE_i}(bps) = \frac{\text{Correctly received TB size(bits)}}{\text{TTI(seconds)}} \quad (3.7)$$

Table 3-1 Summary of SLS parameters

Parameter	Value
Network Layout	7 eNBs, 3 sectors/eNB site, ISD 500m
Link adaptation	Adaptive modulation and coding (AMC) supported
UE parameters	10 per sector, 5 km/h, 3 TTIs feedback delay
UEs distribution	Homogenous; pre-set positions
UE noise	Thermal noise density: -174 dBm/Hz, noise figure: 9dB
Channel model	Urban, Winner II type
Shadow fading	Log-normal, space correlated, zero mean σ = 10 dB
Frequency	2 GHz (Frequency reuse of 1)
Bandwidth (MHz)	5, 10, and 20
Transmission modes	SISO, TxD, OLSM, CLSM
eNB parameters	20 m height, 15 dBi gain, TX power: 43 dBm
Schedulers	Round robin; proportional fair; best CQI
TTI (ms)	100

A pseudo code describing the flow of the developed SLS model is presented in Table 3-2. It mainly summarises the order of the SLS functionalities, which includes cell layout and simulation methodology described earlier in this chapter. A Region of

Interest (ROI) is firstly created as a map, where the area and number of eNBs enclosed within depends on the tier selected for simulation; hence the central eNB site can be selected which has 3 sectors, or a one-tier cell layout which has 7 eNB sites and 21 sectors can be selected, otherwise a two-tier cell layout is selected with 19 eNB sites and 57 sectors as described in Figure 3-6. Thereupon, the eNB/eNBs are positioned accordingly on the ROI map and configured with antenna properties such as transmit power and antenna height (details provided in Table 3-1) for each of the sectors belonging to an eNB.

Table 3-2 Pseudo code describing the flow of functionalities in SLS model

Pseudo code SLS flow

```
(1)   Define ROI
      the cell layout or tier/tiers selected determines the area within ROI map
(2)   Distribute eNB/eNBs within ROI map
      described in cell layout in Figure 3-6
(3)   Create pathloss map
(4)   Create UEs, attach them to an eNB, and distribute UEs uniformly in each sector
(5)   Append network clock to synchronise SLS functionality
(6)   for TTI = 1 - end
(7)       Move UEs
(8)       if UE moves outside ROI
(9)           Relocate UE based on wrap-around algorithm proposed in Chapter 4
(10)      for each eNB
              Receive UE feedback (feedback delay in Table 3-1) and schedule users
(11)          for each UE, do
                  Channel state, LQM, SINR
                  SINR/MCS, LPM, BLER
                  Send UE feedback
(12)  end for
```

The surface area within the ROI map comprises of a collection of points/pixels with a resolution of 10 meters/pixel (demonstrated in Appendix A). Thus, pathloss and shadow fading values (explained in Section 3.2.1) for each of the pixels is encompassed within the ROI map. The pathloss primarily represents the power

density attenuation relative to each pixel, which is mainly due to factors such as distance from a sector antenna to each pixel. The shadow fading on the other hand represents obstacles in the propagation path between a pixel position and a transmitting antenna on the map. A defined number of UEs are then created and randomly distributed within the ROI map: the UEs connect to the nearest/best eNB (in pathloss). A network clock is appended on each entity of the network (e.g. UEs and eNB) to synchronise functionalities such as scheduling in the SLS, and the simulation is run for a number of TTIs (user defined). Thus for each TTI, the UEs move based on a random walk model (5 km/h), covering different pixel positions within the sectors they occupy. The link quality for the UEs on each pixel is utilised to produce the SINR metric, which is then used (i.e. SINR) along with modulation and coding scheme to determine the BLER of the transport block at the receiver. Thus the throughput of each UE is calculated, using Equation (3.7), after each UE has fed-back an acknowledgement to its serving eNB.

3.3.2 Channel modelling

The use of standard and efficient channel models plays an essential role in assessing the system-level performance of LTE networks (or any network standard) in simulation platforms. The channel models represent the effect of the channel on propagating signals between a transmitter(s) and a receiver(s). This is mainly due to the requirement of achieving as close as possible the real life performance of the networks. As a lot of emphasis is placed on making the simulation platforms less complex, the channel models are equally required to be accurate and versatile, but computationally efficient. A common platform was provided by ITU-R identifying a set of test environments (sufficiently covering operating environments and user mobility), which have been effectively used for development, network planning, and

performance verification for 2G and 3G networks [113]. Key factors of the radio propagation environments include multipath propagation, which causes fading and channel time dispersion and also depends on the UEs mobility relative to its eNB. The most commonly used test environments include: indoor office, indoor-to-outdoor pedestrian and vehicular test environments.

The indoor office, indoor-to-outdoor, pedestrian environments are generally characterised by small cell sizes and low power transmissions. The indoor office generally depicts an environment where the UEs and transmitters are all located indoor. The attenuation of pathloss due to obstacles like walls, floors and furniture is modelled with a lognormal shadow fading with σ = 12. A simplified model formulated/provided by 3GPP to model the test environments pathloss (L) is shown in Equation (3.8) [114].

$$L = 37 + 30\log_{10}(d) + 18.3n^{((n+2)/(n+1)-0.46)} \tag{3.8}$$

where L represents the pathloss, n is the number of floors between the receivers and d is the distance between the transceiver.

The indoor-to-outdoor pedestrian environments include low antenna height BSs that are located outside, thus covering pedestrian UEs (average speed of 3 km/h) located on the streets and inside buildings (residential/offices). Lognormal shadow fading with σ = 10 is used for the pedestrian UEs and σ = 12 for the indoor UEs to cover for penetration losses as mentioned earlier. For accurate modelling, the pathloss is further divided into Line-of-site (LOS) and non-LOS: Equation (3.9) represents the pathloss model for the non-LOS case, while Equation (3.10) illustrates a model for both LOS and non-LOS proposed in [115].

$$L = 40\log_{10}(d) + 30\log_{10}(f_c) + 49 \tag{3.9}$$

$$L = 20\log_{10}\frac{4\pi f d_n}{c} \tag{3.10}$$

where f_c is the carrier frequency, and d_n is the sum of n street segments. The vehicular test environment is alternatively characterised by large cells (macrocells), high transmit power, and high cell capacity (assuming limited spectrum). The signal strength diminishes with increasing distance from the transceiver, and is typically used to represent urban and suburban environments with UE speed from 30 to 350 km [113]. The pathloss of the vehicular test environment can be expressed as:

$$L = 40(1 - 0.004 \times \Delta h_b)\log_{10}(R) - 18\log_{10}(\Delta h_b) + 21\log_{10}(fc) + 80 \tag{3.11}$$

where Δh_b is the height of the base station (in meters) form an average rooftop height and $0 < \Delta h_b < 50$ [114]. However, if Δh_b = 15 m and f_c = 2G Hz, the pathloss model is then represented as:

$$L = 128.1 + 37.6\log_{10}(d) \tag{3.12}$$

3.3.3 WINNER channel model

With continuous adaptation of spatial dimension for the 3G and beyond networks, the channel models need enhancement to include the spatial channels in the model. This lead to the development of the spatial channel model (SCM) by the 3GPP/3GPP-2 group in order to access the wireless networks with MIMO functionalities, mainly for outdoor environments at f_c = 2GHz. The SCM was primarily used to test CDMA channels for both link-level simulator and SLS model, where the latter have been used as a standard for system-level evaluations for standards such as LTE, WCDMA, and UMTS amongst others [116]. The SLS SCM was used to test urban macrocell,

suburban macrocell and urban microcell, which are mainly differentiated by their azimuth spread, delay spread and shadow fading pathloss.

Subsequently, the SCM was enhanced mainly to accommodate channel bandwidths of up to 100 MHz (contrary to the SCM suited for 5 MHz), referred to as SCM Extension (SCME) by the Wireless World initiative New Radio (WINNER) group [117]. It was adopted as an ideal test environment for 4G and beyond networks (such as LTE and LTE-A). In addition to the channel bandwidth enhancement, some improvements in the SCME include: extension of carrier frequency to 5 GHz, enhanced pathloss models, and time variant shadowing. The same group, formally named as WINNER II model, shortly developed a further extension of the SCME. This model is well suited for generic SLS models and is able to describe numerous propagation environments for single and multiple radio links for all the defined scenarios [118]. It was modelled to cover a vast amount of propagation scenarios that include: indoor office, large indoor hall, rural macrocell, urban macrocells, and bad-urban microcell amongst many. The channel model is antenna independent (i.e. it can accommodate different antenna patterns and configurations). Moreover, this model supports multi-antennas technologies, polarisation, multi-user, multi-cell, and MH networks. To reduce complexity, different scenarios were modelled using the same approach with difference in key parameters. The channel model has been justified for use in coordinated environments, relaying and MH schemes [119], which are aspects considered in this research, and hence, the channel model is adopted in the SLS for the purpose of the mentioned investigations.

$$PL = A\log_{10}(d) + B + C\log_{10}\left(\frac{f_c}{5.0}\right) + X \tag{3.13}$$

$$PL_{free} = 20\log_{10}(d) + 46.4 + 20\log_{10}\left(\frac{f_c}{5.0}\right) \quad (3.14)$$

where A is the fitting parameter which include the pathloss exponent, parameter B is the intercept, parameter C describes the pathloss frequency dependence, and X is an environment-specific term (e.g. wall attenuations) [119].

3.4 The LTE transmission modes

A key technology in the dramatic improvement of data rate increase in the 4G and subsequent 5G networks is the implementation of MIMO systems. The technology entails configuration of multiple antennas at the transmitter and/or receiver side to achieve diversity or spatial multiplexing in the spatial domain. This is an alternative to Single-Input Single-Output (SISO) transmission which requires a single antenna at both the transmitter and receiver, thus, exploiting only the time and frequency domain [120]. The transmission modes of the LTE network can be summarised into four main modes (from the 7 modes specified in LTE release 8): the SISO mode, Transmit Diversity (TxD), and then the spatial multiplexing modes i.e. open-loop spatial multiplexing (OLSM) and Closed-Loop Spatial Multiplexing (CLSM) [121]. Thus what follows is a brief summary of the transmission modes theory, which is then followed by simulation results evaluating their individual performance in the network.

While the SISO mode uses a single antenna with no diversity in the transmitted signals, TxD uses multiple antennas (usually 2 or 4) to transmit the same signals, using different coding and frequency resources, so as to overcome the limitations in a noisy propagation environment [121]. This is done to achieve better transmission reliability as the different transmitter paths or channels experience different fading/signal attenuation. Though this mode normally requires complete CSI at the

transmitter, it is also possible to implement it using space time block coding (STBC) [122] without the CSI. The use of STBC has been widely adopted as a means of reducing the complexity (especially at the UE side) compared to the use of array receivers to efficiently utilise the TxD transmission mode. A well renowned STBC is the Alamouti-type STBC [123], where the signals and their conjugates are transmitted in two time slots from the different antennas (assuming two transmitting and receiving antennas) i.e. [x_1, $-x_2^*$] and [x_2, x_1^*] respectively. The sequences from the antennas are orthogonal (as the inner product of the sequences amounts to zero) i.e. $x^1.x^2 = x_1x_2^* - x_2^*x_1 = 0$ [124]. The received signal over the two consecutive symbol period is represented by Equation (3.15) and (3.16), where $\boldsymbol{h}_{(1,2)}$ represents the channels, and $\boldsymbol{n}_{(1,2)}$ represents the noise [124]. Thus, STBC improves the data reception reliability without compromising the transmission rate (since two symbols are transmitted in two time slots accordingly): the rate differs in different scenarios depending on the antennas and coding schemes.

$$y_1 = h_1 x_1 + h_2 x_2 + n_1 \tag{3.15}$$

$$y_2 = -h_1 x_2^* + h_2 x_1^* + n_2 \tag{3.16}$$

The spatial multiplexing techniques on the other hand achieve spatial diversity by transmitting multiple independent streams from multiple antennas. The scheme can be represented as;

$$\mathbf{y} = \mathbf{W}\mathbf{x} \tag{3.17}$$

where $\mathbf{y}$ is the output vector, $\mathbf{W}$ is the precoding matrix, and $\mathbf{x}$ is the transmit/message signal matrix.

The length of the vector $\mathbf{x}$ represents the number of layers, which also indicates the total symbols transmitted over the different antennas simultaneously [125]. The precoding matrix maps the symbols to their respective transmit antenna. Thus with appropriate CSI from the UE, the eNB can choose the optimum Precoding Matrix Index (PMI) to maximise the system capacity. OLSM requires less UE feedback, as it does not need channel condition information at the transmitter side (such as PMI feedback), but only requires the rank indicator information (i.e. number of layers required/number of streams transmitted simultaneously). OLSM transmission mode also includes a cyclic diversity delay to avoid inter-symbol-interference: i.e. the signal is supplied to every antenna with a specific delay to achieve frequency diversity. Therefore, at a time instance *k*, the transmission of a vector $\mathbf{x}_k$ can be described as:

$$\mathbf{y}_k = \mathbf{W}\mathbf{D}_k\mathbf{U}\mathbf{x}_k \tag{3.18}$$

where $\mathbf{W}$ represents the precoding matrix selected from the predefined codebook (at both eNB and UE), matrix $\mathbf{D}_k$ and diagonal matrix $\mathbf{U}$ represent the cyclic delay diversity: Equations (3.19) and (3.20) show the matrices $\mathbf{D}_k$ and $\mathbf{U}$ for a 2-transmit antennas [126]: matrices for other number of antennas are provided in Appendix A.

$$\mathbf{U} = \frac{1}{\sqrt{2}}\begin{bmatrix} 1 & 1 \\ 1 & e^{-i2\pi/2} \end{bmatrix} \tag{3.19}$$

$$\mathbf{D}_k = \frac{1}{\sqrt{2}}\begin{bmatrix} 1 & 0 \\ 0 & e^{-i2\pi k/2} \end{bmatrix} \tag{3.20}$$

Similar to TxD mode using STBC, the OLSM mode is suitable where there is abrupt change in channel conditions (such as UE speed) or when channel information is lost [121]. Contrasting to OLSM transmission mode, the UEs signal a PMI in addition to the rank indicator in the CLSM transmission mode. In order to reduce the complexity

from the UEs signalling (i.e. PMI feedback), the matrix is chosen from a predefined codebook for the different antenna configurations (i.e. 2 or 4 transmit antennas) [126]. From Equation (3.17), the output vector $\mathbf{y}_k$ for CLSM mode can be written as:

$$\mathbf{y}_k = \mathbf{W}\mathbf{x}_k \tag{3.21}$$

3.4.1 Evaluation of the transmission modes with varying channel conditions

Recapitulating the different transmission modes, the SISO mode is very simple and does not require any processing in terms of diversity. Hence, the impacts of channel and propagation limitations are more severe in SISO transmission mode compared to the MIMO transmission modes. For the multiple antenna modes however, there is a trade-off in system complexity, as coding schemes and UE signalling are required (depending on the mode) to achieve the capacity enhancement. While the TxD mode performs reasonably well in highly noisy channels, a major limitation of the scheme is the redundancy involved in achieving the diversity. This limitation is improved to achieve better system capacity in the spatial multiplexing modes, which transmit independent streams from the different antennas. The CLSM mode generally performs better than OLSM as it receives UE feedback for the optimum precoding matrix to use for transmission, and therefore has more overheads. This is, however, reduced by a predefined set of precoding matrix so that the UE only feeds back an index of the appropriate precoding matrix from the table (available at both the UE and eNB).

Following the theoretical overview of the transmission modes, the performance of the different modes discussed is demonstrated in this section. Thus evaluation scenarios

were devised to analyse the modes in varying channel conditions. As earlier mentioned, a typical example of varying channel condition is an abrupt increase in UE speed [120, 121], hence, two scenarios were compared in the result; one scenario indicates UE modelled in a 'random walk' speed (5 km/h), while the other scenario represents a high speed UE (moving at 120 km/h). In order to compare the performance on an equivalent platform, the result from equal number of UEs (with same channel characteristics/conditions except UE speed) are simulated to achieve the performance metric, which is throughput in this case. The cell layout used to simulate the network for this performance analyses is shown in Figure 3-8.

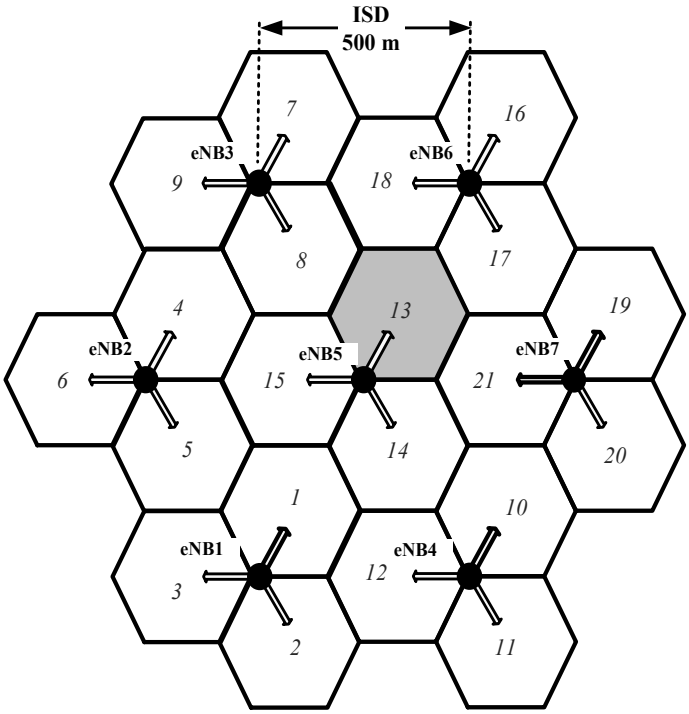

Figure 3-8 Cell-layout for the performance investigation, indicating the sector where simulation results were obtained

A single tier consisting of 7 sites (with 3 sectors each) was simulated: the layout represents a typical urban scenario with an ISD of 500 m. Each sector has 10 UEs,

and the performance metric of the UEs in sector 13 i.e. the target sector are represented in the following results. This is because the sector is in the middle of the layout, and receives interference from all surrounding eNB sites, thus avoiding optimistic results (specifically for UEs in the cells at the edge of the cell layout). Furthermore, the UE performance was averaged over 100 TTIs and aggregated to obtain accurate results for the throughput evaluation.

The CDF of the target sector's UEs throughput is shown in Figure 3-9. The UE throughput is represented using a CDF from 1000 samples (from 100 TTIs of the 10 UEs). A channel bandwidth of 5 MHz (only to run timely simulations) was used. Using the 50^{th} percentile (i.e. 0.5 on the y axis, which is the median of the distribution) as a point of reference, the SISO, TxD, OLSM, and CLSM throughputs are approximately 0.54, 0.63, 0.81, and 0.95 Mbps respectively at UE speed of 5 km/h. With higher UE speed however, the throughputs at the point of reference are 0.23, 0.43, 0.63, and 0.53 Mbps respectively. Matching the theoretical pre-eminence, the result shows a slight improvement at the 50^{th} percentile with the OLSM transmission mode (dashed black line), which is slightly better than the CLSM transmission mode (dashed blue line) at UE speed of 120 km/h with up to 60 kbps. The CLSM mode however performs significantly better with low speed UEs i.e. 5 km/h, which is due to the more detailed UE feedback obtained when using this mode. The graph shows approx. 190 kbps and 370 kbps improvement for the CLSM mode at 50^{th} percentile compared to the OLSM and TxD modes respectively (with UEs speed of 5 km/h).

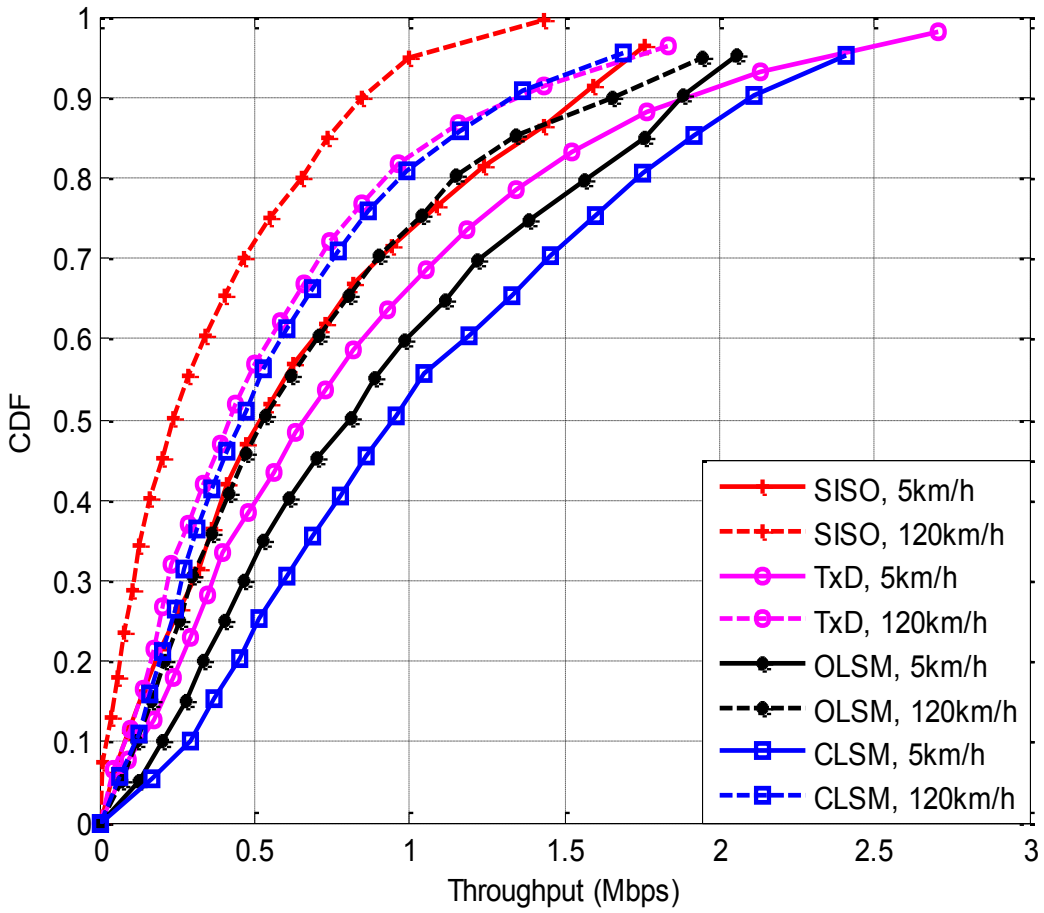

Figure 3-9 CDF of UE throughput in an LTE network with different UE speed for the SISO, TxD, OLSM and CLSM transmission modes

Thus, it can be concluded from the result that UEs achieve better throughput with consistent channel condition using the CLSM transmission mode, while the OLSM and TxD modes are more suitable for varying channel conditions (where UE speed was considered as a factor of the channel variation in this study). Thus, the CLSM transmission mode is used for further simulations in this thesis: this is because the UE movement is simulated based on a random walk in this model i.e. UE speed of 5 km/h.

3.5 LTE Resource allocation/scheduling algorithms

As described in Chapter 2 of the thesis, the LTE physical resources are represented as a time-frequency resource grid, which consists of a number of resource elements. These resources are allocated to UEs in the form of RBs, which is primarily dependent on the channel bandwidth, and then secondarily on the channel condition of the UE (according to the type of resource allocation scheme). Thus what follows in this section is a brief theoretical overview of the common resource allocation algorithms in LTE networks. This will be trailed by simulation results comparing the performance metrics of UEs using the different resource allocation algorithms in the network.

The RLC sits above the MAC sub-layer in the UE/eNB protocol stacks, where it works with the logical channels in the network entities to carry either control-plane or user-plane data [127]. Data is transferred between the MAC sub-layers in the network entities in the form of transport blocks via the DL-shared channel, which highly depends on the number RBs allocated to a UE and the MCS. The scheduler in the eNB's MAC sub-layer carries out the key task of allocating the resources. The scheduler allocates the resources for both DL and UL (depending on the scheduling algorithm). However, this research is focused on the DL aspect of the network, and hence concerted in this section.

Among the different resource scheduling algorithms proposed in literature, the most common ones used for scheduling in the LTE network include the Round Robin (RR), Best CQI (BCQI), and Proportional Fair (PF) schedulers [128]. The trade-off between the schedulers is based on the complexity of the algorithms (which differs for the

different schedulers). From the aforementioned scheduling algorithms, the RR scheduler is most widely used for performance evaluation and comparison due to its simplicity in implementation and uniformity in resource allocation [129]. As the name implies, it schedules the UEs equally in a 'round robin' fashion (one after the other). This, however, comes with a trade-off as UEs with very poor channel condition (usually UEs at the cell edge) are equally scheduled with UEs having very good channel conditions, resulting to lower throughput of the UEs and of the network in general. On the other extreme, the BCQI scheduler assigns resources to the UEs with the best radio link conditions. This is determined by the CQI feedback from the UEs to the eNB, which indicates their channel condition: UEs with higher CQI have better channel quality as described in the earlier part of this section [130]. Thus, this particular scheduler (BCQI) is specifically for achieving higher maximum throughput by scheduling UEs with the best CQI (usually UEs closer to the eNB), compromising on the fairness in scheduling UEs.

A compromise between the two extremes (i.e. simplicity and maximum network/UE throughput) is achieved by the PF schedulers [130]. Unlike the BCQI scheduler, the PF scheduler targets achieving a good UE throughput and at the same time provide fairness to UEs with poorer channel condition. While the schedulers described earlier (i.e. RR and BCQI) are concerned with individual UE or a set of UEs, the PF scheduler algorithm considers all the UEs over a certain period to make scheduling decisions. In this scheduling algorithm, the eNB firstly obtains the instantaneous CQI for each ***k*** UE in a time slot ***t*** in terms of requested data rate $R_{k,n}(t)$. It then keeps track of the moving average throughput $T_{k,n}(t)$ for each of the UEs on *n* RBs within a past window t_c length. Thus, the system latency is controlled by t_c: if t_c is large, it adopts

the BCQI algorithm, and then adopts the RR algorithm when the variable becomes small. The scheduler then gives priority to the UE k^* in the t^{th} time slot and RB n that satisfies the maximum relative channel condition [131].

$$k^* = \underset{k=1,2,\ldots}{\arg\max} \frac{\left[R_{k,n}(t)\right]^{\alpha}}{\left[T_{k,n}(t)\right]^{\beta}} \tag{3.22}$$

From Equation (3.22): if ($\alpha = 1,\ \beta = 1$), it denotes PF algorithm, if ($\alpha = 1,\ \beta = 0$), it then becomes BCQI algorithm, and if ($\alpha = 0,\ \beta = 1$), it denotes the RR scheduling algorithm. The eNB then continuously updates $T_{k,n}(t)$ of each UE in the t^{th} time slot using exponential moving average filter as described in Equation (3.23). Thus, the PF scheduling algorithm treats the RBs independently, updating them in each of the time slots [131].

$$T_{k,n}(t+1) = \begin{cases} \left(1 - \frac{1}{t_c}\right) T_{k,n}(t) + \frac{1}{t_c} R_{k,n}(t), k^* = k \\ \left(1 - \frac{1}{t_c}\right) T_{k,n}(t) \ldots\ldots\ldots\ldots\ldots\ldots, k^* \neq k \end{cases} \tag{3.23}$$

3.5.1 Evaluation of the common scheduling algorithms in the LTE network

Following the theoretical overview of the scheduling algorithms, the resulting performance disparity of the different schedulers is demonstrated in this section. The results are obtained by simulating an LTE network with the same cell layout in Figure 3-8. It represents a typical urban environment with 7 sites (500 m apart) having 3 sectors each, and simulation results are obtained from UEs in a central sector (sector 13, i.e. target sector) to ensure presence of adequate interference from neighbouring sites, hence achieving realistic results. The network was simulated using a 5 MHz bandwidth channel in the CLSM transmission mode: the UEs are modelled for

random walk, hence, the transmission mode is suitable for the performance analyses as demonstrated in Section 3.4.1. The throughput distribution of UEs in the target sector with the different schedulers is shown in Figure 3-10.

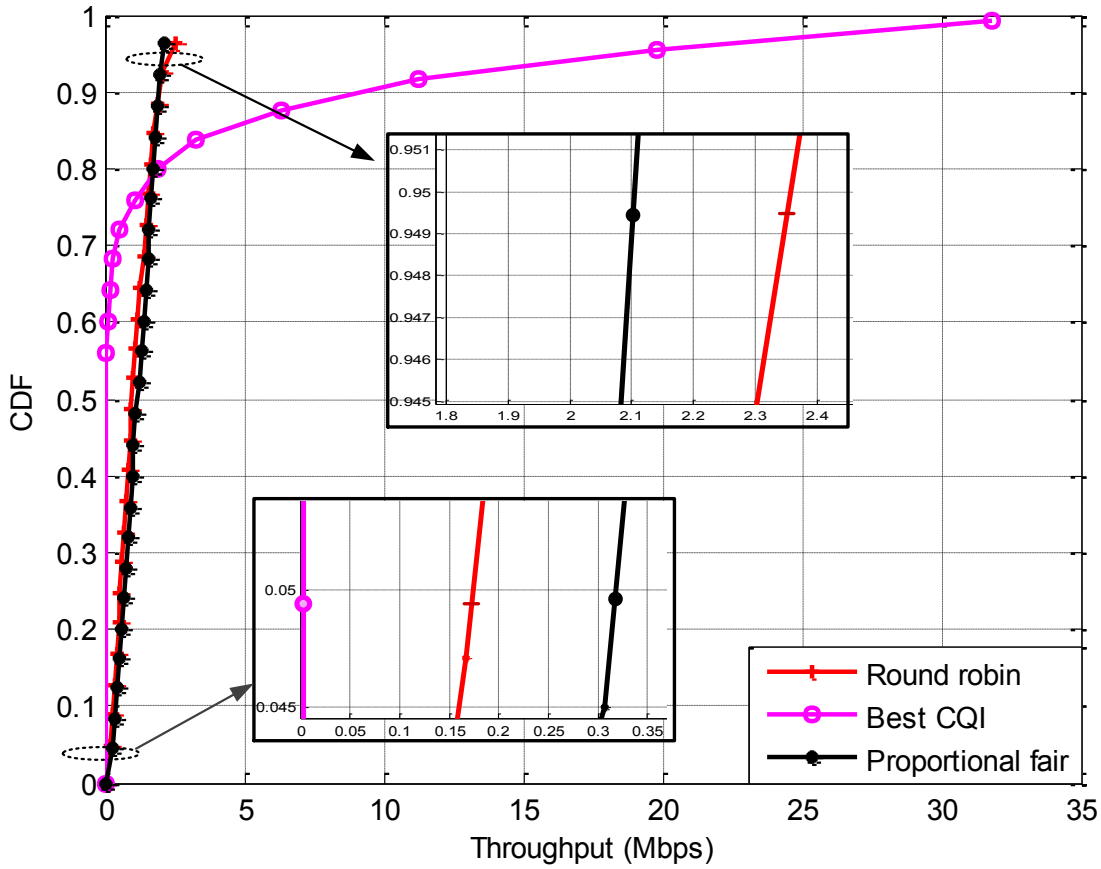

Figure 3-10 Throughput CDF with different schedulers for UEs in target sector

The UE throughput distribution is compared using a CDF in this result for the three scheduling algorithms discussed in this section i.e. RR, BCQI, and PF. For each of the distributions, a total of 1000 UE throughput samples are represented. This is obtained from an aggregate of 10 UEs in the target sector for a total of 100 TTIs. The 95th percentile and cell edge (i.e. 5th percentile) are used as reference points to compare the performance of the different scheduling algorithms. The 95th percentile indicates the best achievable throughput for UEs in the network, signifying UEs closest to the eNBs or having the best channel quality, while the 5th percentile indicates the vice

versa in the CDF. The points of reference are zoomed and included in the result to clearly show the difference in performance at the reference points.

As described earlier, the BCQI scheduler only allocates RBs to the UEs with the best channel conditions. Hence as expected, the UEs throughput is extremely high, up to 19.1 Mbps at the 95^{th} percentile of the distribution, relative to the throughput of the compared scheduling algorithms. For the RR and PF schedulers, the UEs throughputs in the CDF are approximately 2.4 and 2.1 Mbps respectively at the point of reference (i.e. 95^{th} percentile). At the cell edge of the distribution however (i.e. 5^{th} percentile), the BCQI scheduler has a throughput of 0 bps, while the RR and the PF schedulers have 180 kbps and 320 kbps respectively. It can be seen in the result that the PF scheduler performs better at the cell edge, while the RR scheduler performs alternatively better at the 95^{th} percentile. This is because the PF scheduler targets achieving a good throughput, at the same time giving fairness to the cell edge UEs in the network as earlier indicated in Equation (3.22). Thus a balance between serving UEs with best CQI and ensuring acceptable level of performance for cell edge UEs is achieved with varying conditions of α and β variables in the equation (Equation 3.23). The RR scheduler on the other hand is focused on simplicity in implementation for scheduling UEs in the network, regardless of the channel quality i.e. it schedules all UEs equally regardless of their CQI. Hence, UE performance is slightly worse at the cell edge compared to the PF scheduler, but equally significantly better than the BCQI UE performance at the cell edge.

Despite the slightly inferior cell edge throughput achieved using the RR scheduler (relative to PF), it is however commonly used for evaluating system-level UE

performance in cellular network simulators as a "control" or baseline scheduling algorithm [132]. This is because it equally schedules all the UEs on the resource grid of a serving eNB, hence ensuring that the performance metric of all possible positions in the evaluated cell is accounted for in the result. This is particularly of interest for the analyses in this thesis as the UEs are distributed uniformly in the developed SLS, and multiple iterations are run and averaged to ensure that all possible positions (within a cell/sector region) are reflected in the result. Additionally, the use of RR scheduler provides the minimum performance at the cell edge of the cellular network. Thus the RR scheduler is henceforth used for the performance evaluations in this thesis as it has similar performance outcome with the ideal PF scheduler, and results from proposed algorithms in this research can be directly compared with other works in literature (since the scheduler is commonly used as a baseline in literature).

3.6 Analysis of cell edge UE performance in LTE networks

One of the developments in LTE networks is the universal frequency reuse property (reuse factor of 1). Thus the same spectrum is used in all sites/sectors of the network, which generally increases network coverage and system capacity [133]. Though the universal reuse factor has its advantages as earlier mentioned, this leads to degradation of cell edge UE performance, mainly due to incurred inter-cell interference. This is in addition to other limiting factors such as propagation distance and fading. In this section, UEs performance is evaluated using the throughput metric for different LTE channel bandwidths. This study is carried out to analyse the cell edge UE performance relative to UEs closer to the eNB or with better channel conditions, and to also illustrate the data rates when using different LTE bandwidth channels. The cell layout for the performance evaluation is shown in Figure 3-11.

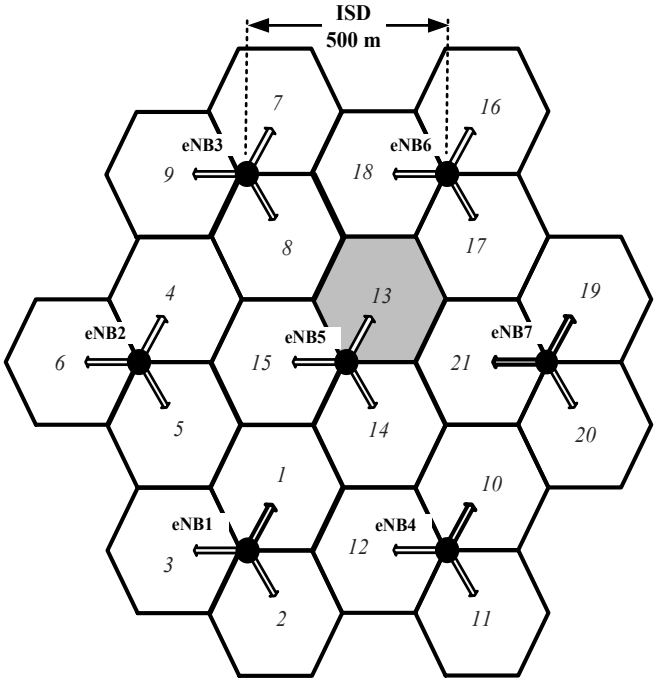

Figure 3-11 Cell layout showing the different sites surrounding the target sector

The cell layout represents a typical urban environment with 7 sites (500 m apart) having 3 sectors each. Similar to the simulation methodology of the previous performance evaluations in this Chapter, the UE metric is obtained from the central sector (sector 13, i.e. target sector) to ensure presence of adequate interference from neighbouring sites and achieve accurate results. The network was simulated using the CLSM transmission mode and the RR scheduler with three different LTE channel bandwidths i.e. 5 MHz, 10 MHz and 20 MHz. The eNB TX power is 43 dBm and the WINNER II channel model was used for the simulation. A total of 105 iterations are run and a CDF of the target sector UEs throughput is categorised into the 5^{th}, 50^{th}, and 95^{th} percentile, which commonly represents the cell edge throughput, median throughput, and best UE throughput (usually UEs closer to the eNB) respectively in a cellular network. Results for the different bandwidths are shown in Figure 3-12, Figure 3-13, and Figure 3-14.

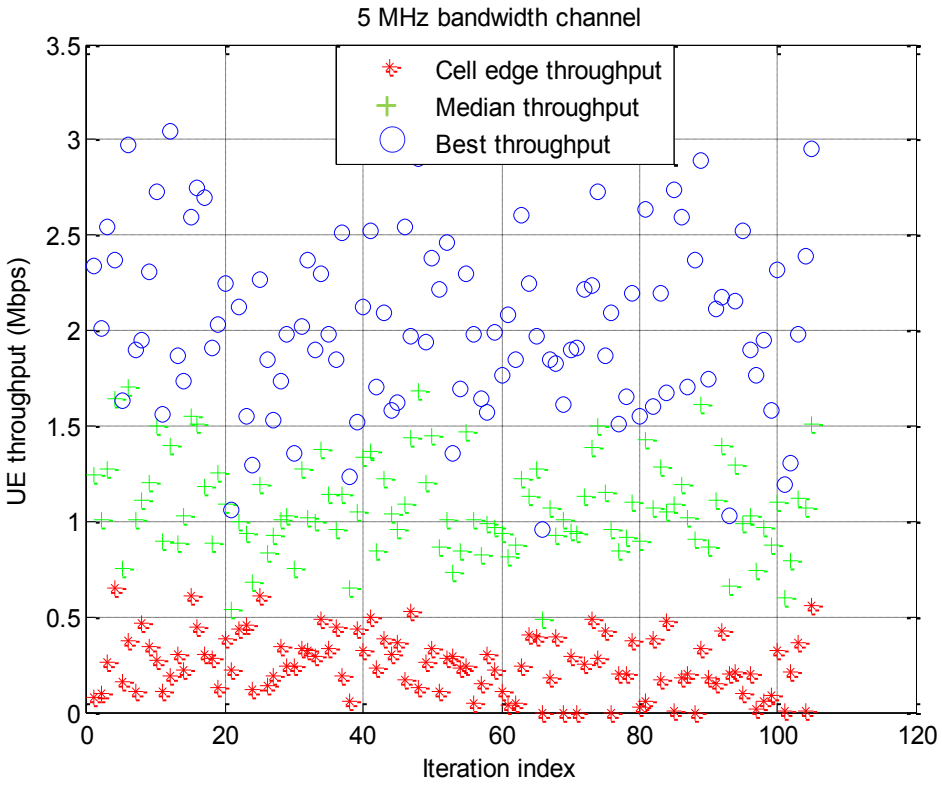

Figure 3-12 UE throughput for a 5 MHz bandwidth channel

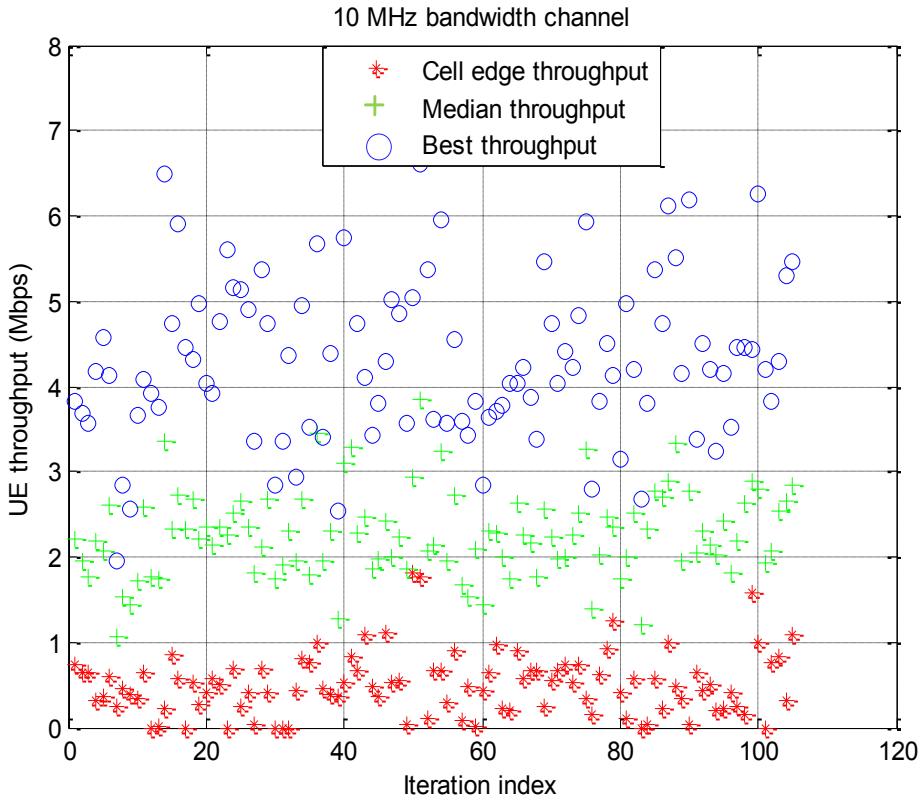

Figure 3-13 UE throughput for a 10 MHz bandwidth channel

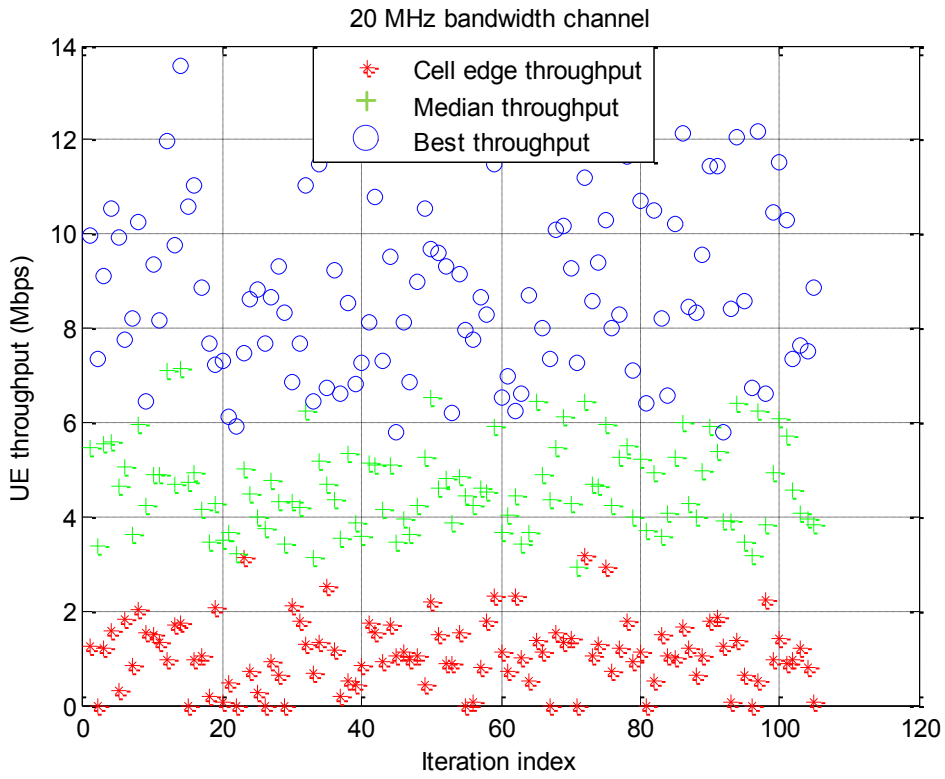

Figure 3-14 UE throughput for a 20 MHz bandwidth channel

In the graphs, the cell edge throughput is indicated by an asterisk marker, the median throughput is indicated by a plus marker, and the best UE throughput is indicated by a circle marker. The graphs demonstrate the vast difference in throughput achieved between cell edge UEs and the best UEs for each of the iterations. The difference between the cell edge UE throughput and the best UE throughput is approximately 1.8 Mbps, 3.8 Mbps and 7.7 Mbps for the 5 MHz, 10 MHz, and 20 MHz bandwidths respectively. It can also be established from the figures that the UEs achievable throughput indicates a unit step for the increasing bandwidths. As an example, taking the median values from the graphs, the throughputs are on average 1.1 Mbps, 2.3 Mbps and 4.6 Mbps for 5 MHz, 10 MHz and 20 MHz bandwidths respectively. As a result, further evaluations in this thesis are carried using one of the bandwidth channels (mostly 5 MHz) as the simulation run time increases with higher bandwidth.

3.7 Novel enhancement to existing state-of-the-art LTE SLS

The preceding sections of this chapter have demonstrated in detail the specifications, and implementation methodology of a state-of-the-art DL SLS used as the benchmark simulation model in this research (the SLS can be found in [105]). An overview of the background functionalities was also included followed by a selective performance evaluation to corroborate the key SLS features including the test environments (e.g. Urban), the channel models adopted (e.g. WINNER channel model) and scheduling algorithms, amongst other features. While the presented SLS is the most complete and highly sufficient simulator available for fundamental LTE network evaluation, it requires the introduction and development of original features and functionalities in order to comprehensively investigate and evaluate advanced 4G networks (e.g. LTE-A) and in extension the envisioned, beyond-the-state-of-the-art 5G technologies. These include novel inter-cell coordination algorithms beyond the current CoMP, D2D communication modelling and algorithms and multihop transmission. Hence, this section highlights some of the main enhancements included in the SLS for the purpose of this research.

The SLS enhancements are summarised in Table 3-3. The benchmark model is first of all de-cluttered by discarding some parameters (such as pathloss map for the ROI, shadow fading map etc.) and ambiguous results, which are normally stored in the memory cache during simulation. This significantly reduces overheads and increases the simulation speed. As such, the method of acquiring UE performance metrics was easily advanced from the norm of aggregating UE performance over some TTIs, to taking the average over multiple iterations i.e. drops (each drop contains an average metric over several TTIs). This further validates the results as the UE metrics is

averaged over a significant quantity of aggregates for consistency. Additionally, UEs distribution is reset in each of the iterations, therefore leading to the UEs covering more geographical locations in their respective cells, hence obtaining UE performance for diverse environments during the simulation.

Table 3-3 Description of some major enhancements to the existing SLS

Functionality	Framework simulator	New SLS developed in this thesis	Remarks
Wrap around interference modelling	Not included	Introduced	Interference to border cells is modelled based on a new algorithm proposed in Chapter 4. The innovation allows a smaller map (just one tier) to be sufficient for simulation, reducing the overheads from pathloss modelling amongst other requirements for a larger map (e.g. two or more tiers)
UE relocation	Random	Handover	In the event of a UE moving outside the ROI in a TTI during simulation, it is handed over to the adjacent cell based on a new wrap around schematic
CoMP Capability	Not available	Introduced	Adjacent cells can coordinate transmission/ beam forming to mitigate interference on cell edge UEs based on a new algorithm implemented in Chapter 4.
Dual mode UE operation	Not modelled	New model introduced	UEs in the simulator can function as cellular UEs or D2D TXs/RXs. Additionally idle UEs can be selected as relays for multihop transmission (novelty of Chapter 5)
Obtaining UE performance metrics	Aggregate over multiple TTIs	Aggregate over multiple iterations	Several iterations are run (with multiple TTIs each), so as to obtain more accurate results, and account for UE performance in different environment

A significant limitation of the benchmark SLS is the absence of interference among UEs in the edge cells/borders cells, hence not fully exploring edge cell interference. This is accordingly compensated for in the preceding evaluation results by both creating a two-tier map (as shown in Figure 3-6) and only taking the metric of UEs in the first tier, and simulating one tier and considering only the central sectors. The creation of larger maps (two-tier map described above) however require extreme overheads as information such as distance metric and pathloss between each UE to its eNB (amongst other features) are required for the whole ROI. In addition the performance metric is only taken from a few sectors. Thus, an original interference modelling technique is proposed (in Chapter 4), allowing the logging of performance metric for all UEs in the ROI (using a smaller map) during simulation, and eliminating the border effect. Consequently, mobile UEs exiting the border cells in one TTI are conveyed to their transit cells in accordance to the schematic of the interference modelling architecture proposed.

Another unique novelty described in this thesis is the modelling of UEs with D2D communication capabilities. This imposes a challenge by means of the need of unique functions able to implement new antenna modelling, new scheduling (when UEs are D2D TXs) and mode selection (UEs can select cellular or D2D transmission mode) etc. Thus, a UE (D2D TX) can transmit to other UE/UEs (D2D RX/RXs) when in D2D mode (a feature not available in the existing platform). Details of the modelling and performance evaluation are provided in Chapter 5. Significantly a further development in the presented work provides the introduction, of multihop transmission as will be also described in Chapter 5. Quite importantly for 5G network applications, idle UEs (UEs not transmitting or receiving) can be selected as relays,

able to transport traffic between a sending and receiving node when required in congested network scenarios.

3.8 Summary

In this chapter, a comprehensive implementation of the LTE SLS used for the purposes of this research investigation was presented. A rare state-of-the-art DL LTE SLS provided by University of Vienna was used as a benchmark for the model devised in this thesis. Thus the detailed implementation of the benchmark SLS and selected performance evaluation of the LTE network features were presented. Additionally, a detailed summary of the major enhancements to the existing SLS was also provided.

There are numerous functionalities that need to be simulated in just a single communication link (between an eNB and a UE), and hence would take excessive simulation time and parameters to depict the process in a single simulation model. This becomes even more complex when implementing SLSs, which involve various network entities (several eNBs and UEs) and would require a more robust platform and computational time in days to simulate a large network. Abstracting the link-level functionalities of the network entities to obtain a metric, which can then be included to achieve the system-level performance of a network, solves this. A common method of achieving this objective is by implementing the models using LQM and LPM as described for the design of the simulation model in the chapter. Specifically, the post-equalisation SINR in this platform was mapped to CQI to achieve a BLER probability of less than 0.1, and subsequently obtain the throughput metric for the system-level performance.

The network layout of the SLS for the research investigation represents a typical macrocell environment using hexagonal grids to characterise the sectors in the network as commonly used in simulation platforms. The antenna gain pattern of the individual sectors was equally illustrated in Section 3.3 of this chapter. Another key element of the SLS is the implementation of a comprehensive channel model, which could accurately but concisely abstract the different propagation models for the network evaluations. The detailed summaries of commonly used channel models for simulation platforms were also presented in the chapter, identifying the WINNER II channel model for implementation in this work. This is mainly due to the vast test environments in the model, which include: indoor office, large indoor hall, rural macrocell, urban macrocells, and bad-urban microcell amongst many. It also includes various multiple antenna configurations and is well suited for higher channel bandwidth modelling (appropriate for 4G and beyond networks with channel bandwidth of up to 100 MHz).

The transmission modes of the LTE network were analysed using the SLS. While the SISO mode has no diversity (as it uses single antenna for transmission), the multiple antenna transmission modes (i.e. TxD, OLSM and CLSM) achieve diversity in the spatial domain. The CLSM mode however incites better performance at a steady channel condition as shown in Figure 3-9: this is because in addition to increasing the transmission rate (by transmitting different streams from multiple antennas), it also includes adaptive transmission based on PMI feedback from the UE. The TxD and OLSM transmission modes however perform particularly well with fast varying channel conditions (as they don't require any UE feedback) as shown in Figure 3-9 for UE speed of up to 120 km/h.

Additionally, the different resource allocation algorithms in the SLS were analysed. The most commonly used scheduling algorithm is the RR scheduler, due to its simplicity (as it allocates resources to the UEs one after the other). Another algorithm discussed was the BCQI scheduler, which only schedules UEs with the best CQI. A balance between the schedulers is implemented in the PF scheduler, which on the other hand allocates RBs to the UEs based on the resource usage rate/transmission for a certain period of time, and hence is most appropriate for multiuser resource allocation. The performance of the scheduling algorithms was equally compared using the throughput metric of UEs in the network. The result clearly indicates the biased resource allocation with the BCQI scheduling algorithm towards the UEs with good channel condition, indicated by the significant throughput gain at the higher end of the distribution and extremely poor throughput at the lower end (typically representing UEs closer to the cell edge). The RR and PF schedulers however indicate a similar distribution of the UE throughputs, with the PF scheduler marginally performing better at the cell edge of the network. Furthermore, the performance disparity between cell edge UEs and UEs closest to the eNB in the LTE network was analysed. The study also presented the achievable throughputs with different channel bandwidths in the LTE network.

One limitation of the SLS however is the absence of proper interference modelling for the sites/sectors at the border of the cell layout. This leads to optimistic results achieved by UEs in the border cells, thereby, affecting the accuracy in the results obtained from the simulator. Thus to achieve accurate results in this chapter, the problem was eliminated by creating larger maps (i.e. increasing the ROI) and discarding results from the border cells as described in Section 3.3.1 of this chapter.

This however requires additional complexity and significant additional time to obtain few results. Hence, the following chapter presents a proposed method of eliminating the border effect, which provides realistic result and UE mobility in the simulator. The enhanced model is then used to implement a CoMP algorithm to improve the cell edge UE performance in the following chapter.

Chapter 4

Inter-Cell/Site Interference Modelling and CoMP for 4G and Beyond Networks

4.1 Introduction

Within the paucity of available system-level simulation models, a common existing limitation is the optimistic performance metrics retrieved from User Equipment (UEs) located in the cells/sectors at the edge of the cell layout (referred to as border cells or edge cells in this thesis). This inhibits the inclusion of key technologies such as Coordinated Multipoint (CoMP) algorithms and also effective handover execution in the models. Some algorithms, which vary in implementation in terms of complexity/overheads, simulation time, etc., have been proposed in literature to eliminate the border cell effect using a general approach referred to as wrap-around (WA). In this direction, this chapter proposes a new algorithm/architecture of eliminating border cell effects using the WA approach.

While traditional WA approach eliminates border cell effect by reconstruction of the maps to form a toroid shape, the proposed architecture is an enhancement of the common approach as it does not require distortion of simulator topologies, and hence is compatible with any flat surfaced maps and cell planning tools. The proposed algorithm entails inclusion of corresponding virtual eNBs (VeNBs) at the border cells without extending (or distorting) the cell layout, which normally requires expanding the shadow fading map amongst other complex functions: pathloss/fading matrices

and UEs are not included in the virtual eNBs. The term VeNBs is used in this context because while actual eNBs are not modelled to encompass the border cells, attributes which contribute to UE interference (such as signalling) are included to calculate the SINR of UEs at the border cells. To further reduce the system complexity/overheads, the VeNBs are uniquely introduced only during interference calculation in the proposed algorithm, and UEs are modelled to transit to corresponding border cells according to the schematic in the implementation. The proposed architecture is simulated and results are presented to conform between the performance metric of UEs in the border cells to the central cells in a one-tier cell layout. The central cells are used as test factor since the UEs within experience adequate interference, hence achieve realistic performance. Simulation results are also provided in the chapter to demonstrate the efficiency of the proposed algorithm in terms of simulation run time, and increase in quantity of UE performance metric logged relative to traditional models.

The work in this chapter has been extended further by implementing a proposed CoMP algorithm based on CoBF (i.e. Coordinated Beamforming). In the proposed algorithm, the adaptive beamforming technique is employed so as to steer antenna beams of neighbouring eNBs in the event where UEs served at the same time (by the different eNBs) are situated/located in a common cell border of the neighbouring cells. The proposed algorithm was simulated in the model, and results are presented in the chapter to show the performance improvement in terms of SINR and goodput (i.e. net throughput) of the cell edge UEs compared to traditional transmission scenarios (without any cell or site coordination/CoMP). The implementation of the proposed algorithms and simulation results are preceded with theoretical overview of the

technologies/algorithms (i.e. WA and CoBF) and their comparison with current related research work in the respective schemes.

4.2 Challenges in 4G+ networks simulation platforms

A major requirement of System-Level Simulator (SLS) platforms is to effectively emulate complex cellular topologies such as the 4G LTE/LTE-A [134] networks with all the supporting features as close as possible to real-case deployment scenarios, so as to considerably reduce CAPEX and OPEX in the network development. As described in the preceding part of the thesis (Chapter 3), the conventional manner of simulating such complex topologies is to implement a two-tier network (with a total of 57 sectors and 19 sites) and subsequently evaluate the performance of UEs from the inner tier [105] (i.e. first tier, with 21 sectors and 7 sites) as shown in Figure 4-1: for clarity in description, the two-tiers in the cell layout are distinguished by shaded and un-shaded sectors for the first tier and the second tier respectively.

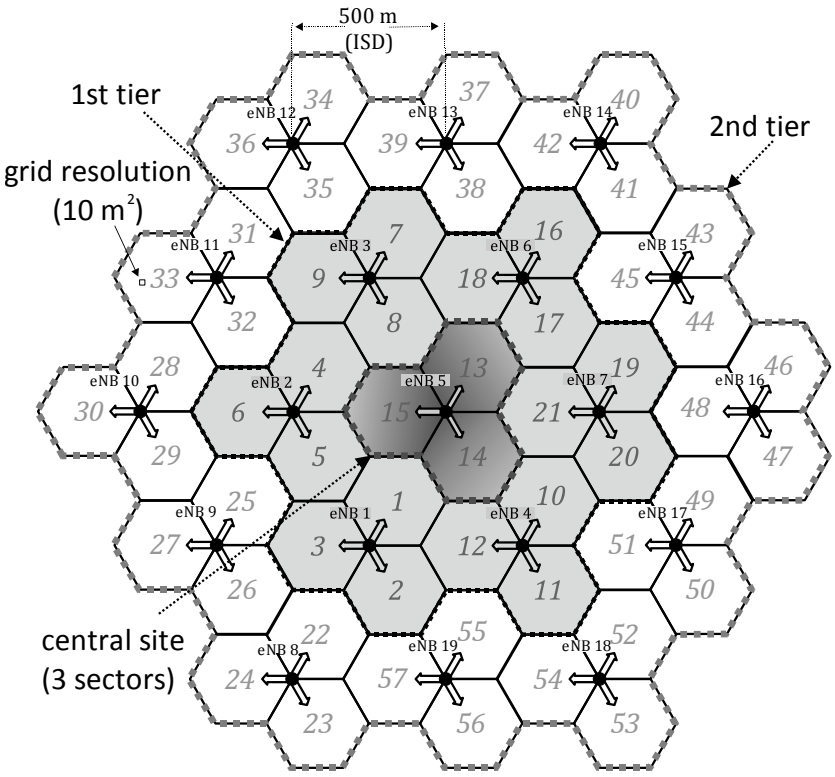

Figure 4-1 Typical SLS topology comprising two tiers, 19 sites and 57 sectors

For example when two tiers are simulated with 10 UEs per sector, a total of 360 UE performance results is discarded: i.e. only performance results of the UEs in the 21 sectors of the first tier (shaded cells in Figure 4-1) are logged. This is because the outer sites usually provide overoptimistic performance (such as goodput), due to the absence of proper interference modelling. Alternatively, only one tier is simulated and the central site is accounted for the evaluation of performance while the 6 remaining sites are again discarded. It is evident that due to the plethora of parameters that need to be accurately modelled, such approaches are impeded due to the computational expense that arises from the nested iterations that represent multiple users. An example using the two-tier layout is when obtaining a distance metric (required for pathloss and other distance dependent modelling in the simulator) and signalling overhead from eNBs signalling for 570 UEs is generated, while only 210 UEs result is actually utilised.

Additionally in single-tier simulations, advanced features of LTE-A such as CoMP [54] and handover cannot be simulated reliably. An example is a UE transiting outwards from sector 33 (in Figure 4-1), which needs to be handed over to an adjacent site/sector. As a result of the above, it is necessary to develop a platform that will effectively eliminate the interference modelling limitation (by eradicating the border cell deficiencies) without wasting computational power and resources. The most popular approach for this purpose is termed wrap-around (WA) [135, 136].

4.2.1 Traditional wrap-around modelling implementation

The WA modelling concept has been widely adopted as a viable means of achieving simulation efficiency with SLS platforms. Taking into consideration that topologies in WA approaches vary, the main concept thereof is a number of sectors shaped in a

toroid as proposed in [135]. In this particular topology, a regular flat surfaced map is formed as a rhombus, which consists of a set of cells (up to 25 in this example) as shown in Figure 4-2 (a). The top and bottom of the rhombus layout is then attached together (firstly joining the horizontal ends, then the vertical sides) to form a torus as illustrated in Figure 4-2 (b). Therefore each of the cells in the architecture is surrounded by neighbouring cells, hence allowing mobile UEs to transits across the cells without any boundary.

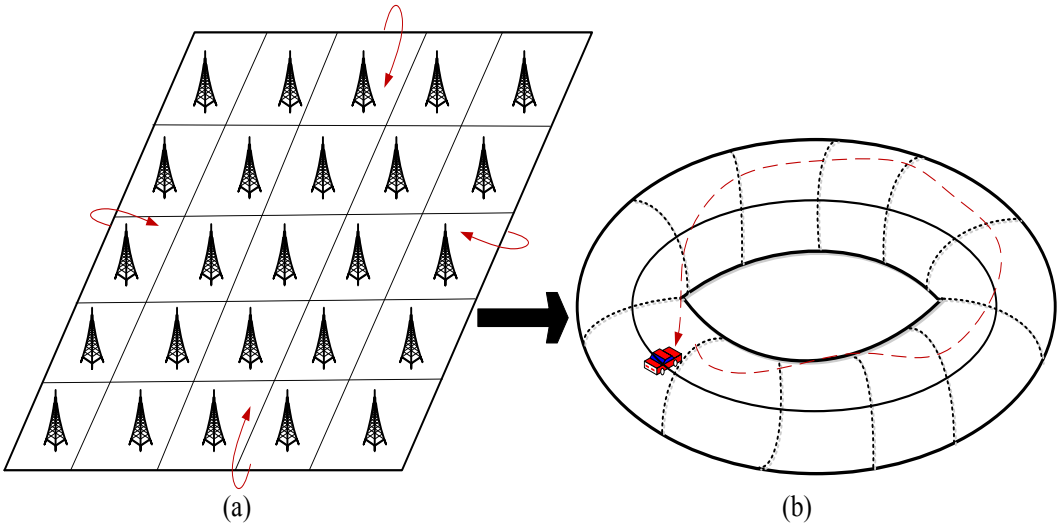

Figure 4-2 Illustration of a typical WA implementation [135]

4.3 Efficient interference modelling for 4G+ networks

Although the concept of the toroid-shaped wrap-around seems like a viable solution, it does not allow for the use of real path-loss maps from network planning tools, such as Capesso [137, 138]. As the capability of using network planning is a very sought-after feature, several approaches use a 'flat' surface topology [104, 139, 140], similar to the model for this research investigation. Therefore, in these simulators, WA is not possible without major restructure and loss of the aforementioned network planning capabilities. Motivated by this apparent dead end, a novel method for modelling interference across all the sectors of a one-tier network topology is proposed [141].

One of the main advantages of the proposed approach is that, although it presents conceptual similarities with WA approaches, it allows for use with limited resources and can be implemented as an extension to any 'flat-surfaced' SLS platform.

The technique proposed here involves the creation of just one tier of sites, and the inclusion of virtual eNBs (VeNBs) in the same positions as they would appear on the second tier, only during the phase of calculation of interference. In this process, all features of the eNBs are replicated (such as antenna configuration, azimuth, etc.) to their respective positions outside the first tier. As expected, this process does not create additional overheads on the complexity of the system. Figure 4-3 shows the configuration of the proposed scheme, where VeNBs represent the replicated eNBs that are introduced during the calculation of interference.

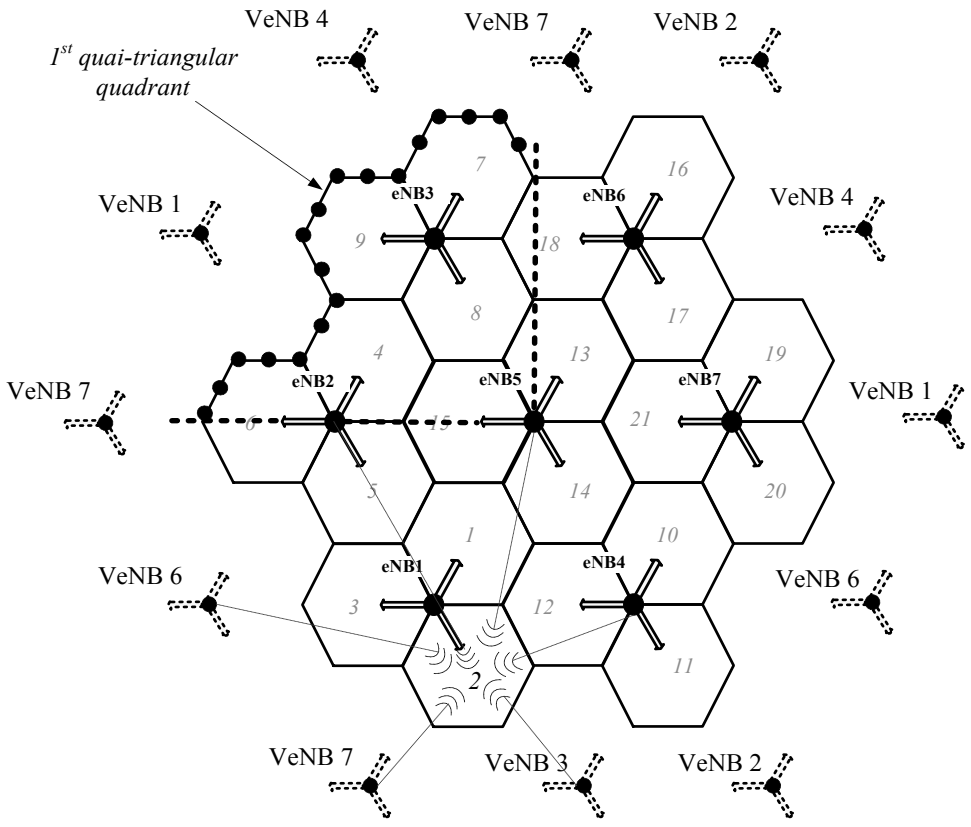

Figure 4-3 Proposed cell layout with VeNBs and quadrant in the ROI

The topology of the simulation platform described in Chapter 3 was used, which meets the LTE-A standard definitions [142]. However, this technique can be applied to any flat-surfaced topology. It can be seen that all the outer sites have been properly provided with 6 equidistantly positioned neighbouring eNBs (similar to the central site).

Taking Sector 2 as an example from Figure 4-3, the complementing eNBs are 6, 7, and 3 (represented as VeNBs with the same numbering since they are copies of their respective 'real' counterparts), in addition to the existing surrounding sites (i.e. 2, 4, and 5). This compensates for the lack of a full set of enclosing eNB neighbours, and therefore allows results to be taken from all the sites rather than only from the central site. It should be noted that, in the proposed technique, the shadow fading map is not expanded and therefore additional calculations for the space correlated fading or additional UEs are not required. Another major advantage of the proposed technique is that it doesn't distort the topology of the flat surfaced maps (which requires additional complex processing) as shown in Figure 4-2, allowing it to retain its compatibility with real maps like Capesso [138]. Additionally, the proposed scheme is computationally efficient and reduces variation amongst eNB models compared with the two-tier approach across the ROI (which—in some cases—is considered beneficial). This is because all 7 sites seen in Figure 4-3 not only have the same number of neighbours, but also in most cases the exact same eNB replicas. The technique adheres to the concept of WA, as outer sites are 'enclosed' by their complementing VeNBs, and it is envisaged that such an approach can extend any configuration of sites/sectors, without extending the Region of Interest (ROI).

Furthermore, as WA techniques usually do not impose geographical limits on the 'random walk' of UEs this is also accounted in the proposed architecture. Thus, UEs in the cellular network are handed over from a parent eNB to a new parent eNB according to the direction of transit. In the proposed approach, the ROI is divided into four quasi-triangular quadrants (as illustrated in Figure 4-3), and their intersection is the centre of symmetry. In the case where a UE leaves outside the quadrant at the end of one TTI, it is handed over to the symmetric counterpart of its last location in the next TTI (described in Appendix B). This is an additional enhancement to SLS platforms such as [103, 104], where UEs are relocated to random positions in the ROI in the event of the aforementioned circumstance.

4.3.1 Performance evaluation of proposed interference modelling

A set of simulations have been performed in order to assess the performance of the proposed approach. For this purpose, the new proposed architecture is used to extend the MATLAB SLS platform described in Chapter 3. To that extent, the focus lies on investigating whether the modelling of interference in the outer sectors is similar to that of the central sectors. In addition, the computational efficiency of the one-tier WA system is compared with the conventional non-WA simulation. The cell layout for the simulation set up emulates a typical urban environment with multiple sites (7 in this case) which are 500 m apart, with each site having 3 sectors. Equal number of UEs are distributed in all the sectors (10 UE per sector), to establish an even load between the eNBs in the performance evaluation. The Proportional Fair (PF) and Round Robin (RR) schedulers are used to compare the results, where varying number of multiple iterations are run to achieve equal samples for performance comparison. A detailed summary of the simulation parameters are presented in Table 4-1.

Table 4-1 A detailed summary of simulation parameters

Parameter	Value
Network Layout	7 eNBs, 3 sectors/eNB site, ISD 500m
Link adaptation	Adaptive modulation and coding supported
UE parameters	10 per sector, 5 km/h, 3 TTIs feedback delay
UEs distribution	Homogenous; pre-set positions
UE noise	Thermal noise density: -174 dBm/Hz, noise figure: 9dB
Channel model	Urban, Winner II type
Shadow fading	Log-normal, space correlated, zero mean, σ=10 dB
Frequency (GHz)	2 (with frequency reuse of 1)
Bandwidth (MHz)	5
Transmission modes	CLSM, 2 TX and 2 RX, maximum of 2 streams
eNB parameters	20 m height, 15 dBi gain, TX power: 43 dBm
Schedulers	RR; PF
Number of iterations	100; 294; 42

Traditionally, in SLS platforms, there are several degrees of freedom during the simulation. For example, the shadow fading map is produced using a lognormal space-correlated function, the UEs movement is simulated based on 'random walk' models and their positions are picked in a uniform fashion across each sector. The increase of the entropy in the aforementioned is needed in order to closely approach 'real-life' situations and take into account different environments. The approach in such platforms is to run multiple iterations/drops and aggregate the UE performance results, taking, thus, an average over different simulated environments [101].

Nonetheless, this approach poses a significant challenge, especially when the target of the simulation is a direct comparison between different systems. One way of reducing the performance fluctuation in the multiple iterations is to use the same shadow fading map during all the iterations. Using the same map reduces one degree of freedom making a direct comparison more accurate; however, a particular consideration in terms of systems comparison regards the random positioning of the UEs. In a network layout with ISD of 500 m (and regular 166.667 m hexagonal sectors), the area of each sector is approximately 7217 m^2. For a map resolution of 10 m^2, this is equal to 722 UE possible positions. Even after 200 iterations with 10 UEs per sector, the expectation value of positions not accounted for is $1999^{722} / 2000^{721} \approx 45$ [143]. In other words, an area of 450 m^2 of each sector is not evaluated while other areas are included multiple times in the aggregated performance and—as a result—the evaluated goodput is skewed. It should also be noted that the above expectation value takes into account a perfectly uniform random function. Unfortunately, computer-assisted simulators typically use pseudorandom number generators, which can significantly increase the expectation of non-accounted positions and degrade the accuracy of the simulated performance.

To circumvent the above problem, for the first set of simulations presented here, a set of 100 iterations comprising pre-determined UE positions is devised using rejection sampling [144]. The restrictive condition in this case is $R \leq [N / M]$, where R is the maximum number of sample repetitions, M is the number of observations and N is the length of the set (i.e. the possible positions of the UEs). The predetermined positions are used in conjunction with the same shadow fading map and the RR scheduler in order to study two specific sectors of the topology that represents different scenarios

with regards to interference modelling. Shown in Figure 4-3, these are sectors 5 and 2. In Sector 13, no WA is needed as the sector belongs to an eNB that is surrounded by 6 neighbours and is therefore used as a reference (i.e. control) sector in the evaluation methodology. On the other hand, Sector 2 provides the most optimistic results as it is in the edge of the ROI. As mentioned in the introduction, the case of Sector 5 is also studied, as it is adjacent. These sectors are evaluated in terms of SINR in Figure 4-4 and goodput performance in Figure 4-6 and Figure 4-5.

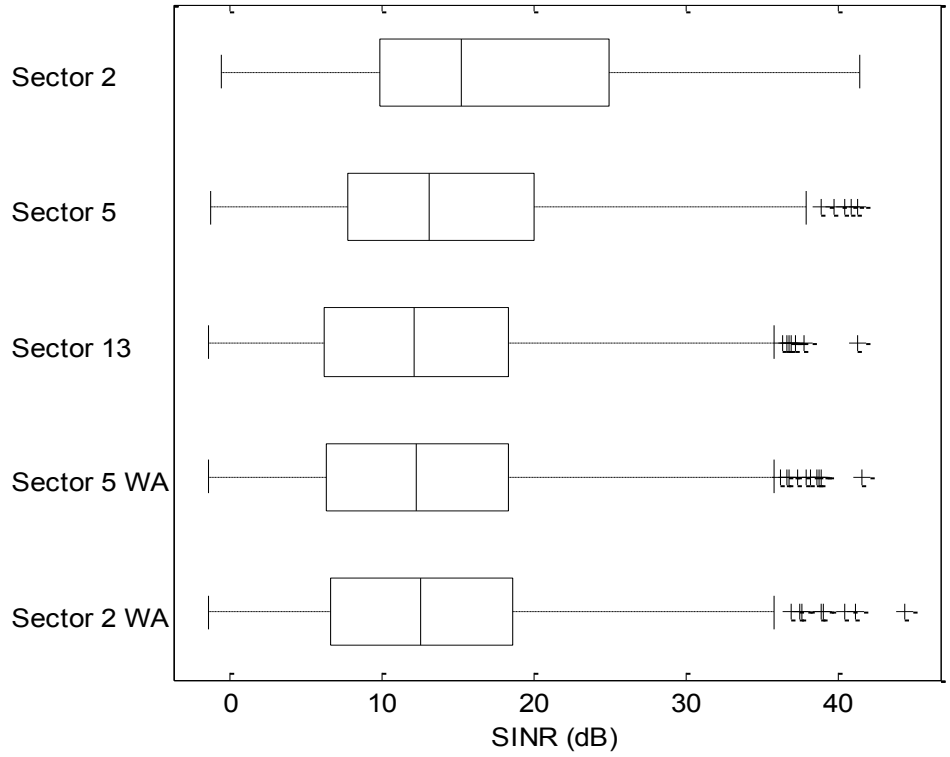

Figure 4-4 Boxplot showing the SINR of UEs in the investigated sectors

The SINR of the UEs in the investigated sectors is represented using a boxplot in Figure 4-4: values are averaged for each UE over 100 TTIs (i.e. 1000 samples in total for each sector). The box within represents the interquartile range (IQR), which is the 25th (Q1) to 75th (Q3) percentile. The vertical line inside the box is the median. The whiskers indicate the lower (Q1-1.5(IQR)) and upper (Q3+1.5(IQR)) fences, while

the plus signs (+) after the upper fences denote the outliers. As shown in the result, Sector 2 without WA provides a significantly higher SINR than the 'control' Sector 13 (which de facto has proper interference modelling, as it is surrounded by sites) and Sector 5 is in between these two. As expected, when WA is enabled, sectors 5 and 2 provide similar results to Sector 13 (i.e. medians of 12.19 dB, 12.47 dB, and 12.09 dB respectively). The minute differences are attributed to the random walks (the only degree of freedom that was allowed between multiple iterations of the simulation). In contrast, when WA is not enabled, Sector 5 results in a median of 13.01 dB, while Sector 2 deviates considerably with a median of 15.23 dB. The UE goodput for the corresponding sectors of Figure 4-4 is presented in Figure 4-5 and Figure 4-6 in the form of CDFs.

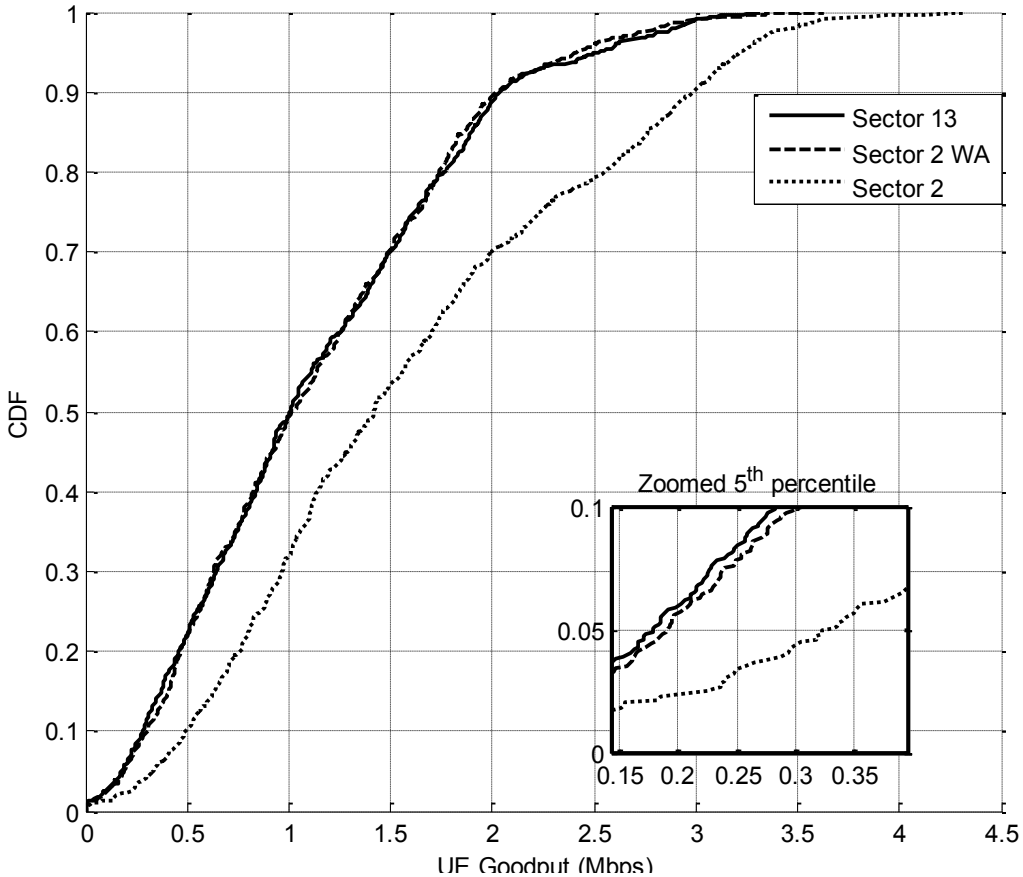

Figure 4-5 CDF of sector 2 with WA and without WA

The graph inset indicates the 5th percentile, showing the goodput of users at the cell-edge of the cellular network. It can be seen from the CDF plot in Figure 4-5 that Sector 2 shows a much more optimistic goodput (139 kbps difference at the 5th percentile) compared with Sector 13, indicating the lack of proper interference. The difference is more subtle for the case of Sector 5 in Figure 4-6 (25 kbps difference at the 5th percentile) but significant nevertheless. With the introduction of WA this problem is rectified and Sector 2, as well as Sector 5, both with WA closely follows the trend of Sector 13.

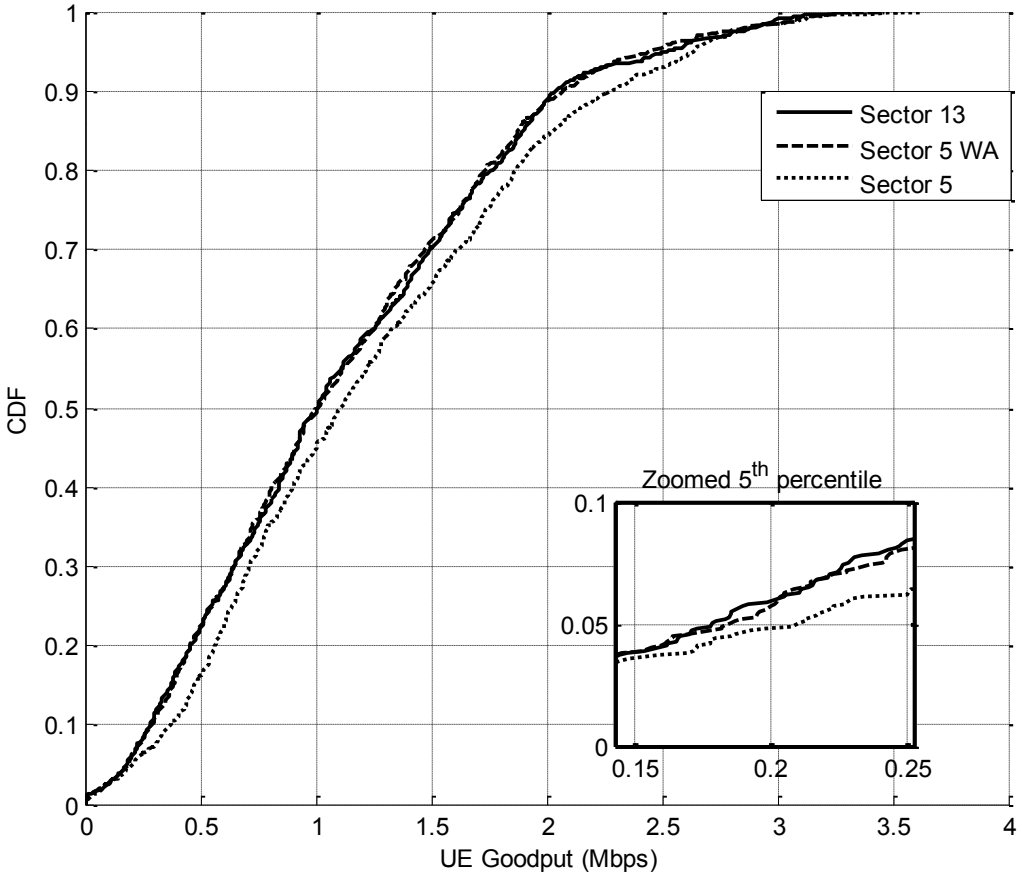

Figure 4-6 CDF of sector 5 with WA and without WA compared to sector 13

The last simulation is devised in order to evaluate the efficiency of the system in conventional testing, i.e. where different shadow fading maps are used with random sampling of positions. For this purpose, the system is tested with two different

scheduler configurations: i.e. RR and proportional fair PF [128], for a total output of 8820 UE goodput (i.e. net throughput). In addition, the simulations involve the UE selection from the whole ROI with and without WA, and the comparison to the central site (i.e. sectors 13 to 15 of Figure 4-3). The results in terms of spectral efficiency are presented in Figure 4-7. As shown in the result, taking results from all of the sites across the ROI without WA provides again highly optimistic results for both schedulers. Taking the cell edge SE as an example in the figure (y-axis), there is a difference of approx. 44% and 30% with RR and PF schedulers respectively when the goodput from UEs in all the sites are taken with and without WA included. Whereas, enabling WA provides goodput performance on a par with the central site (which is used as a control in this performance evaluation).

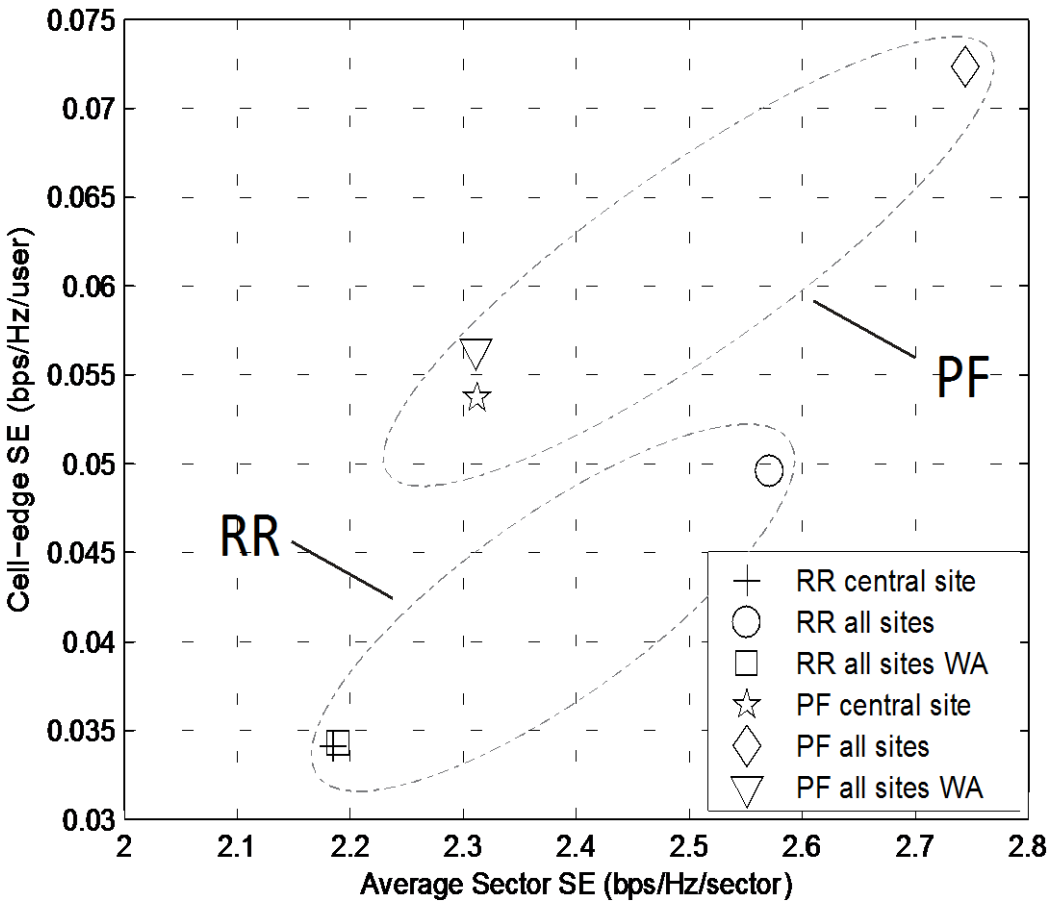

Figure 4-7 SE of the evaluated sites/sectors using RR and PF schedulers

A significant advantage of the proposed technique is the ability to retrieve more statistical results in shorter time (for a period of a single iteration) during each simulation compared with the models without WA. Hence, Table 4-2 shows the number of useful statistical results for the two cases, i.e. with WA, where UEs over the whole ROI are selected, and without WA, where only the central site is selected and UEs outside the central site are not created.

Table 4-2 Simulation efficiency for SLS with and without WA

Method	Iterations	Total useful UE goodput samples	Average time per UE/iteration/TTI (s)
Without WA	294	8820	10.17
With WA	42	8820	3.64

Indeed, that is the best-case scenario of parameterization for a simulator without WA in order to achieve computational efficiency. For the purpose of direct comparison the system was set in such a way that both scenarios produce the same number of useful statistical results, albeit with different number of iterations. The simulation was run on an Intel i5 processor at 3.3 GHz. It can be seen that there is an almost three-fold increase in simulation efficiency even taking into consideration the aforementioned best-case scenario for the simulator without WA. This proposed method comes with some added complexity to the SLS, which is however still significantly better than the traditional WA implementation. This is because the traditional implementation requires complete distortion of the cell layout throughout the simulation, while the proposed method only requires the VeNB attributes

specifically during the calculation of interference, and runs normally (as if WA was not modelled) for most part of the simulation run time. This does not affect the simulation results because UE performance metric is not taken from the VeNBs.

4.4 Inter-cell coordination in LTE-A networks

As discussed in Chapter 2, inter-site coordination is a vital feature of the 4G networks in order to achieve the performance capability specified for the standards. An example is the LTE/LTE-A standard with a reuse factor of 1, where the cell edge UEs experience even more interference (since the cells/sectors reuse the same spectrum) in addition to the diminishing signal strength due to the distance from their serving eNBs. Thus, the 3GPP specified CoMP transmission and reception schemes in addition to radio access techniques for the LTE/A networks [54]. The CoMP schemes are primarily specified to improve the cell edge UE performance in the network, by using the X2 logical interface to establish coordination between different sites/sectors in the network.

The CoMP standard could be achieved by implementing CoSH/CoBF (which will henceforth be referred to as only CoBF to avoid confusion) or JP [52]. However, the focus in this thesis is on the CoBF scheme for interference avoidance in the DL of the LTE network. One reason for adapting the preferred CoMP scheme is the trade-off in complexity and performance improvement. Though the performance improvements of both schemes are similar [145], the JP scheme however has more overheads. This is because while the CoBF scheme requires only a single eNB to transmit to its serving UE, the JP scheme requires multiple eNBs to serve a single UE at the same time and requires more complex processing such as inter-eNB synchronisation and additional

logging of control information [58]. Thus, these trade-offs has seen the CoBF scheme most popularly adopted in most research investigation [145-147]. A key technique for achieving the CoBF scheme is by adapting an antenna signal processing technique referred to as beamforming [121].

4.4.1 Beamforming

Beamforming is a signal processing technique where multiple antennas are used to steer or form antenna beams in a desired direction [121]. This is achieved by weighting the magnitude and phase of the antenna signals. The signals can be weighed from both the receiver and transmitter side to improve the signal transmission/reception of a UE (or a group of UEs) in particular location(s) of a cell. With the massive requirements for 4G networks (e.g. in terms of data rate), the adaptive beamforming technique [148] (i.e. continuous beamforming to suite moving receivers) is considered as a key element in aiding to achieve the high data rates. Thus to achieve beamforming with an array of antennas, a distance (τ) is required between the antennas where the signal from each antenna (in an antenna array) is multiplied by an array steering vector **a(θ)** (i.e. **a(θ)** = [1 $e^{-j\theta}$ … $e^{-j(M-1)\theta}$]) as shown in Equation (4.1) [121]:

$$s_0(t) = s(t),$$

$$s_1(t) = s(t-\tau) \approx s(t)e^{-j\theta},$$

$$s_{M-1}(t) = s(t-(M-\tau) \approx s(t)e^{-j(M-1)\theta} \quad (4.1)$$

Written as a vector,

$$\mathbf{s(t)} = \begin{bmatrix} 1 \\ e^{-j\theta} \\ e^{-j2\theta} \\ e^{-j3\theta} \\ . \\ e^{-j(M-1)\theta} \end{bmatrix} .s(t) = \mathbf{a(\theta)}.s(t)$$

where **a** is the array steering vector. Thus, the output of the individual antennas is represented as:

$$y(t) = \mathbf{W} \cdot \mathbf{a}(\boldsymbol{\theta}) \cdot s(t) \tag{4.2}$$

where **W** is the weight vector. Figure 4-8 illustrates beamforming as represented in Equations (4.1) and (4.2). In the example, the beam is steered to two different angles (90 degrees and 60 degrees), where $M = 4$, and the spacing between antenna elements $d = 0.5\,\lambda$.

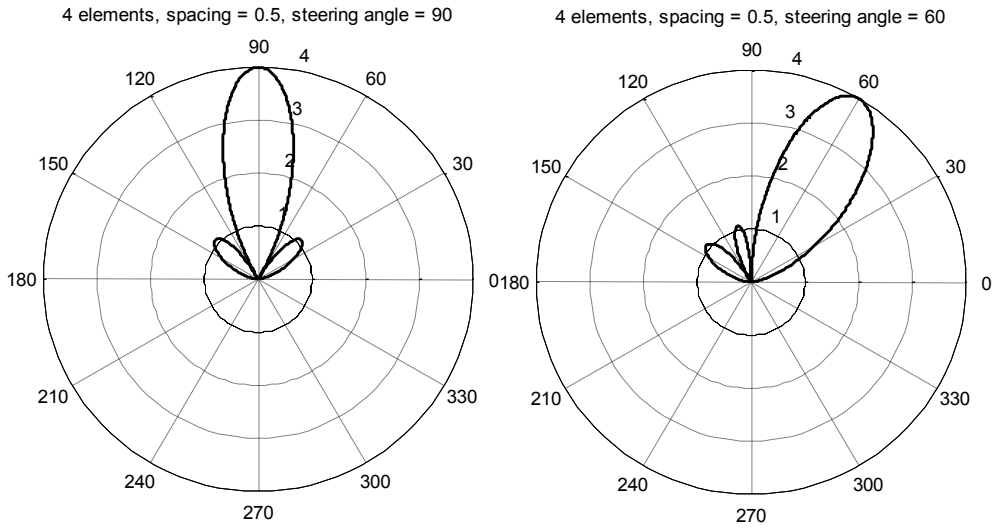

Figure 4-8 Illustration of Antenna beams steered to different directions

4.5 CoMP algorithm based on UE location

To investigate the performance gain of inter-site coordination in LTE networks, an algorithm based on beam steering (as described in the previous subsection) is implemented. For the purpose of this investigation, the sectors will be referred to as cells (i.e. 3 cells belonging to a site). Figure 4-9 illustrates the setup of the simulated scenario, where 2 cells (belonging to different sites) with a common border (i.e. cell edge) in a single tier cell layout was investigated. As shown in the figure, cells 13 and

21 satisfy the condition required for the simulation set up: since they have a common border (referred to as a conflicting border in this context) and belong to different sites i.e. 5 and 7 respectively. Additionally, the WA interference modelling described earlier was included in the model (i.e. all the edge cells are surrounded by VeNBs), to ensure realistic results from the performance investigation.

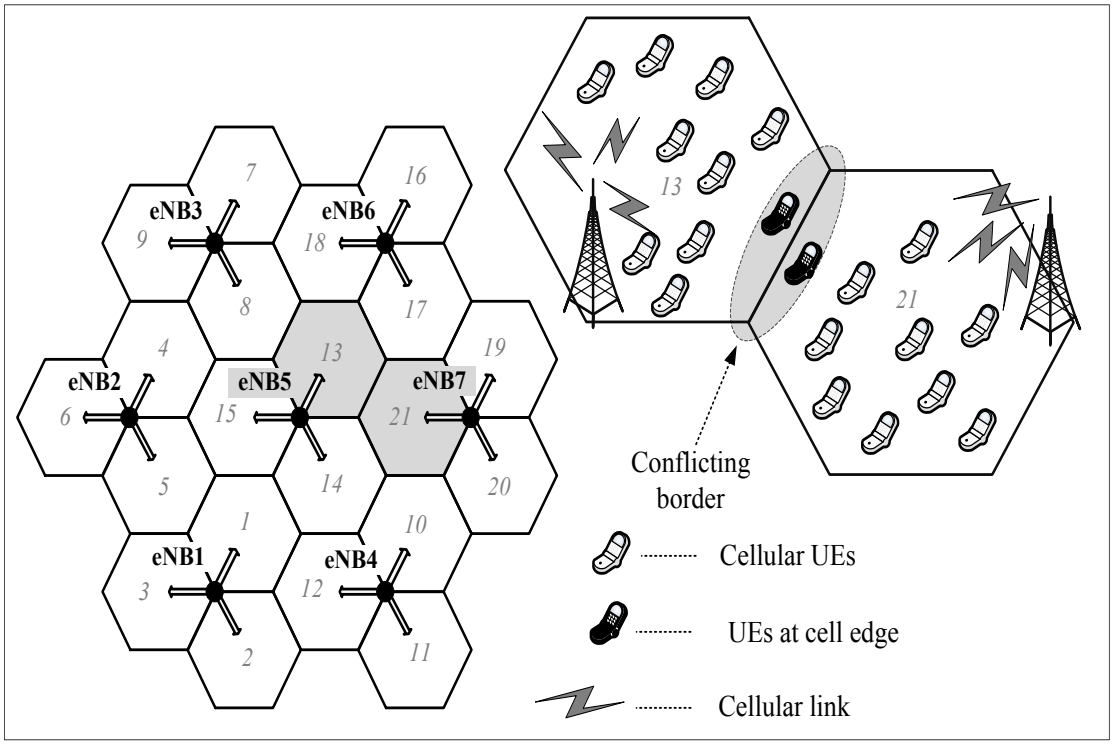

Figure 4-9 Illustration of cooperating cells and "conflicting border"

Similar work has been carried out in [145, 149, 150] for CoBF in the DL of an LTE network. The listed research literature have demonstrated substantial improvement of the cell edge UE performance with the algorithms proposed. A common limitation from the literature however is the requirement of explicit CSI to be shared between cooperating cells prior to transmission. While this has been shown to be very useful as detailed CSI (such as PMI) for all the UEs are shared between eNBs in the cooperating cells/sites, the notion is considering a non-limited backhauling capacity to

share such unambiguous CSIs. Studies have however shown that the backhauling capacity in real life is rather an issue as it has a limited capacity and could be highly saturated with explicit CSI [151] (especially with numerous cooperating sites/cells).

Inspired by the achievement of the aforementioned literature and considering the limitation on backhauling capacity, this work focuses on achieving CoBF with limited CSI compared to the existing works. Thus, an algorithm is implemented in this section, which does not require detailed CSI feedback from the UEs but rather considers the UE location (determined by the eNB) as the required parameter. A drawback of the obtaining the UE location feedback in this proposal is that it could require additional component such as GPS at the eNB or inclusion of some existing localisation algorithms to determine the UE positions accurately. This could however be less complex compared to additional unambiguous CSI (such as PMI) required for each UE to normally required at the eNB.This significantly reduces CSI requirement on the UEs, leaving only instantaneous location of the cell edge UEs to be shared between adjacent cooperating cells. The algorithm for the CoMP implementation is shown in Table 4-3. Some parameters were defined to establish a platform for varying the conditions in the algorithm. These include distance thresholds Th_1 and Th_2, indicating the distance between the positions of the UEs in the cells to their respective cell edge in the different cells. The variables θ_1 and θ_2 were also set to represent the angle/direction of the "conflicting border" of the cooperating cells in the respective cells. Finally, indexes I_1 and I_2 are defined to indicate the presence of cell edge UEs in the respective cells for each TTI.

Table 4-3 Detailed description of the CoMP algorithm implementation

Algorithm Beam steering conditions for cooperating cells in algorithm

(13) θ_1 : angle of conflicting border for cell 1
(14) θ_2 : angle of conflicting border for cell 2
(15) Th_1 : distance threshold for cell edge of cell 1
(16) Th_2 : distance threshold for cell edge of cell 2
(17) Inter-cell coordination = 0
(18) $I_1 = I_2 = 0$ (*reset interference index log*)
(19) **for** each TTI
(20) ***if*** inter-cell coordination = 0
(21) **for** $UE_i \rightarrow UE_n$ in coordinating cells
(22) $UE_i pos$ = position of the i^{th} UE relative to serving eNB
(23) $UE_i\theta$ = angle of the i^{th} UE relative to serving eNB
(24) ***if*** UE_i is attached to cell 1
(25) ***if*** $UE_i pos > Th_1 \,\&\, UE_i\theta >= \theta_1$
(26) $I_1 = 1$
(27) **else if** UE_i is attached to cell 2
(28) ***if*** $UE_i pos > Th_2 \,\&\, UE_i\theta >= \theta_2$
(29) $I_2 = 1$
(30) ***end*** **for**
(31) ***if*** inter-cell coordination = 0 & $I_1 = I_2 = 1$
(32) *steer beam of cell 1 in this TT1*
(33) *inter-cell coordination = 1 (set inter-cell coordination index)*
(34) ***if*** inter-cell coordination = 1
(35) Steer *beam of cell 2 in this TT1*
(36) in*ter-cell coordination = 0 (reset coordination index)*
(37) **else** *transmit normally (I_1 or $I_2 \neq 1$ i.e. no interference)*
(38) *inter-cell coordination = 0 (reset coordination index)*
(39) ***end*** **for**

Thus, when a UE in cell 1 is further than Th_1 and is in the direction of angle θ_1 (relative to its serving eNB), it is then tagged as a cell edge UE: same as the case with a UE in cell 2 for Th_2 and θ_2. Hence, the indexes I_1 and I_2 are set to 1 if UEs

served by the different eNBs/cells are located at the conflicting borders (in the same TTI). The duration of the coordination scheme spans for two TTIs. In the first TTI, if the conflicting border comprises of UEs served by different cells, the beam from one of the cells is steered away from the cell edge, and vice versa in the next TTI. This is done to establish fairness in the scheme (since each cell edge UE is covered in one of the TTIs), and the impact of signal from interfering cells is eliminated at an instance for the UEs in the cell edge.

The architecture for the algorithm is demonstrated in Figure 4-10 to Figure 4-12. The graphs describe how the eNB beams are steered in the simulator and how they affect the UEs at the cell edge of the network in this simulation set-up. As described earlier, the antenna beams normally extend over to the neighbouring cells (as it emulates a typical macrocell with eNB transmitter power of up to 43 dBm i.e. approx. 20 W). Thus the signal coverage from a sector antenna/site antenna is not perfectly restricted within its cells, and hence appears as interference (or dominant signals) to UEs at the cell edge of neighbouring cells. This is even a bigger problem with the recently deployed 4G networks such as LTE, as the same spectrum is reused in all sectors: hence having possible cell edge UEs being allocated the same set of RBs at the same time by their individual serving eNBs. Figure 4-10 illustrates the normal/fixed direction of the antenna beams for the non-adaptive antennas, which is also the initial direction of the beams at the start of the simulation. Figure 4-11 shows the direction of the beams in time t_A, while Figure 4-12 shows the beam direction at a later time t_B in the event of UEs at the conflicting borders. Figure 4-11 clearly shows the variation of the antenna beam (dashed line) from cell 2 at t_A (one TTI) steered away from the cell edge. UE (1,1) no longer receives interference from cell 2. Similarly in

Figure 4-12, the antenna beam in cell 1 at the following TTI is steered away from the cell edge and UE (1,2) is not any more limited by interference from cell 1.

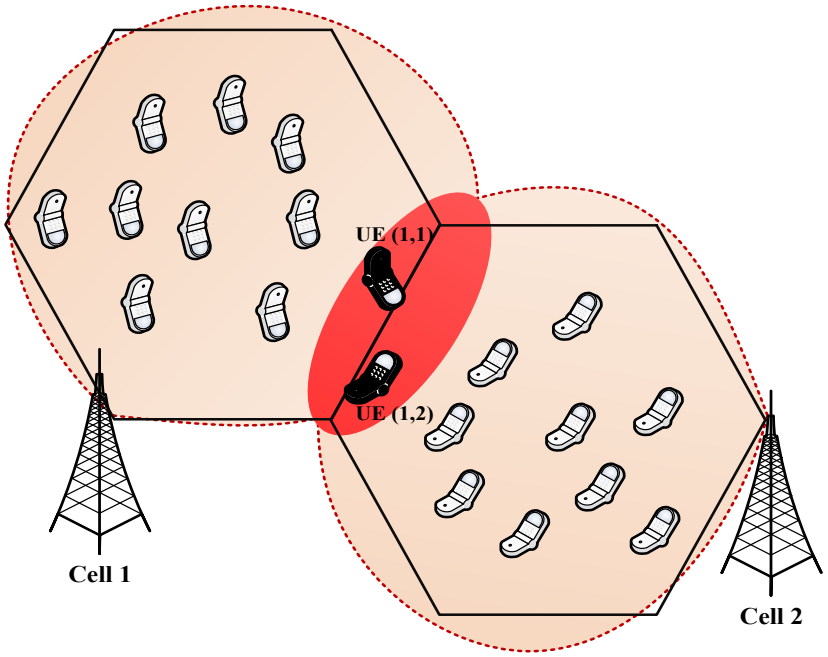

Figure 4-10 Illustration of fixed beams for non-adaptive antennas in SLS with UEs served by different cells at a common border

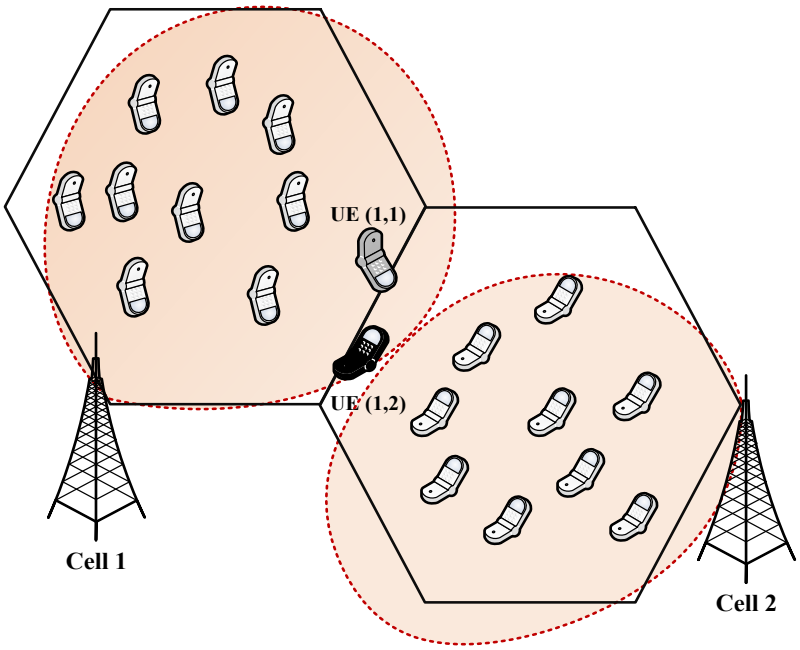

Figure 4-11 Illustration of beam directions at 1st time slot

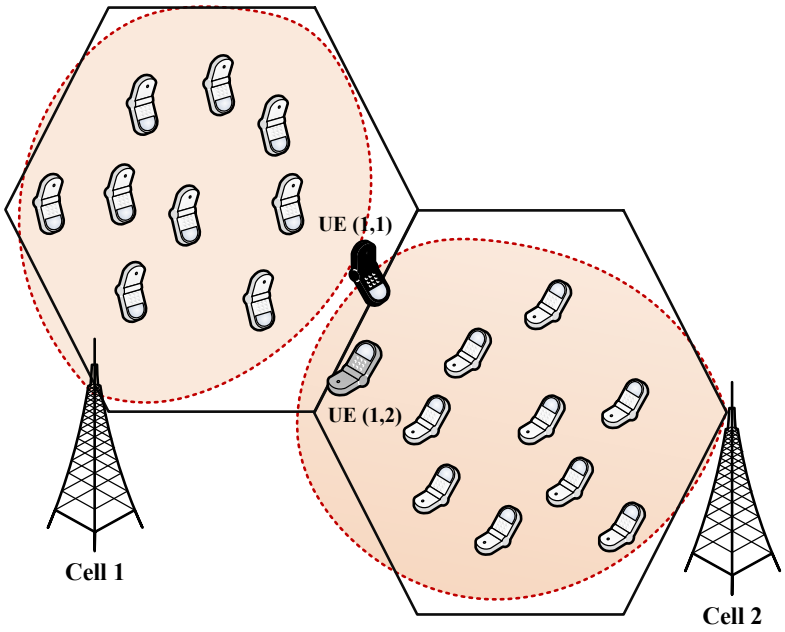

Figure 4-12 Illustration of beam directions at 2nd time slot

Although the CoMP scheme implemented has shown better performance compared (as shown in the following results) to traditional transmission scheme without the need for detailed CSI, the technique equally has its challenges. One major challenge in the scheme is the requirement of the individual UEs positions and angle relative to their serving eNBs for the duration of the transmission intervals. Although it is practical to achieve this, it requires additional equipment (such as GPS) at the eNB. However, several literature have proposed schemes to efficiently determine the location of UEs (both indoor and outdoor), either based on comparing time delay of received signals, or by UEs cooperating to unambiguously determine their positions [152, 153]. Some renowned algorithms for determining the location of UEs based on their signal include MUSIC (Multiple Signal Classifier) and ESPRIT (Estimation of Signal) [154]. The detailed description of the location algorithm is out of the scope of this work, but the implementation could be accessed in the references provided.

4.5.1 Performance enhancement with proposed CoMP algorithm

The performance of the CoMP algorithm is illustrated in terms of goodput and SINR in Figure 4-13 and Figure 4-14 respectively for the cooperating cells (i.e. 13 and 21). It is compared with the performance of the same cells when no inter-cell coordination is involved. As described earlier, the effect of simulation entropy (caused by UE random movement and lognormal shadow fading amongst others) is restrained by reusing the same shadow fading map for all the iterations, where accurate performance metric of the UEs is then achieved by averaging over the number of iterations. For these results, a total of 100 iterations were run, hence, averaging 1000 samples of the UEs metrics for each of the cells (i.e. 10 UEs per cell). The simulation parameters are kept the same with Table 4-1, where the RR scheduler is used in a 5 MHz bandwidth channel with the CLSM transmission mode (to compare the different results using the same parameters).

As shown in Figure 4-13, the goodput is considerably higher with the CoMP algorithm included compared to when the normal transmission scheme (without CoMP) is employed. The graph inset indicates the cell edge (i.e. the 5^{th} percentile of the CDF) for the goodput distribution of the cooperating cells. As shown in the result, the cell edge goodput without CoMP is 85 kbps. With the CoMP scheme implemented however, it is shown that the cell edge goodput has improved with over 100 kbps. The trend of the increase in the performance metric (goodput) is consistent over the distribution, with a similar improvement of 150 kbps at the median (50^{th} percentile) of the CDF. The distribution then becomes similar/close at the 95^{th} percentile with about 2 Mbps for both scenarios. This is because the impact of the interfering signals is only

present for the UEs closer to the cell edge and less for UEs closest to the serving eNB (whose performance are indicated at the higher end of the distribution).

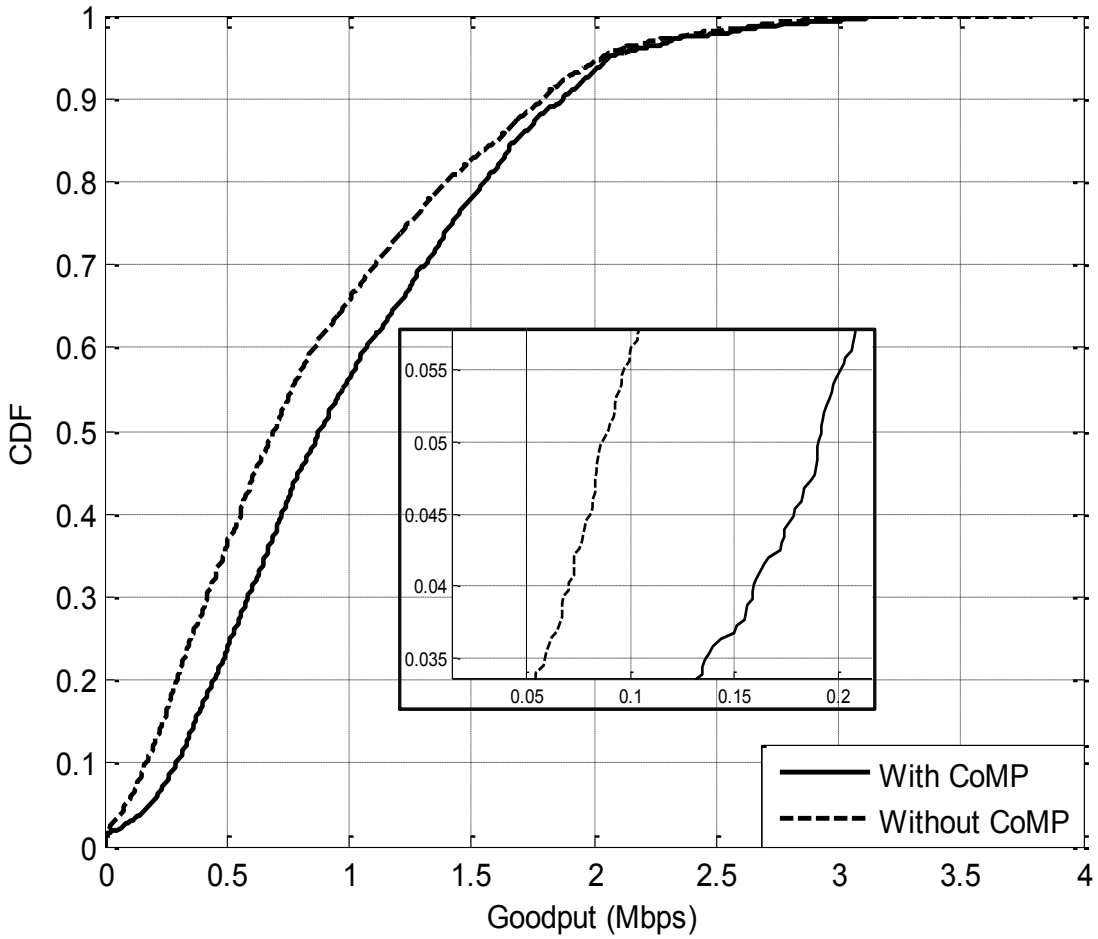

Figure 4-13 UE goodput CDF with and without inter-cell coordination

To further illustrate the improvement of the CoMP algorithm, the SINR distribution of UEs in the cooperating cells is evaluated in Figure 4-14. Similar to the goodput comparison in Figure 4-13, the SINR distribution with CoMP is compared with that of the normal transmission scheme (without CoMP), using a box plot in this result. As expected, the SINR of the UEs with CoMP is better than when CoMP is not included in the transmission for the investigated cells. The median value in the result is 7.9 dB and 10.7 dB with and without CoMP respectively. This indicates an increase of up to

2.8 dB at the median of the transmission scenarios. The median value is used to compare the performance as it indicates the centre point of the distribution with consideration of the outliers.

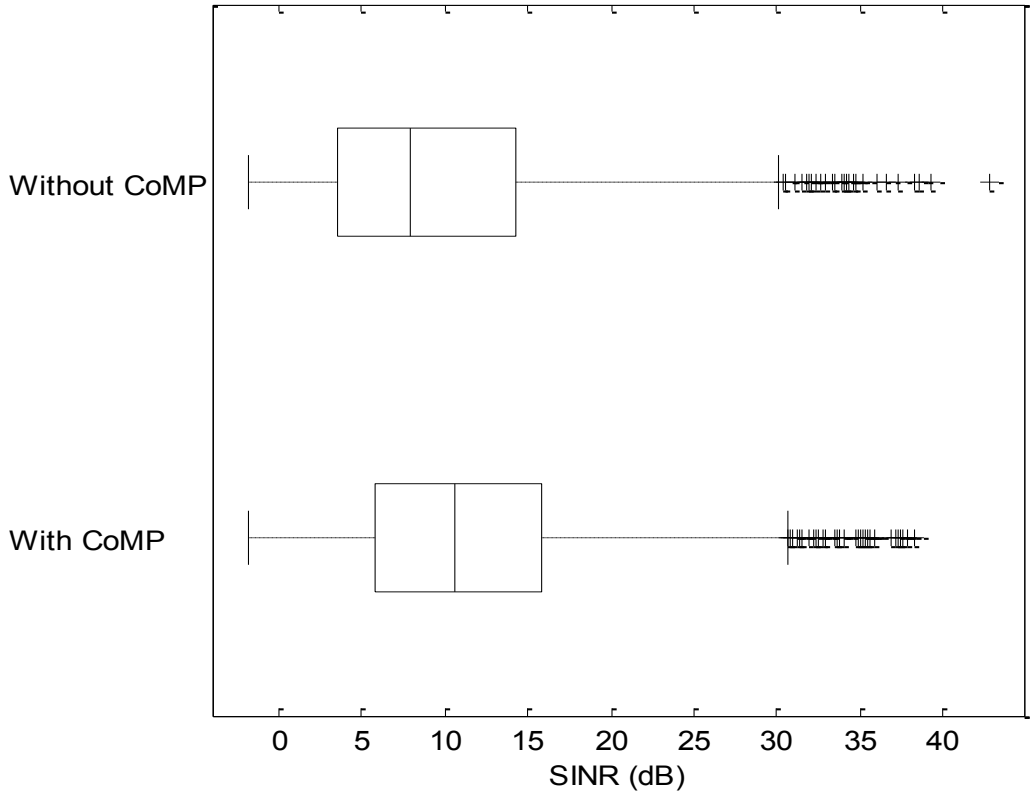

Figure 4-14 UE SINR distribution for the cooperating cells

4.6 Summary

Following the detailed description of the LTE SLS model in the previous chapter, this chapter presented a proposed technique of interference modelling for 4G networks (such as LTE). Additionally, a CoMP algorithm was proposed and implemented in the SLS to illustrate the performance gain of inter-cell coordination in the LTE network.

The proposed inter-cell interference modelling approach presented in the chapter is shown to increase efficiency while reducing the number of required wireless sites and

mobile users in a LTE SLS platform. The method, which is based on WA, shares significant common ground with traditional techniques; however, it does not require a specific toroid-shaped topology. Instead, the technique proposed involves the simulation of one tier of sites, and the duplication of VeNBs at indicated positions exclusively during the interference calculation. Consequently, all features of the eNBs are replicated, avoiding—thus—additional overheads on the complexity of the system. Additionally, the UEs moving from the edge/border cells are accordingly handed over to the transiting cells/sites instead of the random deployment of the UEs in typical simulators (without WA). As a result, it can be implemented in any existing SLS platform without major restructure. The simulations have shown that the technique provides similar interference modelling on the edges of ROI to the central sectors of the network. In addition, the method allows for the simulation of advanced LTE features, such as CoMP to be performed in a one-tier topology, using less memory and achieving an almost three-fold computational efficiency over traditional SLS configurations.

Furthermore, the CoMP algorithm implemented in this chapter has shown to improve both the goodput and SINR of UEs closer and/or at the cell edge of the LTE network. The algorithm implemented is based on the adaptive beamforming technique, where eNBs cooperate with neighbouring cells/sites to steer their beams in a coordinated manner, and therefore, minimise the impact of interference on UEs around the cell edge of the network. Compared to some existing methods which require complex pre-processing between the coordinated cells and even the UEs involved, the proposed approach requires only the direction of the UEs from their serving eNBs (which was assumed to be efficiently acquired). The algorithm is then accomplished continuously

in 2 consecutive TTIs to ensure fairness to the UEs at the cell edge of the coordinating cells: i.e. the coordinating cells sequentially steer their beams away from the cell edge in the event of the cells serving UEs at a common cell borders. This is in contrast to the normal concurrent transmission of neighbouring cells, resulting to poorer performance of the cell edge UEs. The results presented show over a fold of increase in terms of the goodput of the cell edge UEs in the cooperating cells. It also shows significant improvement of the UEs SINR (with approx. 3 dB gains) compared to the traditional transmission scheme.

Chapter 5

Device-to-Device Communication and Multihop Transmission for Future Cellular Networks

5.1 Introduction

This chapter analyses Device-to-Device (D2D) communication as an essential add-on technology to the currently developed 4G and subsequent 5G cellular networks. The technology enables User Equipment (UEs) in close proximity to communicate directly, hence taking some load off the eNBs by reducing UE traffic, and maximising cellular Resource Block (RB) utilisation amongst other advantages. Thus, a comprehensive LTE-A System-Level Simulator (SLS) that includes D2D communication was devised to investigate performance gains of the technology in cellular networks. This was achieved by further developing the state-of-the-art DL SLS model described and enhanced in chapters 3 and 4 respectively, by vitally modelling the UEs to possess dual mode capabilities i.e. D2D and cellular mode (a feature not readily available in the few existing models). Hence, a UE can transmit to its receiver (RX) when it's in D2D transmitter (TX) mode, in compliance with the specified UE parameters of the 3GPP standard.

Subsequently, the performance gain of a hybrid network (consisting of UEs in both D2D and cellular mode) is analysed in this chapter. This includes detailed simulation results illustrating the proximity and power gain of D2D UEs compared to regular cellular UEs, leading to performance improvement in terms of throughput and SINR

of the cellular network in general with D2D transmission included. Despite the promising gains of D2D technology in cellular networks, one key issue identified and currently focused on in recent research is interference management in the hybrid network. This is because cellular RXs get inherent interference from D2D TXs within the same cell/sector in addition to interference from neighbouring eNBs (considering a DL implementation). Thus in this direction, an efficient power control algorithm based on power reduction was proposed in this chapter to mitigate interference, in addition to the study of performance gains of adopting the technology in the network. The D2D TX power is varied based on cell edge SINR of cellular UEs at a set minimum threshold in the proposed algorithm. Hence, a maximum SINR threshold was also set so that the D2D TX can transmit at maximum power when the cell edge SINR is above the minimum threshold and up to the maximum threshold to ensure fairness to the D2D transmission.

A target of future cellular networks is the achievement of Gbps individual user experience. Thus, the work in this chapter is further extended to include Multihop (MH) transmission in the hybrid networks. While MH transmission exists in traditional cellular networks, current studies are focusing on using D2D UEs to relay traffic and improve cellular UE experience in the networks. Extending the current literature, MH transmission for relaying D2D traffic is considered in this thesis. This is mainly due to the greatly projected D2D UE performance (due to close proximity transmission), leaning towards achieving the projected UE experience of future cellular networks.

5.2 Modelling of D2D UE in SLS

In order to investigate performance of D2D communication in cellular networks, a new model had to be implemented, extending the functionalities of the state-of-the-art SLS presented in Chapter 3. In summary, the benchmark SLS consists of eNBs and UEs within a Region of Interest (ROI), which are created as a map and includes the pathloss, antenna gain etc. among other features of a 4G cellular network. The cell layout represents a typical macrocell with a number of sites (500 m apart) having 3 sectors each. With WA interference modelling implemented in the SLS (as proposed in Chapter 4), only a single-tier is therefore required for the performance investigations as shown in Figure 5-1, hence reducing overheads with adequate interference modelling.

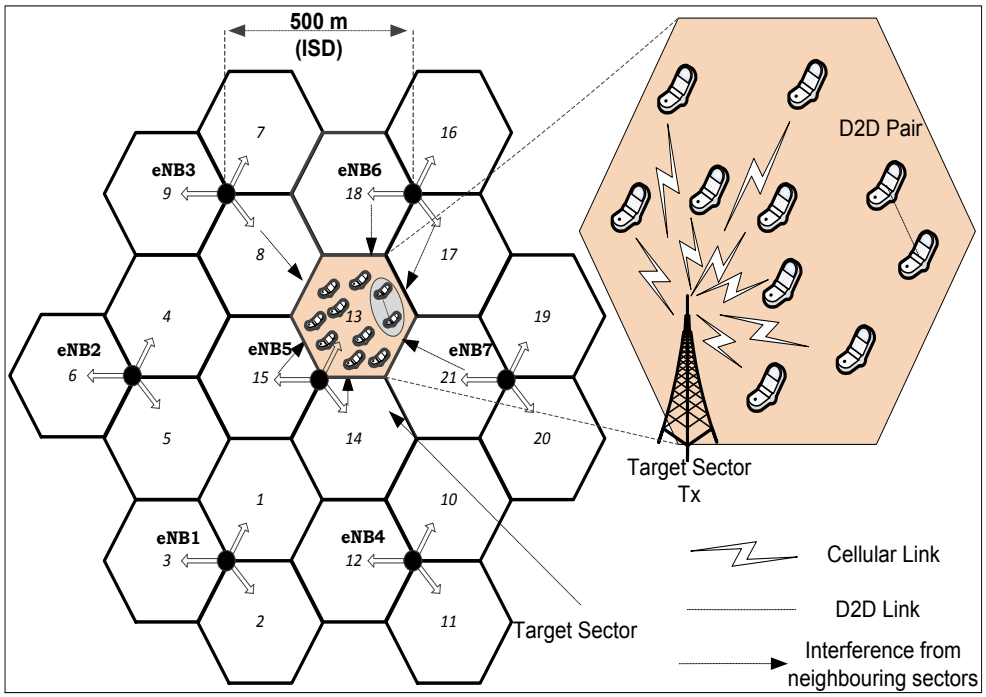

Figure 5-1 Cell layout with UEs in both cellular and D2D mode in target sector

The performance metric of the hybrid network is taken from sector 13, referred to henceforth as the 'target sector' in the context of this chapter. The target sector consists of 10 UEs, where 8 UEs are in cellular mode while 2 are in D2D mode. The

ratio of D2D to cellular UEs is considered to be 20% as cellular UEs continue to be predominant constituents of the network. All other sectors in the model consist of 10 UEs (all in cellular mode), and the respective eNBs are continuously transmitting to their UEs. This was done to ensure that UEs in the target sector experience interference from neighbouring eNBs (especially for UEs at the cell edge). The model emulates a multi cell topology, where a cluster of multiple active cells/sites causes interference to adjacent UEs (due to signalling and transmission) to achieve realistic results. It can also be noticed that the D2D pair are located at the cell edge of the layout in Figure 5-1. This was done to achieve a good SINR for the D2D RX (from the D2D TX) by minimising the interference impact from the eNB as the DL resources are reused in this model. It has been demonstrated in [67] that the further away the D2D UEs are from the eNB, the better their SINR when reusing the DL resources.

The sector eNBs are equipped with directional antennas (the azimuth varies depending on the sector), with antenna height of 20 m, measured from the average roof top of a typical urban environment [112]. The D2D TX and RX are equipped with an omnidirectional antenna of 1.5 m height, with maximum transmitter power ($P_{D\max}$) of 23 dBm i.e. approx. 0.2 W: in accordance to the specified parameters for LTE UEs in the 3GPP standard which can be found in [109]. Figure 5-2 illustrates the antenna gain pattern relative to the pathloss of the target sector eNB (with azimuth of 30 degrees) and the D2D TX in the ROI. The target sector eNB has a maximum antenna gain of 15 dBi, while the D2D TX has a maximum antenna gain of 0 dBi. It is shown in the figure that the pathloss is considerably lower closest to the TXs (both eNB and D2D UEs) and increases further away. The pathloss level (in dB) of the

regions surrounding the TXs is indicated by the colour chat in the figure. The simulation parameter are summarised in Table 5-1.

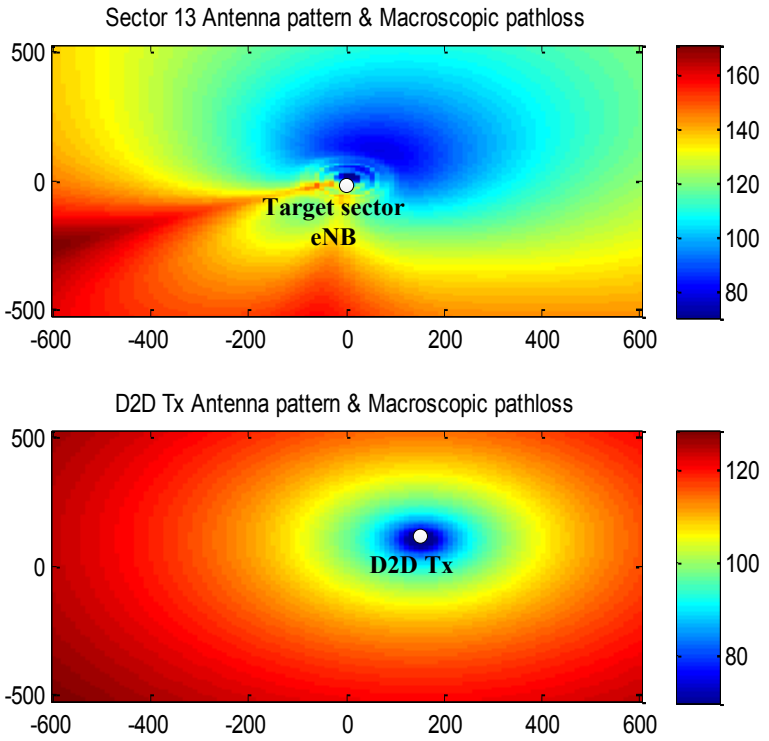

Figure 5-2 Pathloss and antenna pattern of D2D TX and target sector eNB

Table 5-1 D2D and cellular UEs parameters in SLS model

Parameter	Value
Network Layout	7 eNBs, 3 sectors/eNB site, ISD 500m (with WA)
UE parameters	10 per sector, 5 km/h, 3 TTIs feedback delay
UEs distribution	Homogenous; pre-set positions
UE noise	Thermal noise density: -174 dBm/Hz, noise figure: 9dB
Channel model	Urban, Winner II type
D2D Tx parameters	1.5 m height, 0 dBi gain, maximum TX power: 0.2 W
Distance between D2D pair (m)	10 – 50 (steps of 10)
D2D Tx power (W)	0.05 – 0.50 (steps of 0.05)

Frequency (GHz)	2 (with frequency reuse of 1)
Bandwidth (MHz)	5
Transmission mode	CLSM, 2 TX and 2 RX, maximum of 2 streams
eNB parameters	20 m height, 15 dBi gain, TX power: 20 W
Schedulers	RR
Number of iterations	100

The functionalities involved in D2D communication can be broadly classified into 2 main tasks; the UE mode selection, and D2D transmission. Figure 5-3 shows a pseudo code summarising the mode selection for UEs in the developed SLS model: the D2D transmission aspect, which includes peer-to-peer traffic is described in the following subsection. A ROI is first of all created, where eNBs and UEs are configured accordingly within, to include their respective antenna types and other parameters. The ROI also includes the shadow fading maps, and pathloss maps amongst other environmental features. The UEs are uniformly distributed within the sectors, and are attached to their serving eNBs based on the channel SINR (which is determined by the signalling from the eNBs). The UEs are modelled based on a random walk model, and are selected as D2D candidates in the target sector if they are less than or equal to 10 m apart (between a pair of UEs). Thus a D2D TX and RX are selected between the pair, while the rest of the UEs remain as cellular UEs as described in Figure 5-3.

The model maintains the simulation methodology as in the previous implementations (from the preceding chapters), where multiple iterations were run and aggregated over several TTIs (100 TTIs in this case). This is adopted to closely emulate real life conditions and diverse environments during simulations. Thus, the result from the

performance investigation represents metrics from various environments experienced by UEs in the network (for both cellular and D2D).

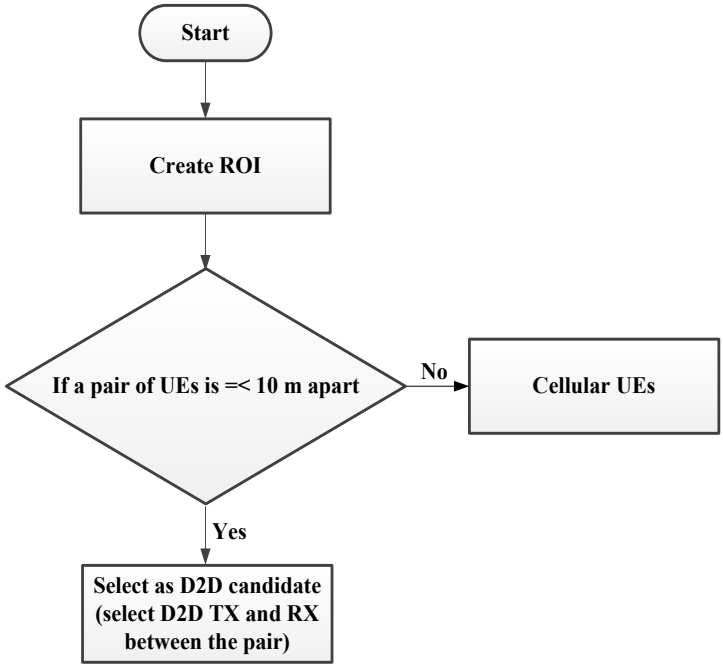

Figure 5-3 Pseudo code summarising mode selection in the devised SLS model

As described earlier, the simulation platforms typically involve some entropy. These include creating of the shadow fading map using lognormal space-correlated function, and simulating the UE movement based on 'random walk' models. These causes some discrepancies in the different iterations, which is commonly resolved by reusing the same shadow fading map for all the iterations during the simulation [101]. As the model depicts a multi-cell scenario (with up to 7 sites in this case), the interference signal experienced by the cellular UEs in the target sector comes from the D2D TX and the neighbouring eNBs. Similarly, the D2D RX interference comes from the eNB of its occupying sector i.e. the target sector and from the eNBs of neighbouring sectors as well (as illustrated in Figure 5-1). The DL interference power and SINR of the cellular UEs in the target sector is represented in Equation (5.1) and Equation (5.2) respectively.

$$P_{C\text{int}f} = P_{eNB_{(j\to K)}\text{int}f} + P_{D2D\text{int}f} \tag{5.1}$$

$$SINR_{UEi\to N_{TS}} = \frac{P_C}{P_{C\text{int}f} + N_0} \tag{5.2}$$

where $P_{C\text{int}f}$ is the interference power to cellular UEs in the target sector, $P_{D2D\text{int}f}$ is the interference power from D2D transmission, and $P_{eNB_{(j\to K)}\text{int}f}$ is the interference power from sector's neighbouring eNBs (where $K = 6$), P_C is the received signal power for $UEi \to N_{TS}$ (where $N = 8$ in this model i.e. total number of cellular mode UEs in target sector) from the sector's eNB, and N_0 is the noise power. Similarly, the D2D RX SINR in the model is expressed as;

$$SINR_{D_{RX}} = \frac{P_d}{(P_{eNB_{(j\to K)}\text{int}} + P_{TS\text{int}f}) + N_0} \tag{5.3}$$

where the received signal power form the D2D TX is P_d, and $P_{TS\text{int}f}$ is the interference power from the eNB of the target sector.

5.3 Performance gains of D2D communication underlaying the LTE network

D2D communication promises tremendous potential gains as an add-on technology to the cellular networks. This includes proximity gain i.e. high data rates with close distance between communicating devices, reuse gain i.e. simultaneous use of radio resources by both cellular and D2D links, and hop gain i.e. use of either UL or DL for full transmission between D2D transceivers [65]. Thus, the technology is implemented to analyse the theoretical performance gains in the LTE-A network, specifically, the proximity and power gain of D2D transmission with maximum reuse

efficiency (i.e. reuse of the whole cellular resources for D2D communication) in this section.

The D2D communication was modelled to be network assisted (i.e. the sector eNB has some control over the D2D transmission), where the D2D TX reuses the RBs of its occupying sector simultaneously with the cellular UEs. The eNB involvement significantly reduces overheads and requirement on the UEs (which have constraint abilities) during D2D communication. An example of the sector eNB involvement includes assisting in D2D session setup [155]. A D2D session could be set up by the eNB for UEs at close proximity, after the serving gateway has detected potential D2D UEs traffic (e.g. UEs in close proximity requesting similar services) [38]. The study in this thesis however only focuses on the UEs performance, and hence D2D UE set-up is simply modelled based on proximity between UEs as shown in in the preceding subsection. Though D2D communication is modelled to be network assisted, the D2D traffic is however assumed to be between the D2D pair, without involvement of the eNB to reduce its load. Each iteration assumes random 'drops' of the cellular users, while 2 UEs in close proximity are assigned as a D2D pair (i.e. TX and RX) in compliance with the peer discovery method described in [38]. The mean goodput of the D2D RX with increasing D2D TX power and proximity between the pair is shown in Figure 5-4.

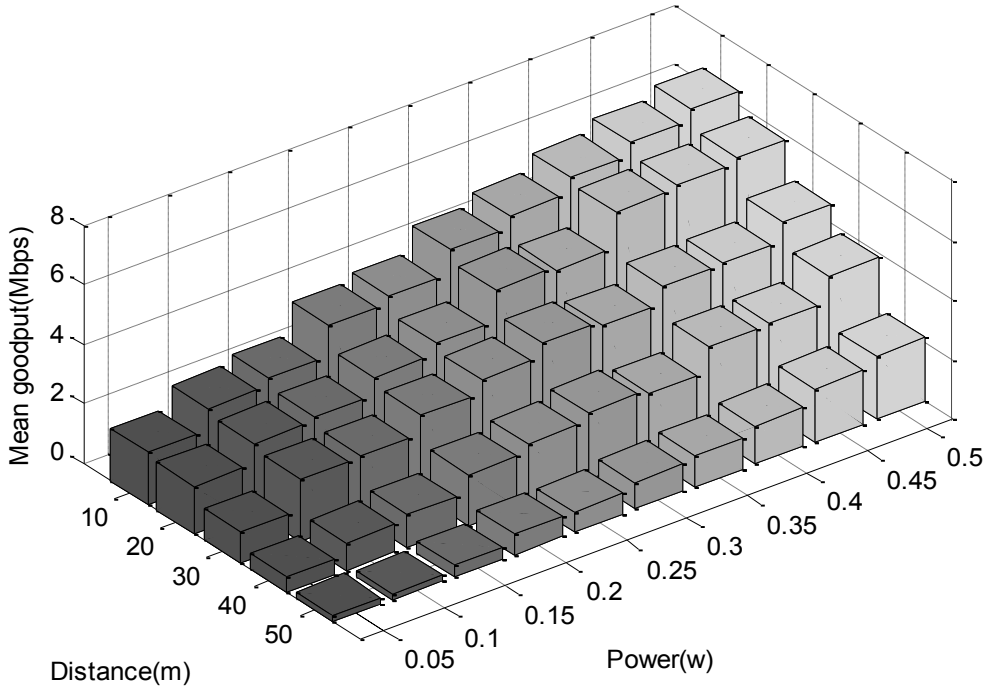

Figure 5-4 Mean goodput of D2D RX with increasing D2D TX power and distance between the D2D pair

The result shows the goodput for a range of distances between 10 m to 50 m, and increasing D2D TX power from 50 mW to 500 mW. While the average UE TX power in the LTE specification is 0.2 W [109], increased TX power levels were simulated to demonstrate the impact of transmission power on D2D RX and cellular RX performance in this study. As expected, the result shows significant goodput gain when the D2D pair is closer, and when the TX power is increased. Taking the average TX power as an example in the result (i.e. 0.2 W), the D2D RX mean goodput is up to 3.5 Mbps when the pair are 10 m apart and 0.8 Mbps when 50 m apart. Furthermore, it is shown that the D2D RX goodput increases significantly with increasing TX power, attaining up to 6.49 Mbps mean goodput for the highest TX power in this study i.e. 0.5 W.

Additionally, the impact of D2D TX power to the cellular UEs is demonstrated in Figure 5-5. To ensure a common platform for comparison in the graph, the D2D RX position was fixed for all variations, and equal number of samples (1000 samples each for the D2D and cellular RXs) were obtained and averaged for the different D2D TX power levels.

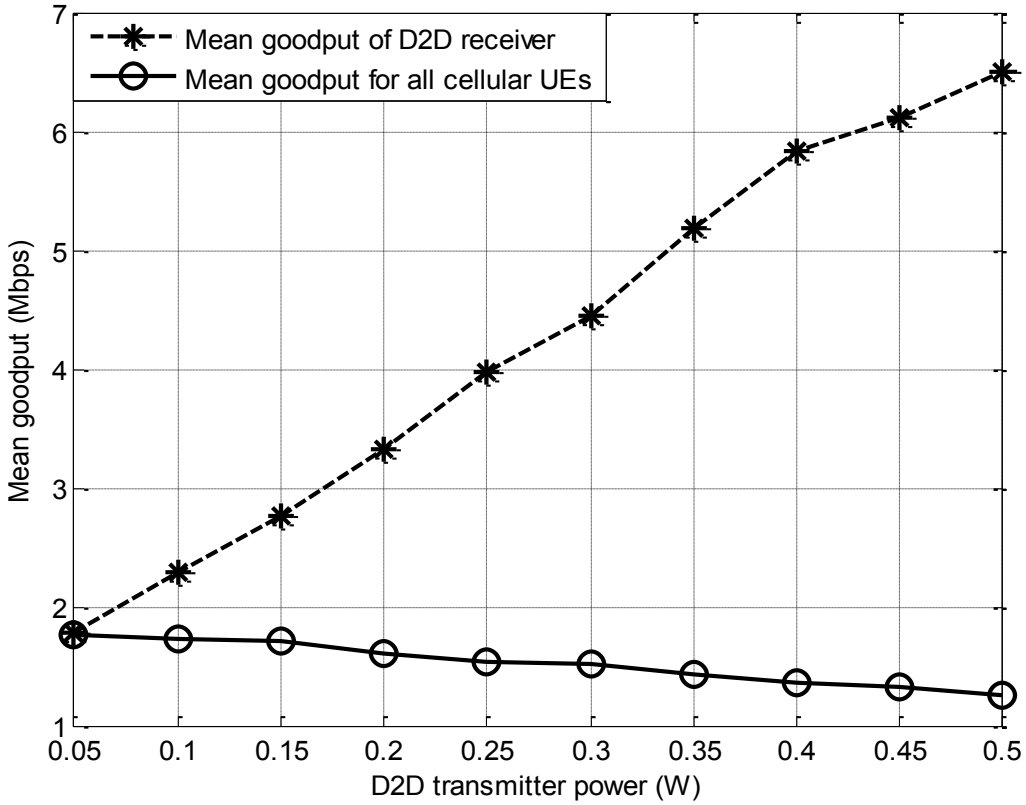

Figure 5-5 Mean goodput for cellular and D2D UEs in target sector

Even at a very low D2D TX power of 50 mW, it is shown that the mean goodput of the D2D RX was similar to that of cellular RXs, which is approx. 1.8 Mbps in the figure. It should be noted that while one or more of the cellular RXs performed better than the D2D RX for the different power levels, most of the users performed worse when power was increased. This is mainly due to interference impact from D2D transmission, and the close proximity between the D2D pair i.e. 10 m in the study. This resulted to a better overall mean D2D RX goodput, compared to that of the cellular RXs.

However, while degradation of the cellular RX performance is not significantly high (less than 1 Mbps for all the variable D2D TX powers up to 500 mW), the D2D RX improvement was more evident in the graph, with more than 4 Mbps increment when D2D TX power is 500 mW. Thus, it can be concluded from the results that the overall performance of the target sector could be improved with efficient power control between the D2D TX and sector eNB. A concerning factor in this solution would be the distance between the D2D pair, which will determine the goodput that could be achieved by the D2D TX power (as demonstrated in the graph of Figure 5-4). The goodput of UEs in the target sector is represented using a CDF in Figure 5-6.

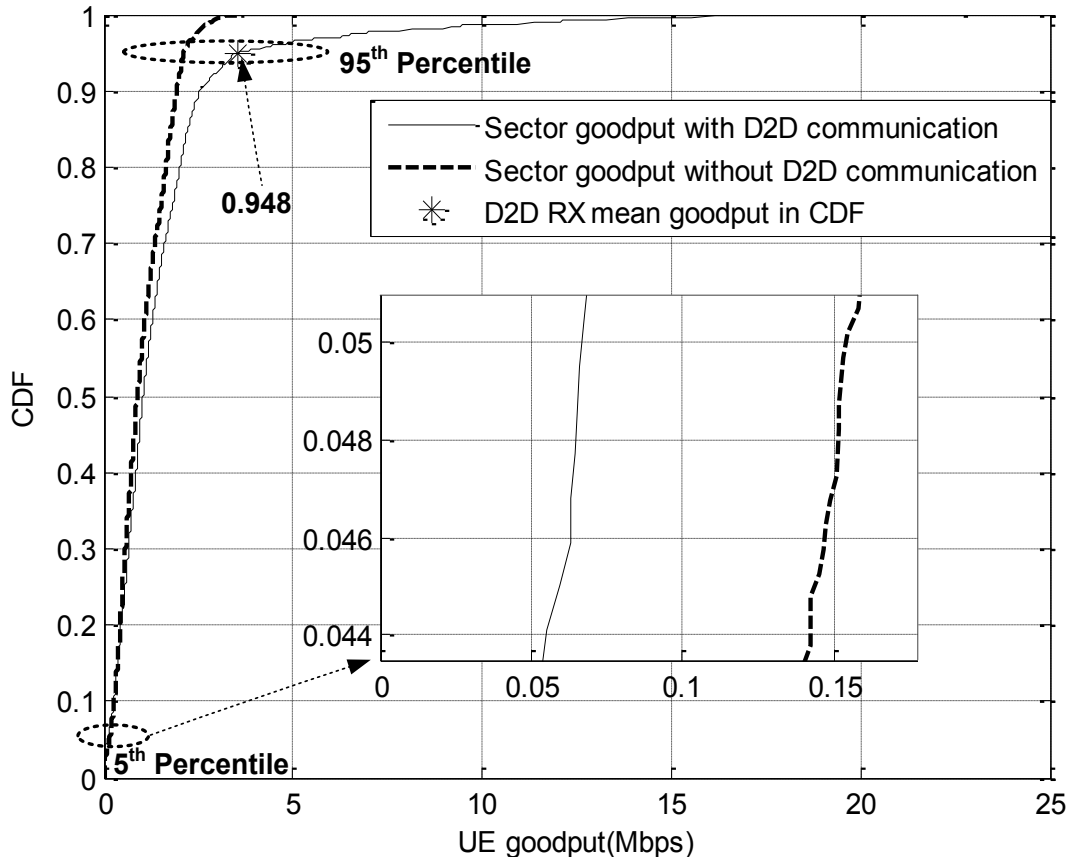

Figure 5-6 CDF of UEs goodput distribution with and without D2D transmission

In the graph, the 5th percentile represents the cell edge performance (i.e. for UEs furthest from the eNB or having poorer channel conditions), while the 95th percentile shows the best UE performance in the target sector. Thus, the CDF for two different

scenarios is compared to illustrate the performance gain in the result: one scenario includes D2D UEs, while the other scenario emulates a typical network with only cellular UEs. Both eNB and D2D TX power were at maximum, and the minimum distance between the D2D pair (which is 10 m in this study) was also maintained for the D2D transmission inclusive scenario during the simulation. A total of 1000 samples were plotted for each of the scenarios compared in the graph.

The result shows that achievable goodput of UEs in the sector is greater even with just a single pair of D2D UE included. This is particularly evident at the higher end of the distribution (from 70th percentile). The asterisk marker indicates the goodput position of the D2D RX in the empirical CDF. On average, the D2D RX performed better than 94.8% of the cellular users in the same sector. However, the goodput of the cell edge UEs has shown to degrade by almost 100 kbps when a pair of D2D UEs is included in the sector. This is shown by the graph inset of the result (in Figure 5-6), which shows cell edge goodput of 60 kbps and 150 kbps with and without D2D communication included respectively. The performance degradation results from interference impact of the D2D TX in the hybrid network as demonstrated in Figure 5-5.

5.4 Interference mitigation in hybrid network

Despite the potential gains of D2D communication in LTE-A networks demonstrated by the results in the preceding section, a major limitation and design question is the interference management between UEs of the different modes (i.e. D2D and cellular mode) in the network [65]. This is mainly because D2D UEs utilise the same frequency and time resources simultaneously with the cellular entities of the network. An example using a single cell scenario is shown in Figure 5-7.

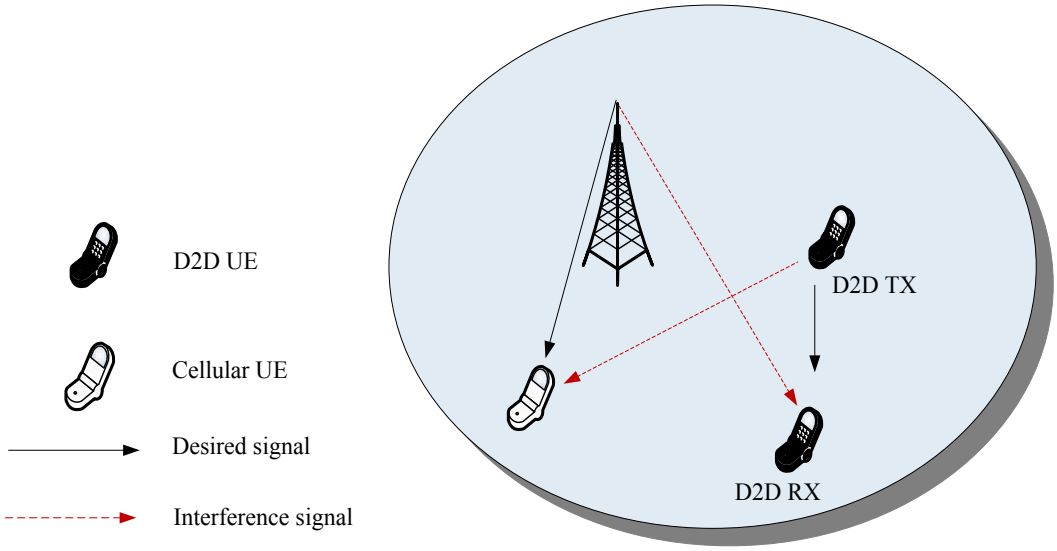

Figure 5-7 Illustration of D2D interference in a single cell using the DL resources

Considering a DL implementation for this research investigation, the description of the interference limitation is focused on only the DL aspect (where DL cellular RBs are reused for D2D transmission). As shown in the figure, a D2D TX may cause interference to the cellular UEs receiving DL traffic at the same time [65]. Using the earlier described scenario (from the system model in Figure 5-1), the inclusion of the technology compromises the intra-cell interference (interference between entities in the same cell or sector) of the resource allocation/transmission in the network: as the DL implementation of the LTE network is based on OFDMA, inter-symbol-interference is eliminated with the use of guard intervals (hence eliminating intra-cell interference) [139]. Generally, a common solution for improving the SINR of UEs in different cells is by implementing power control in the cellular networks [156]. Extending this to the hybrid network (a network with both cellular and D2D UEs), the power control scheme could equally mitigate interference between the UEs of the different modes in the network.

5.4.1 Current research initiatives

Research papers in literature have proposed the allocation of reserved RBs for D2D communication, which are orthogonal or separate from that of the cellular UEs [157, 158] in order to mitigate intra-cell interference. While there is no interference between UEs in the different modes (i.e. cellular and D2D modes) when using the orthogonal sharing method, this however leads to low resource utilisation, and therefore lower achievable throughput in the hybrid network [159]. This is because both the cellular and D2D UEs will have limited available resources for transmission in the resource sharing mode. In [67], a simple power control was proposed to minimise the SINR degradation of cellular UEs in a single cell scenario. Interference to UEs was considered however only between the cellular and D2D channels within a single cell (abstracting the interference signals from the neighbouring cells). A multi-cell D2D network was studied in [160, 161], where the proposed algorithms in the literature require centralised coordination between a set of cells. In [161], both the D2D TX and eNB are continuously transmitting at full power, and all the UEs (both in cellular and D2D mode) return instantaneous CSIs to the eNB. This introduces massive overhead in addition to the UEs geographical location (which requires a GPS as reported in [160]) required to implement the proposed interference mitigation algorithm. For the implementation in [160], the cellular UE is further required to evaluate and report information of victim (of interference) D2D UEs to its eNB, hence, increasing overhead at the UE side.

Following the analyses from the current literature, a novel power control algorithm, which involves D2D TX power reduction, is proposed in this thesis. The proposed algorithm aims to achieve a better overall performance of both the cellular and D2D

UEs, with minimum complexity/overhead and maximum resource utilisation in the hybrid network. Hence, the alteration of the D2D TX power in this model is based on simple UE feedback to a single eNB in order to minimise overheads, while the D2D UEs reuse all the cellular RBs so as to improve resource utilisation [159] compared to the existing method, such as in [158]. Additionally, interference is not only considered from eNB and D2D TX (as in [67]) in the simulation model, but also from neighbouring eNBs surrounding the target sector as shown in the system model and from Equations 5-1 to 5-3. This is because the performance of the UEs in the sector will be affected by the presence of interference power from neighbouring eNBs signalling and transmissions (especially at the cell edge) in addition to the interference power from the D2D TX or sector eNB.

5.5 Proposed power control algorithm with power reduction

The detailed procedure of the proposed power control algorithm is shown in Figure 5-8.

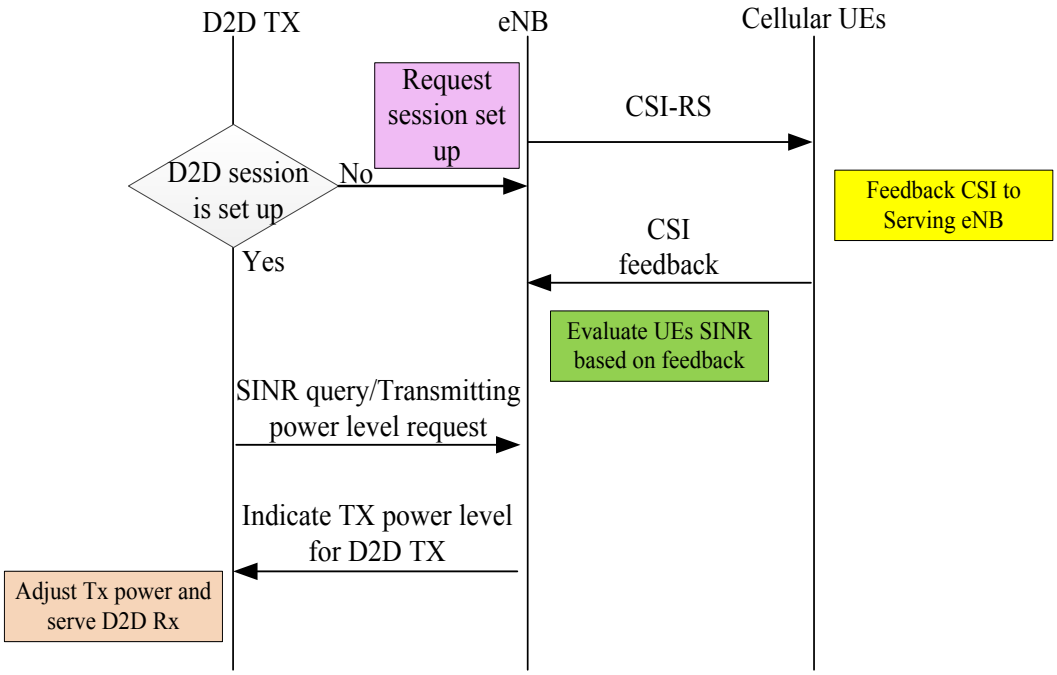

Figure 5-8 Procedure of the proposed power control algorithm

The algorithm requires control signal sharing between the cellular transmitter (eNB) and the D2D TX. As it is the case for a typical LTE network signalling, the eNBs (the target sector eNB in this instance) transmits CSI reference signals (CSI-RS) in order for the UEs to measure and estimate the DL channel [162]. UEs in the target sector then feedback their CSI to the sector's eNB, which includes the link quality as experienced by the CSI-RS. Unlike the algorithms in [160, 161], the CSI of the D2D UEs is not reported to the sector eNB to minimise overhead.

In this algorithm, a minimum SINR threshold is then defined (MIN_{th}), which is compared to the instantaneous cell edge SINR of the cellular UEs ($cellUEs_{CE}$). Additionally, a maximum SINR value (MAX_{th}) is equally set to achieve minimum D2D transmission gain: MIN_{th} indicates the minimum cell edge SINR for cellular UEs, while MAX_{th} indicates a set value where interference impact from D2D transmission will have minimal effect on the cellular UEs to achieve MIN_{th}. A D2D session set up is then initially requested by the D2D TX, which is required just once to initiate D2D transmission. Subsequently, the D2D TX then sends a request for D2D transmission power level from the target sector eNB periodically. The power level of the D2D TX is classified into four groups (shown in Table 5-2) from the maximum D2D TX power i.e. $P_{D\max}$, and selected according to the difference between the instantaneous SINR of the cellular UEs compared to both MIN_{th} and MAX_{th}. The D2D TX then adjusts $P_{D\max}$ based on the outcome of the target sector's SINR evaluation (for the cellular UEs). This is in contrast to [161], where both the eNB and D2D TX were set to transmit at full power throughout the simulation. This is then

repeated continuously to maintain a good performance of the cellular UEs, while avoiding maximum power usage of the D2D TX for the entire TTIs.

Table 5-2 Conditions for D2D TX power reduction in power control algorithm

Conditions for D2D TX power allocation
Set $\boldsymbol{MAX_{th}}$ and $\boldsymbol{MIN_{th}}$
if TTI = 1 *(D2D TX power =* $\boldsymbol{P_{Dmax}}$*, eNB transmit power= maximum)*
else *(for all cellular UEs in target sector)*
for $\boldsymbol{j}$ = TTI 2 : end
$\boldsymbol{P}$ = *cell edge SINR from TTI j – 1 (for cellular UEs)*
if $\boldsymbol{P \leq MIN_{th}}$,
D2D TX power = $\boldsymbol{P_{Dmax}/4}$
if $\boldsymbol{P \geq MAX_{th,}}$
D2D TX power = $\boldsymbol{P_{Dmax}}$
if $\boldsymbol{MIN_{th} < P < MAX_{th}/}$ 2,
D2D TX power = $\boldsymbol{P_{Dmax}/2}$
if $\boldsymbol{MIN_{th} < P <}$ *3* $\boldsymbol{MAX_{th}/}$ 4 && $\boldsymbol{P > MAX_{th}/}$ 2,
D2D TX power = $3\boldsymbol{P_{Dmax}/4}$
end ***for***
end ***if***

While the value of $P_{D\max}$ is acquired from the 3GPP standard in [109], the minimum D2D TX power is acquired from the performance evaluation in Figure 5-5 in the preceding section. The result shows that ample D2D performance gain can be achieved with minimum interference impact on the cellular UEs in the same sector with a D2D TX power of 50 mW. Hence, the inclusion of MAX_{th} ensures fairness to the D2D transmission while minimising the interference impact on the cellular UEs.

5.5.1 Performance evaluation of proposed power control algorithm

The SINR and goodput distribution of the target sector UEs are presented using boxplots and CDF respectively in this section. The graphs are evaluated using

different scenarios: in one scenario, both the D2D TX and target sector eNB are transmitting at maximum power (max. power) throughout the simulation, while the power control algorithm proposed in Figure 5-8 was implemented in another scenario. In order to critically assess the result, a third scenario was included where the D2D TX transmits at average power ($P_{D\max}/2$) throughout the simulation period, hence establishing an intermediate test factor scenario for the two extremes i.e. with maximum power and with power control. The SINR of each UE is averaged over 100 TTIs in each of the multiple iterations to achieve accurate results and evaluate diverse environments in the simulation. Thus, a total of 1000 samples were considered for each of the UEs (both cellular and D2D RXs) in the results. The SINR distributions of the D2D RX and cellular UEs for the different scenarios evaluated are shown in Figure 5-9 and Figure 5-10 respectively.

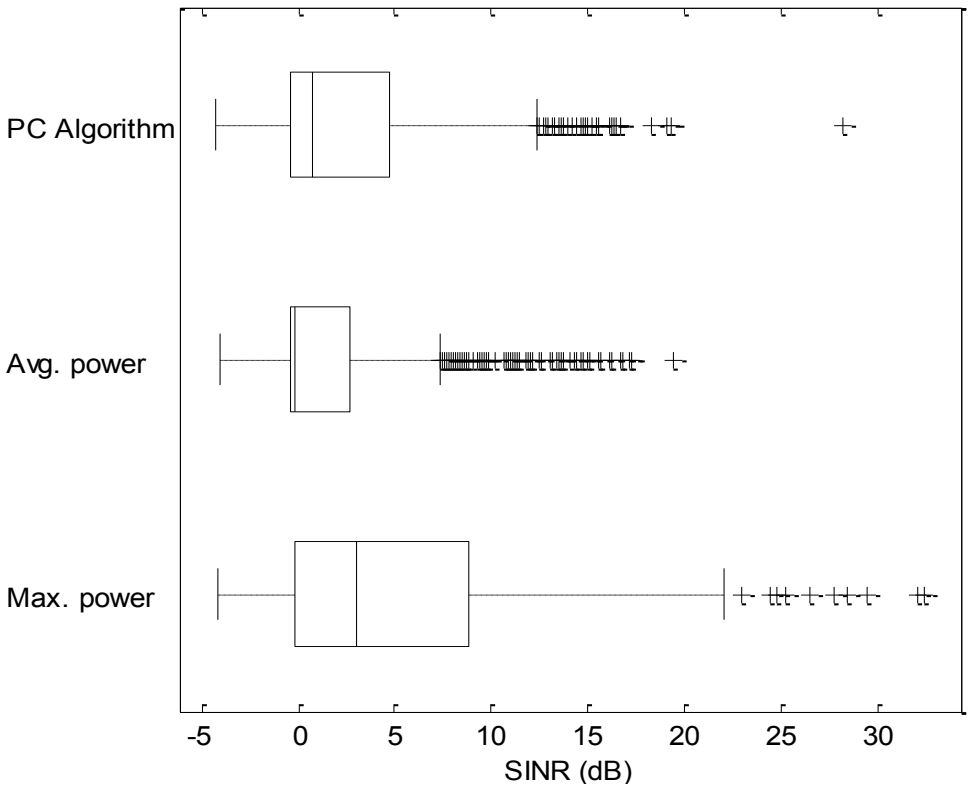

Figure 5-9 SINR distribution of the D2D RX with and without power control

As expected, the scenario with maximum power is significantly better with a median SINR of 3.0 dB, as opposed to -0.1 dB for the average power scenario for the D2D RX (shown in Figure 5-9). Although the SINR of the D2D RX is lower with the power control algorithm (median SINR of approx. 2 dB), it however equally outperforms the average power scenario. This indicates sustained performance of the D2D RX, which is as a result of including the MAX_{th} variable in the algorithm as explained in the preceding section.

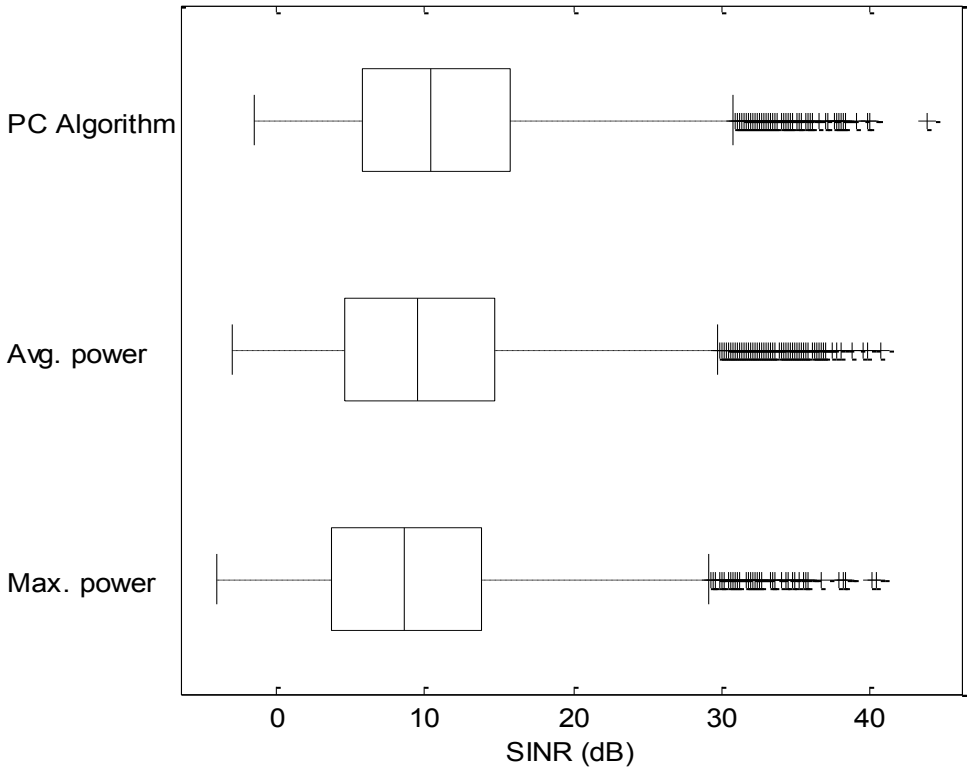

Figure 5-10 SINR distribution of the cellular UEs in the target sector

Unlike the D2D RX performance, the power control included scenario shows better SINR performance for the cellular UEs compared to the other scenarios in the graph presented in Figure 5-10. The result shows that the cellular UEs SINR with the power control algorithm has a median of 10.5 dB in contrast to the average power and

maximum power scenarios with median SINRs of 9.5 dB and 8.7 dB respectively. Another important outcome from the result of the power control scenario is that the lower fence (which represents the 5th percentile on a CDF graph) is equally better with approx. 3 dB gain compared with the maximum power scenario.

The overall SINR of the target sector UEs i.e. cellular and D2D RXs for the different scenarios studied are presented in Figure 5-11: with a total of 9000 samples from the target sector UEs. The median of the target sector SINR with power control is 10.5 dB, which was better than the median in the average power scenario of 9.1 dB and 8.5 dB for the maximum D2D power scenario. The lower bound fence SINR of the target sector has equally improved with up to 2.4 dB in the power control scenario over the maximum power scenario.

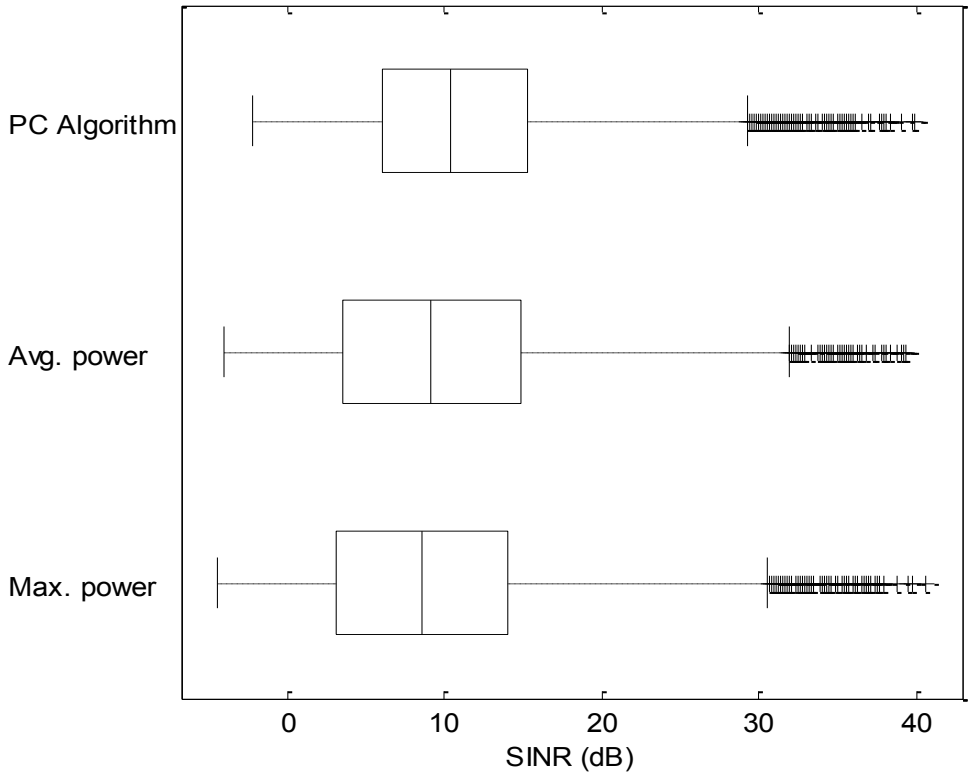

Figure 5-11 SINR distribution of both cellular and D2D UEs in target sector

Additionally, the goodput distribution of the UEs in the hybrid network is presented in Figure 5-12. Extending the scenarios studied in Figure 5-6 i.e. with and without D2D transmission, the power control scenario (with D2D transmission) is included in this result. The zoomed graph inset highlights the cell edge of the UEs in the target sector. It is shown that while the goodput distribution with the power control scheme still maintains the performance improvement trend of the traditional D2D transmission scheme, the latter has also shown over 3 fold improvements in the cell edge performance in the sector. It also shows that cell edge goodput with the power control scheme marginally edges that of the non D2D transmission scheme (which does not have any form of intra-cell interference, contrary to the D2D inclusive scenarios).

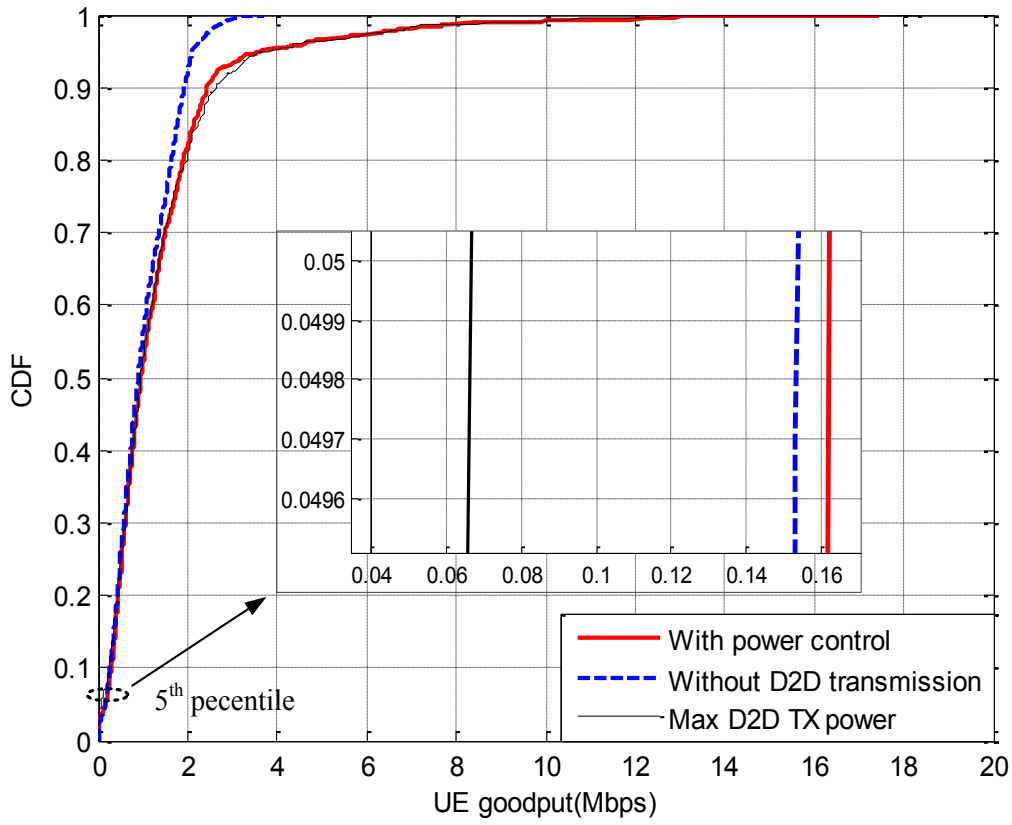

Figure 5-12 Goodput of target sector UEs with and without power control scheme

5.6 Multihop transmission for relaying D2D traffic

The performance gains of D2D communication underlaying cellular networks have been comprehensively studied in the preceding sections of this chapter. The study has demonstrated the proximity and power gain of D2D communication, and also the impact of interference from D2D transmission on cellular UEs in the same cell. Additionally, a novel power control algorithm was proposed and implemented to mitigate interference between cellular and D2D UEs, in the direction of current research initiatives [157, 158].

It has been projected that a key goal for future cellular networks is to achieve Gbps user experience [163]. Thus the work in this chapter is further extended to include Multihop (MH) transmission for D2D traffic as a viable option to further improve the user experience (in terms of throughput and SINR) in the network. MH communication entails using relay stations (fixed or ad hoc) as intermediate nodes between base stations and their corresponding mobile hosts (i.e. UEs in this context) [74]. This has been considered over the years as a solution to increase network capacity, cell coverage, and hugely reduce call blocking in cellular networks. Hence, applying the concept of MH in D2D communication could be useful in achieving its envisioned potential [164]. This will especially be more useful when applied in circumstances of poor channel conditions or long distance transmission (between D2D pairs) for the direct links in D2D communication.

Like every useful transmission scheme, MH transmission requires additional functionalities in order to be effectively accomplished, which includes relay selection and session set-up [165]. This study however focuses on illustrating the performance

gain of the transmission scheme as an additional functionality to D2D communication. Nonetheless, one way of achieving relay selection is by exchanging pilot signals between potential relay nodes (i.e. nodes within the path of the sending and receiving nodes) to establish the most suitable node/path based on the channel quality to the intended receiver [165]. Equation (5.4) represents a common combination method to determine ideal relay nodes, where the 'minimum' function (min) is used to appraise the node with the best channel condition, known as the max-min CSI relay selection [80, 165].

$$h_i = \min(h_{SRi}, h_{RiD}) \tag{5.4}$$

where h_i represents the instantaneous channel quality, h_{SRi} represents the channel gain between the source node and the relay node, and h_{RiD} represents the channel gain between the relay node and destination node.

Thus in the devised model, the distance based relay selection method [80] was adopted: i.e. an idle UE closest to the D2D RX is selected as the ideal relay for MH transmission. The relay selection scheme has less complexity, as it does not require frequent update of channel information of the relay candidates by the transmitting node. Despite the simplicity of the relay selection scheme, it is nonetheless rarely considered in cellular environments for MH communication. This is mainly because of the signal vulnerability due to deep fading when it travels long distances in the network (which typically has a large area i.e. macrocells). However, since D2D communication entails short distance communication, this method is considered in this work as a more efficient relay selection strategy. From Equation (5.4), the distance based relay selection scheme can be represented as:

$$d_i = \min(d_{SRi}, d_{RiD}) \tag{5.5}$$

where d_i represents the distance, d_{SRi} is the distance between the D2D TX and idle node, and d_{RiD} represents the distance between the idle node and the D2D RX.

The same system model from Figure 5-1 is reused for this investigation. The difference in the system set-up is with the presence of an idle UE between the D2D pairs in the target sector as shown in Figure 5-13. The typical handshake process in relay selection was alternatively represented by additional delay in the model to achieve more accurate evaluation. This is traditionally executed by the source node broadcasting ready-to-send pilot signals, and the potential relays (idle UEs) replying a clear-to-send signals in consecutive TTIs as mentioned earlier [80].

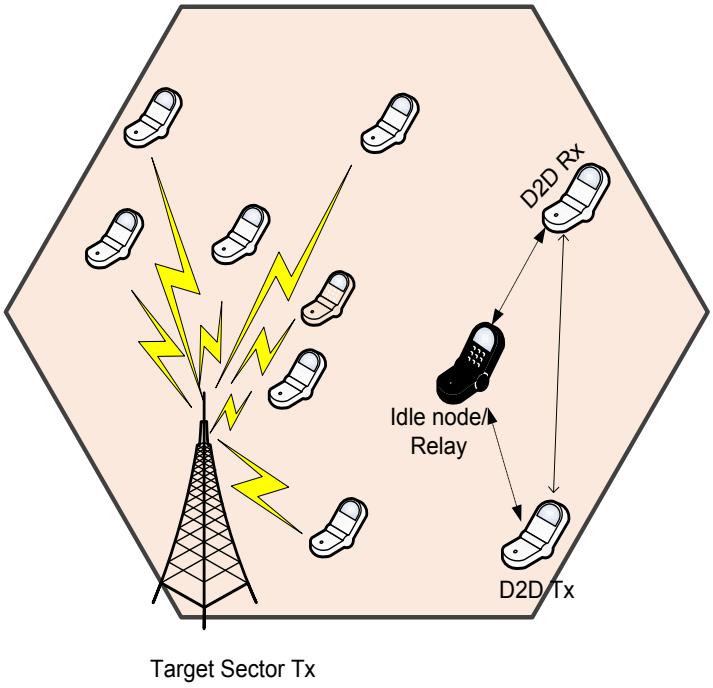

Figure 5-13 Illustration of MH D2D transmission set-up

Additionally, a two-hop (i.e. one relay) MH communication is implemented between the D2D pair to reduce complexity of the system. A non-contention based MH transmission scheme was adopted for this model; hence, the D2D TX and relay node

transmit simultaneously, assuming a full duplex MH transmission [165]. The full duplex MH transmission has its limitation as it may require some interference coordination (since both D2D TX and Relay node are transmitting simultaneously). Considering the low power (0.2 W) required for D2D MH transmission, this limitation is however considered to be minimal and assumed to be perfect in this study.

5.6.1 Performance evaluation of the MH transmission scheme

As mentioned earlier, the focus in this investigation is on the increase of performance gain for D2D UEs with MH transmission compared to the Single Hop (SH) transmission, in view of attaining substantial upsurge in user experience for future networks. Thus, the results presented in this section specifically illustrate the end-to-end D2D RX performance in the network (performance at the D2D RX with allocated RBs from the D2D TX) with less emphasis on relay selection methods as investigated in some of the aforementioned literature. Nonetheless, the D2D RX performance with SH transmission for different distances between the D2D pair (between 10 to 40 m) was included in the results as a benchmark for comparison. The results are mostly represented using a CDF, where the 95^{th} percentile was used a reference point to compare the distributions. This is because the reference point indicates the best achievable goodput in the network i.e. for UEs closest to eNB or with best channel conditions.

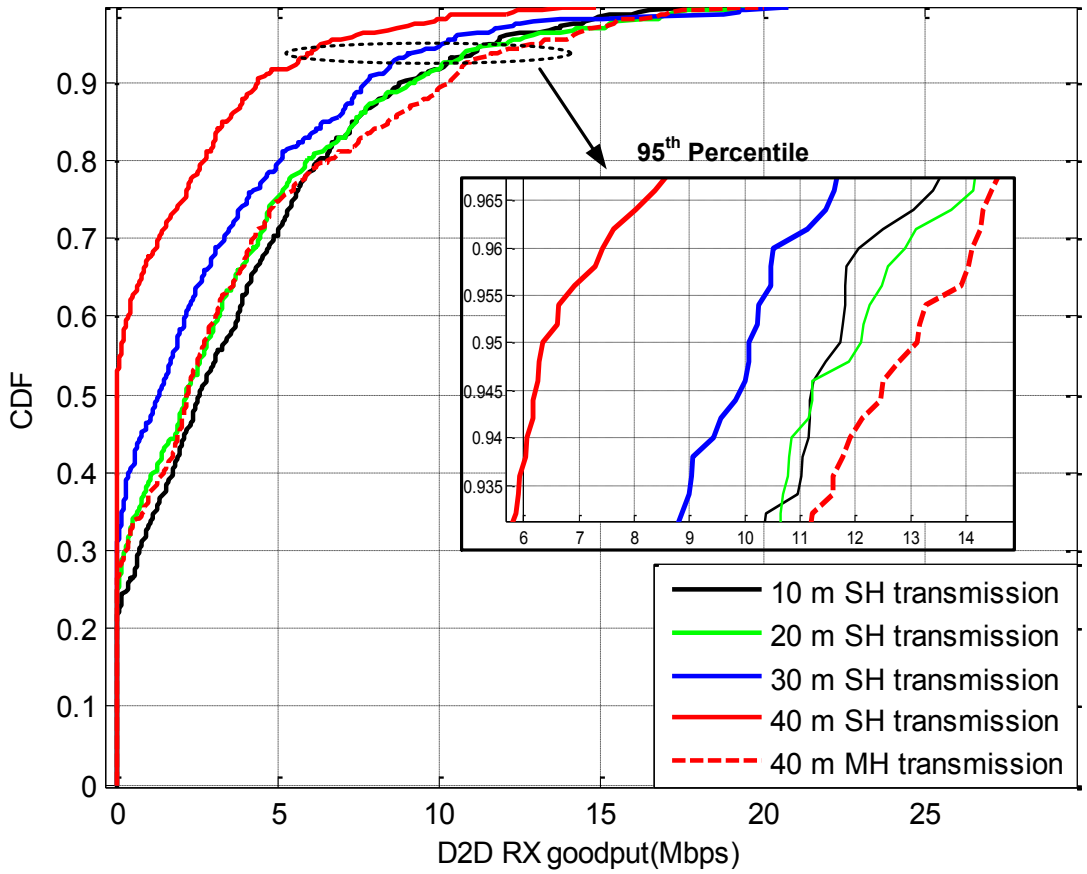

Figure 5-14 Goodput distribution with increasing distance between the D2D transceiver

In Figure 5-14, the goodput distribution of the D2D RX with MH transmission is compared with increasing distance from its transmitter (i.e. D2D TX), using SH transmission. As expected, the D2D RX goodput decreases with increasing distance between the pair for SH transmission. The D2D RX goodput with MH transmission was included in the result, selecting the furthest distance in this study i.e. 40 m, to illustrate the performance gain compared to the SH distributions in the result. The result shows significant goodput gain with relay assisted (i.e. MH) D2D communication for longer distance transmission between the pair. While the goodput of the D2D receiver was 12.1 Mbps at the 95th percentile of the distribution for 10 m

between the pair, the equivalent with 40 m distance between the pair was 4.1 Mbps with SH transmission. With MH transmission however, the D2D UE significantly outperforms the SH transmission scenario at the point of reference (i.e. 95th percentile, with 40 m distance between the pair) attaining over 6 Mbps difference in goodput. To distinctively clarify the result in Figure 5-14, the mean goodput of the D2D RX distribution is provided in Figure 5-15.

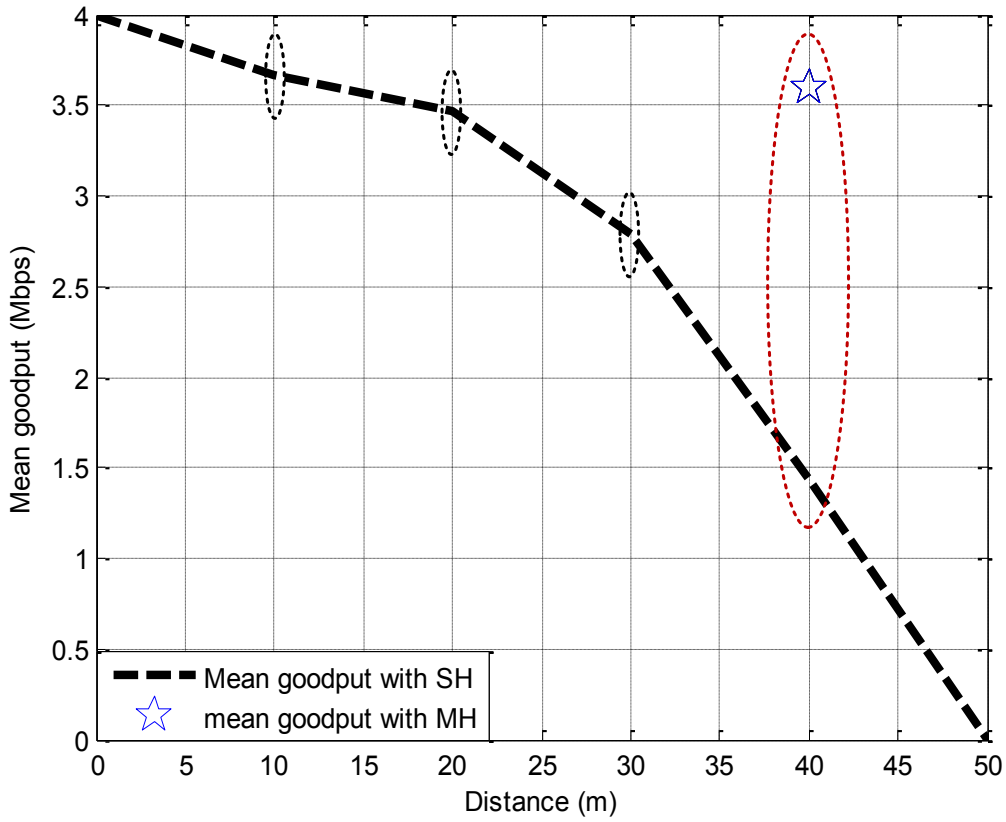

Figure 5-15 Mean goodput of the D2D RX with increasing distance between the D2D pair

The mean value of the distribution takes the outliers into consideration (i.e. extreme bursts in a distribution), hence considered as a good tool to illustrate the central tendency of a distribution. As shown in the result, the mean goodput of the D2D RX was 3.7 Mbps for 10 m distance between the D2D pair, and approx. 1.5 Mbps when they are 40 m apart with SH D2D transmission. Similarly in the result, the mean

goodput of the D2D RX with MH transmission is also included. The result shows that the mean value of the D2D RX is better with MH transmission with up to 2.2 Mbps compared to SH transmission with the same distance between the D2D pair (i.e. 40 m in this study).

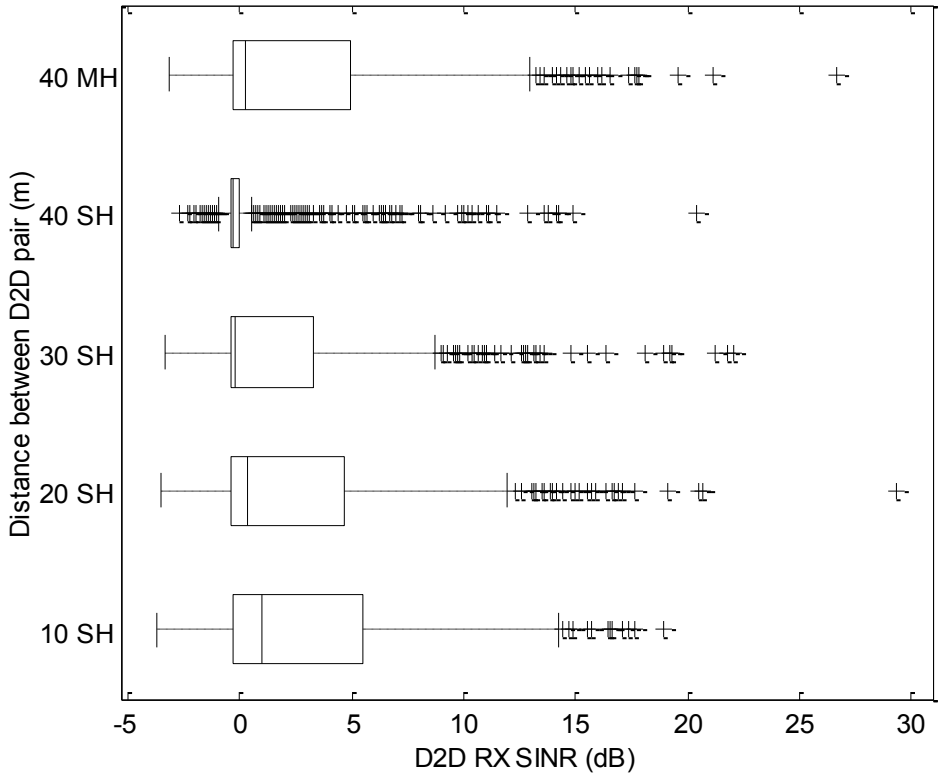

Figure 5-16 D2D RX SINR with increasing distance from the D2D pair

The SINR distribution of the D2D receiver is evaluated between the different distances in Figure 5-16 using a boxplot. It can clearly be observed that the SINR is much better for the D2D UE when MH transmission is used instead of SH. The median of the UE with 40 m between the D2D pair is less significant when compared to 20 m SH transmission (0.2 dB and 0.3 dB for 40 m and 20 m respectively). The minimal difference in the performance is associated to the additional delay in the relay selection for the MH transmission. The overwhelming outliers for the 40 m distance in the results are from the fluctuating performance from the different iterations. This is however considered in the result since the point of reference (i.e. the

median value in this result) takes the outliers into consideration. However, the median value remains consistent between the different distances i.e. the mean SINR keeps decreasing with increasing distance between the D2D pairs as expected.

In addition to these results, the goodput distribution for both cellular and D2D UEs (where applicable i.e. for D2D inclusive scenarios) in the target sector is shown in Figure 5-17. The three different scenarios compared include: a complete cellular transmission scenario, a cellular transmission with SH D2D transmission/scenario included, and cellular transmission with MH D2D transmission scenario. While the cellular UEs were mobile during the simulation (random walk), the D2D mode UEs which includes the relay/idle UE were fixed to establish a common ground for comparison in the D2D inclusive scenarios (i.e. for the MH and SH D2D transmission scenarios); thus the D2D pair were 40 m apart in both scenarios.

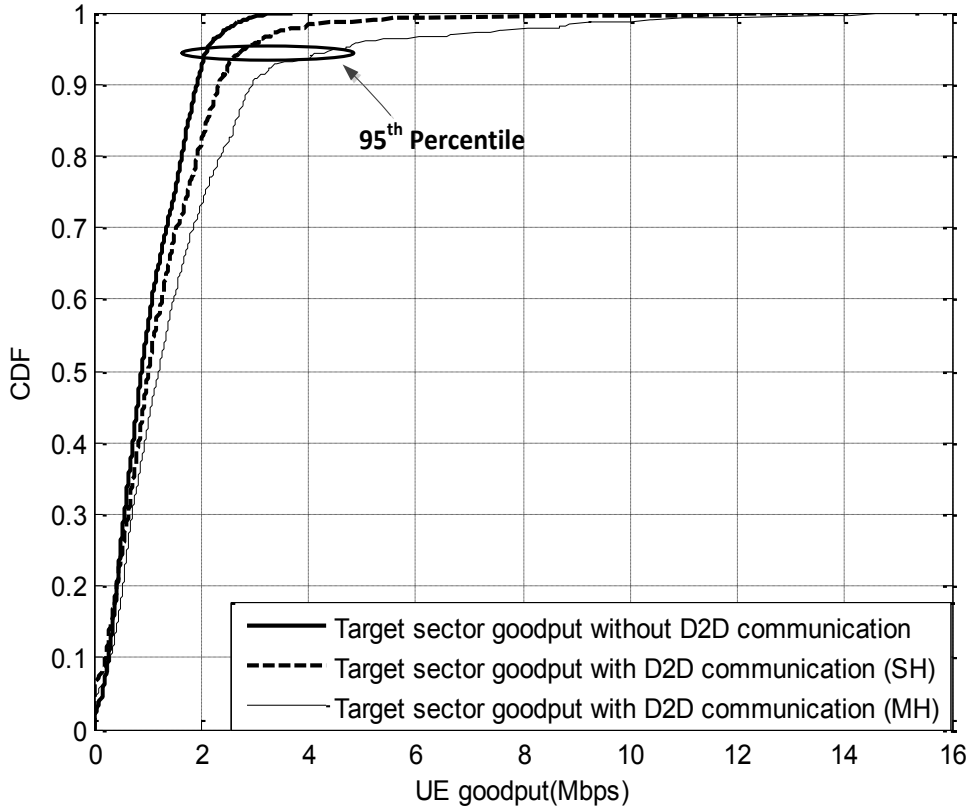

Figure 5-17 Target sector UEs goodput with SH and MH D2D transmission

From the results in Section 5.3, it has been established that the target sector's UE goodput improves, especially at the point of reference (95^{th} percentile) with up to 0.8 Mbps when D2D communication was included. This result further shows significant improvement of up to 2 Mbps when the D2D traffic was carried via MH transmission compared to SH transmission. This totals approx. 3 Mbps goodput gain with MH D2D communication compared to a cell with only cellular transmission. Thus, this shows that MH D2D communication can further increase the achievable goodput in a LTE-A network that includes D2D communication.

5.7 Summary

Following the detailed comparative study in the previous chapters of this thesis, D2D communication has been identified as one of the promising add-on technologies to achieve the envisioned data rate increase in the future wireless networks. One major advantage of the technology is that it reuses cellular network resources while using small power transmission, without the need for opportunistic transmission (i.e. transmitting only when cellular UEs are idle) as it is the case for CR, or additional infrastructure as required for small cells in HetNets. Thus in this chapter, D2D communication as an integral part of an LTE networks has been explicitly studied.

The performance gain of the technology in the network was evaluated using simulation results from the LTE SLS implemented in the preceding chapters of the thesis. The result shows that a D2D RX can achieve over 3 Mbps mean goodput at close proximity and maximum transmission power from the D2D TX, which is better than 2 Mbps achieved by a traditional cellular mode UE at close proximity and/or similar channel conditions from its serving eNB. One major issue of the hybrid

network (i.e. consisting of UEs in both cellular and D2D mode) however is the impact of interference from the D2D transmission, as it occurs simultaneously with cellular transmission in the same cell/sector. The cell edge performance of the investigated sector has been shown to diminish with over 100 kbps with just a single D2D pair transmission. Thus a power control algorithm was implemented with the aim of achieving the performance gain of including the technology, while restoring the performance degradation at the cell edge of the investigated sector. The algorithm entails setting a minimum and maximum SINR threshold so as to achieve a minimum performance for the cellular mode UEs, while avoiding complete deferring of the D2D mode UEs performance. In this way, the D2D TX power is varied based on simple CQI feedback from the cellular UEs, which is then evaluation by the eNB. Simulation results show that the SINR of the cellular UEs has improved with almost 3 dB gain compared with continuous maximum power transmission of the D2D TX, while the D2D RX still performs better than a scenario with continuous average power transmission.

Additionally, MH transmission for D2D traffic has equally been identified and studied as a viable option of further improving the performance gain of D2D communication in the LTE network. A simple model was devised using a single relay (i.e. a total of 2-hops) between the D2D pair, where a simple distance based relay selection was employed. Simulation results showed that the D2D RX achieved over 2 fold increase in SINR when using MH transmission from the same distance between the D2D pair. The result also shows that a sectors' goodput has improved with almost 2 Mbps with MH D2D transmission compared to the traditional D2D transmission.

Chapter 6

Research Summary and Future Work

6.1 Introduction

In this chapter, the research drive for this thesis is first of all summarised. It substantiates the motivation for research on projected secondary technologies for the current 4G LTE network standard and subsequent 5G networks. Thereupon, a comprehensive summary and outcomes of this research are presented, which includes results from the performance investigations and proposed algorithms implemented in the research carried out. The thesis highlights leading research organisations, their initiatives, and technologies projected for implementation of the future cellular networks (i.e. 5G). Principally, this thesis develops a comprehensive DL LTE SLS which includes 4G and beyond capabilities. This includes a new proposed interference modelling technique, which advances the traditional WA approach by maintaining flat surface topology, and hence applicable to any flat surfaced map with less overheads. Subsequently, the thesis was further extended to include inter-cell coordination (CoMP) with a proposed algorithm based on UE location. Furthermore, an effective power control algorithm based on power reduction was proposed, and MH transmission for D2D traffic was studied to maximise the gain of UEs to attain higher data rates for future cellular networks. Finally, the chapter concludes by presenting/suggesting additional topologies and future research directions that could further enhance the investigated technologies in this thesis, and the cellular network performance in general.

6.2 Research drive

The continuous reduction in terminal costs and mobility has influenced continuous popularity of mobile communication in recent times. These advantages have inclined rapid research towards integrating wireless networks to add user mobility to the enormous data rate offered by the wired medium, such as fibre optics/optical networks. The network has grown over the years from providing basic voice services to the current trend of including real-time HD video and high-speed data services to end users. With the bandwidth bottleneck in the wireless networks however, mainly due to limiting factors such as fading, pathloss, and transceiver equipment constraints amongst others, numerous standards have been continuously developed to satisfy the increasing demand of these earlier mentioned services to the growing subscribers. The network evolution has led to the currently deployed 4G network standards such as the LTE (under the auspices of the 3GPP). The LTE network is specified to provide up to 100 Mbps and 60 Mbps DL and UL respectively with the initial release (LTE release 8), and up to 1 Gbps (for both DL and UL) for the recently standardised LTE-A i.e. release 10 and beyond [126].

The LTE networks have edged other 4G standards such as WiMAX 2 (i.e. IEEE 802.16m) [46] due to its flat all-IP architecture and significantly lower latency, in addition to its backward compatibility with existing 3G technologies (this significantly eases migration from the widely deployed 3G networks). In addition to the earlier mentioned drawbacks of the wireless network transmission, one of the performance limitations of LTE networks is the cell edge UE constraints associated with the universal reuse factor of the network i.e. all cells/sectors use the same spectrum. Hence, the cell edge UEs suffer from inter-cell/inter-sector interference

from transmission by the neighbouring eNBs. Thus the 3GPP have identified CoMP (inter-cell/site coordination) as a viable scheme in proffering solution to this limitation, which includes implementing CoSH/CoBF or JP schemes to achieve coordination in the DL of the network: UL CoMP implementation is specified to be vendor specific [52]. This has in turn channelled research towards providing and/or optimising algorithms to efficiently carry out CoMP in the LTE networks. In order to test these algorithms however, an efficient simulation platform is required to accurately represent the network. This greatly reduces CAPEX as the algorithms are critically tested and analysed prior to field deployment or enhancements. The availability of such platforms is however very limited, and hence hinders vast tests and algorithms in the research community. Thus, it has been prioritised as a key objective to firstly implement a comprehensive LTE SLS, which adheres to the 3GPP standard models and includes the projected technologies investigated, as a giant initial step to the accomplishment of this research.

Additionally, numerous candidate technologies are projected as key factors in achieving the dramatic data rates anticipated for the forthcoming 5G networks. These technologies include D2D communication, CR, and Heterogeneous implementation of the networks (i.e. HetNets) amongst others [32, 33, 157]. While all the mentioned technologies are equally promising in achieving their targeted aim, D2D communication is of particular interest in this research. One reason for this is that the technology has the ability of reusing the whole cellular resources simultaneously with cellular transmission in the network. This is achieved by short distance transmission (between 20 m to about 100 m), to attain high performance gain with very low power requirement. For technologies such as CR however, the secondary/unlicensed UEs

only access the spectrum when the primary/licensed UEs are not using them (referred to as opportunistic transmission). It further requires complex spectrum sensing algorithms prior to the utilisation by the secondary UEs. In the case of HetNets, additional fixed infrastructures (i.e. low power base stations) are required to increase the capacity of the network. The D2D technology however still has more power efficiency as it requires just about 0.2 W transmitter power in the LTE network for the D2D TX, without the need for any additional infrastructure. As an example, up to 1 W [166] TX power could be required for a small base station in a Pico cell.

One major limitation and design question for adopting the D2D technology is the impact of interference with the simultaneous transmission from both D2D TX and cellular TX (i.e. eNB), considering a DL implementation. In this perspective (i.e. DL), the D2D RX gets interference from the eNB, while the cellular RX gets interference from the D2D TX. A straightforward solution proposed for this problem is by reserving part of the cellular RBs for D2D communication. While this ensures orthogonal resource utilisation between the two modes (i.e. cellular and D2D), it however compromises the maximum resource reuse capability of the technology [155]. Another approach currently investigated is the application of power control to mitigate this interference in the hybrid network (network with both cellular and D2D transmission) [66].

Thus, this thesis endeavours to address these issues by first of all implementing and optimising an efficient LTE SLS platform to accurately and timely obtain performance metric for the UEs in the network. Consequently, performance gain of inter-site coordination is equally illustrated by implementing a CoMP algorithm to

improve cell edge UE performance in the network. Furthermore, D2D communication as an integral part of the LTE network is also evaluated. This includes MH transmission for D2D traffic and implementing a power control algorithm to mitigate the impact of interference in the network while utilising maximum resources for D2D communication.

6.3 Thesis summary and outcomes

In this thesis, the evolution of wireless networks to the current 4G standards (such as mobile-WiMAX and LTE) was thoroughly detailed to begin with. The LTE network was shown to be more popularly adopted compared to other 4G standards with reports from GSA showing over 90 LTE networks commercially launched during 2012, and additional 83 networks anticipated in different countries around the world by the end of 2013. On major reason highlighted for the dominance of LTE network standard is its backward compatibility (it has support for legacy systems such as GSM and HSPA), in addition to increased data rates mentioned in the preceding section.

Advances towards achieving multi-Gbps data rate for future 5G networks were studied. Projects spearheaded by the EU such as METIS-2020, 5G-now, COMBO, MiWaves, are currently leading research with sufficient funding available to achieve this initiative by the year 2020. Some measures identified in the study to achieve the dramatic data rates increase includes adopting new protocols, procuring additional spectrum, and/or implementing additional technologies to enhance the network capacity. Some of these technologies include massive MIMO, CR, CRANs, D2D communication, and HetNets amongst many. Further emphases were placed on enhancing the user interface to improve the capacity of the networks in the study. This

is required to enable seamless utilisation of different RATs by the UE in the future networks. One of the studies illustrated the implementation of the function (i.e. migration capability to the different RATs by the UE interface) using a new protocol referred to as 'policy router' in the core network.

One major limitation of wireless communication in general is the availability of radio spectrum (RF between 3 kHz to 300 GHz), which is not only finite and congested but also expensive to acquire. Acquiring new spectrum is currently considered as an extreme option for the 5G networks as mentioned earlier. However, it was identified from studies in this thesis that while the occupied spectrum for the TV band is currently underutilised, the cellular spectrum is however congested with increasing subscribers. Some of the studies showed that only an average of 11% of the TV band was actively used at the time it was conducted. Emerging technologies such as CR and D2D communication have been employed as prospective tools in maximising the use of the currently available spectrum in literature. Hence, this thesis focuses on efficient spectrum utilisation of the congested cellular spectrum within the currently deployed 4G networks (specifically LTE network) as an initial step towards achieving the implementation of the future network. This was achieved by implementing key functionalities such as inter-cell coordination (i.e. CoMP) and D2D communication in the network. As explained in the preceding section the CoMP functionality was implemented to improve cell edge performance, while D2D communication was employed to achieve maximum resource (i.e. RB) utilisation in the network.

To assess the performance of these technologies, a comprehensive DL SLS was implemented. The simulator completely adheres to the LTE specification and includes

appropriate channel models such as WINNER II model, the ability to simulate different channel bandwidths, and different MIMO transmission schemes such as TxD and CLSM. The SLS was implemented by abstracting the link-level functionalities using a LQM, which then outputs an SINR metric that is mapped to a LPM to determine the BLER, and subsequently the net throughput (i.e. goodput) of the UEs in a multi-cell macro network. To achieve accurate results for diverse environments, the system is run for several numbers of iterations, where the UE performance is averaged over multiple TTIs (for each of the multiple iterations). With the discrepancies from the multiple iterations due to entropies from common models such as 'random walk' UE movement and creation of the shadow fading map using lognormal function, a single shadow fading map is used (for all the iterations) to make this effect subtle as commonly done. This has been shown to minimise the aforementioned entropies and attain as close as possible realistic results from the simulations.

Consequently, an efficient inter-site interference modelling technique for 4G networks was proposed. The technique was implemented as advancement to the 'wrap around' interference modelling approach. The proposed architecture ensures more UE performance metric is logged in SLS platforms by ensuring all the cells/sectors simulated are surrounded by equal eNB sites to achieve realistic results and eliminate 'border cell' effect (cells/sectors on the border of a flat SLS model without neighbouring sites). The proposed architecture entails duplicating virtual eNBs on a single tier map to compliment the cell borders without extending the map or network entities (such as eNBs and UEs), which are introduced only during interference calculation. It also includes UE relocation algorithm where UEs are accordingly relocated to their transit eNBs in accordance to the handover functionality and to

allow easier implementation of technologies such as CoMP to be easily implemented in the network. Thereupon, the model was extended further to include a proposed CoMP algorithm, where the adaptive beamforming technique was employed to reduce interference on the cell edge UEs of the cooperating cells. The algorithm spans two TTIs, where the antenna beam is steered away from a 'conflicting border' (common cell edge of the cooperating cells) i.e. in the event of UEs from the different cells occupying the conflicting border in one TTI, and vice versa in the following TTI. Simulation results shows over 1 fold improvement (in terms of throughput) and approx. 3 dB gain in terms of SINR for the cell edge UEs in the cooperating cells.

Furthermore, D2D communication as an integral part of future cellular networks was investigated. The technology was additionally modelled in the LTE SLS to investigate the performance gain and efficient resource utilisation in the network. Results show up to 3 Mbps mean goodput for a D2D pair in close proximity with maximum D2D transmitter power, better than an average of 2 Mbps achieved with cellular transmission for UEs closest to the eNB (indicated by the 95^{th} percentile of a CDF). In spite of the high data rate achieved by close proximity D2D transmission, the impact of interference from the cellular and D2D transmission further hinders the achievable throughput (especially at the cell edge of the network). Thus, a power control algorithm was proposed to mitigate the impact of interference in the hybrid network (network consisting of both cellular and D2D UEs). The algorithm was implemented by setting a minimum SINR threshold so that the cellular UEs achieve minimum performance, and equally a maximum SINR threshold to establish farness to the D2D transmission as well. Hence if the cell edge SINR of the cellular UEs is above the maximum threshold, the D2D transmitter transmits at maximum power, while the

transmit power is varied according to some conditions to achieve performance gain for both cellular and D2D UEs in the network. Simulation results show over two fold of improvement in the cell edge throughput of the hybrid network with the power control compared to when both eNB and D2D transmitters transmit at full power for the whole TTIs. It equally shows improvement in the overall SINR distribution of the UEs in the hybrid network. Additionally, MH transmission for D2D transmission was investigated in the hybrid network. Contrary to some recent studies where D2D UEs are used to relay cellular UEs traffic, the use of idle nodes to relay D2D traffic was implemented. Simulation results show over 3 Mbps improvement in a single D2D Receivers goodput with MH transmission (for the same distance between the D2D pair with single hop transmission).

6.4 Future directions

This section summarises key features that could be further investigated in addition to the achievements in this thesis. Particularly, inter-site/cell coordination and critical evaluation of D2D communication underlaying the cellular networks have been carried out in this research. The solution for the inter-site/cell coordination in this thesis was provided by implementing a CoMP algorithm, employing the CoBF/CoSH techniques to improve cell edge UE performance. The D2D evaluation features solution to key issues anticipated for the technology's implementation in the forthcoming networks, in terms of interference management and performance enhancement of the technology itself. This was achieved by implementing a proposed power control algorithm based on power reduction and including MH transmission for D2D traffic in the networks, where numerous simulation results were presented and discussed in the thesis using a developed state-of-the-art SLS for the performance

investigations. The technologies investigated (i.e. CoMP and D2D communication) and solutions proposed can be further studied or enhanced by exploring additional investigation topologies and also combining them with some other promising technologies as follows:

6.4.1 Efficiency in implementing CoMP schemes

The CoBF/CoSH technique was adopted for the CoMP scheme implemented in this thesis. This scheme requires coordinated resource allocation/ beam forming between cooperating sites/cells so as to mitigate interference on cell edge UEs, where all the resources to a single UE is allocated by its serving eNB only. The algorithm proposed in this thesis yielded substantial improvement in the cell edge performance of the users in the cooperating cells as demonstrated in Chapter 4. Another alternative CoMP scheme proposed by the 3GPP is the JP. The latter scheme has however received less popularity in the research community, as it requires cellular resources i.e. RB to a single UE from multiple eNBs at the same time. While this could be highly beneficial, it however burdens the reduced latency prioritised to be kept minimal in current 4G and subsequent 5G networks, in addition to complexity [54]. Nonetheless, both CoMP schemes employ the X2 interface to exchange information between the cooperating cells alike. The X2 is a logical interface that is established in the EPC to make possible a communication path between eNBs in the LTE network [58]. The interface is used to carry out handover processing and/or achieve coordination by exchanging signalling information to succour processes such as CoMP in the network. A significant requirement for the LTE-A and most probably in future cellular networks is in terms of reduced latency [167]. This could however be compromised by the additional delay from the X2 interface processes (such as information exchange and coordination) involved in achieving the CoMP schemes,

especially for the JP scheme. This is because the X2 interface is not only required for control information in this scheme, but also to convey data/resources from the cooperating sites, hence adding overwhelming requirements on the virtual interface.

One promising solution highly anticipated for this limitation is by including centralised processing specifically, using the CRAN [92, 167] architecture. CRAN is an evolutionary step in BS implementation where Radio Remote Heads (RRHs) are connected using an optical transport unit to a centralised point (i.e. cloud) responsible for all Baseband Unit (BBU) processing [168]. This is an improvement to the traditional implementation, where every BS represents a single unit, which consists of its own RRH, and BBU entities closely connected together (for 3G networks implementation). The traditional implementation has shown to place a heavy burden on individual BS maintenance in terms of the CAPEX and OPEX as shown in Figure 6-1 [168]. The figure estimates the expenditure of maintaining traditional base station sites, which shows the heavy requirement from base station hardware and site support for each of the distributed sites in a traditional cellular network.

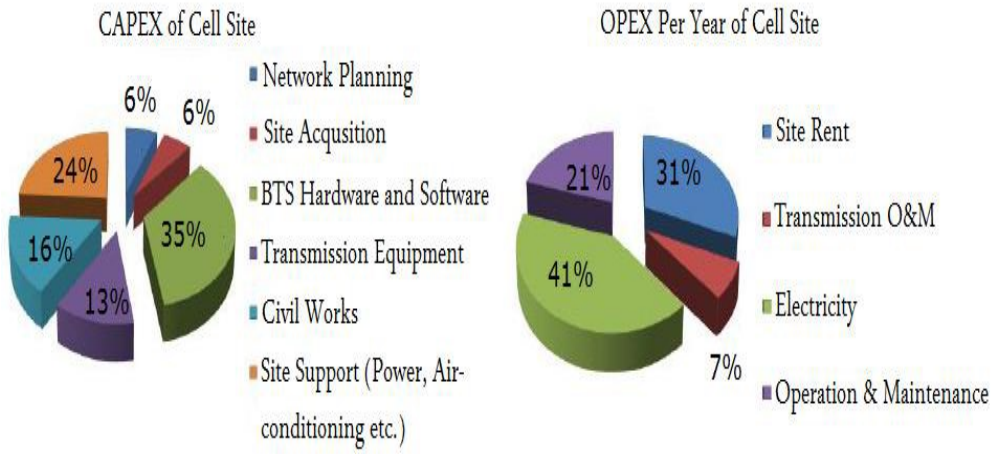

Figure 6-1 CAPEX and OPEX analysis for a site [168]

A general representation of the CRAN is shown in Figure 6-2 [168]. While CRAN is being widely researched on and exists of recent, the enhanced development relative to the CoMP schemes (such as the algorithm implemented in this thesis) is to take advantage of the high bandwidth and minimal delay of the BBU's in the pool when employing the X2 logical interface. Thus in addition to reduced latency due to the centralised processing in the network, the implementation will significantly increase energy efficiency and CAPEX/OPEX of the network in general. This would also allow for easier implementation of highly complex CoMP schemes (such as JP) with reduced latency and overheads in future cellular networks.

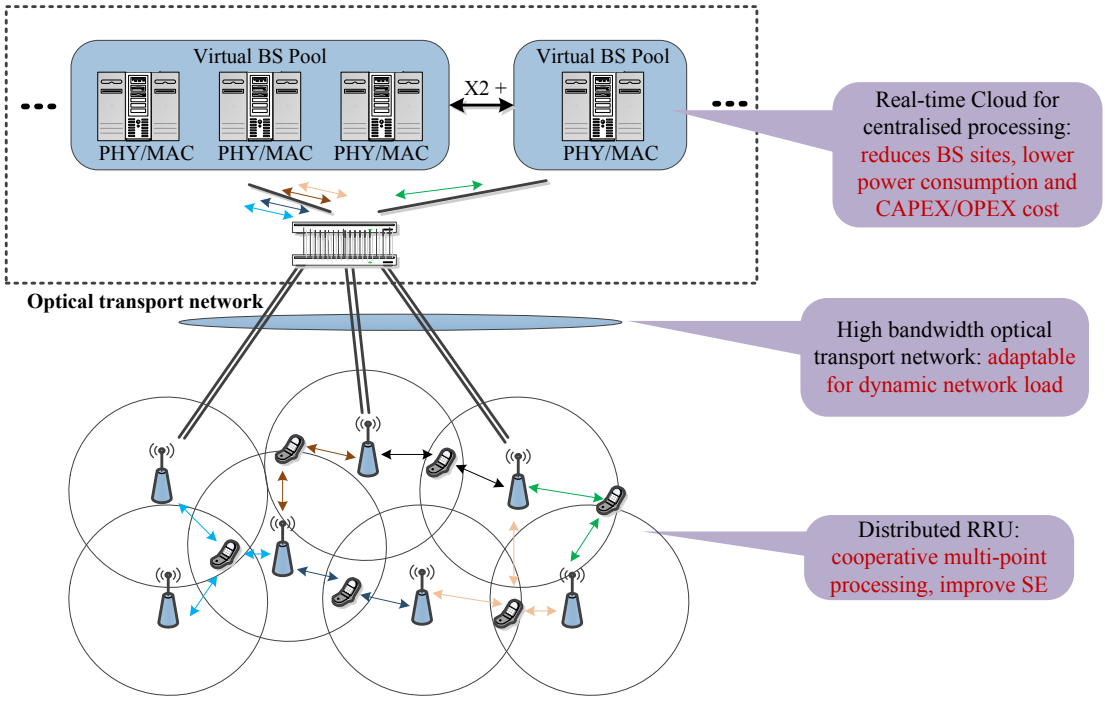

Figure 6-2 High level representation of CRAN architecture [168]

6.4.2 Enhanced investigation scenarios and implementation for D2D communication

In this thesis, performance gain of D2D communication underlaying the cellular network has been explicitly demonstrated using several simulation results. The results

have revealed significant UE performance gain with the technology due to the direct link and close proximity of D2D pair during transmission. The interference impact from the simultaneous transmission (i.e. D2D and cellular) has been shown to deteriorate the cell edge performance in the network, which was mitigated by implementing a novel power control algorithm based on power reduction in the thesis.

The SLS model utilised for the investigations in this work comprised of multiple cells, hence ensuring that sufficient interference have been duly considered from neighbouring cells to the D2D and cellular UEs analysed (in addition to interference from the different modes within the same cell). The performance metric was considered for UEs in a single sector (i.e. the target sector in this thesis), where a pair of D2D UEs was considered. While this approach is sufficient for the investigation [67], tens of iterations with multiple TTIs each (the UE performance is averaged over multiple TTIs in each of the iterations) was furthermore run to consider diverse simulation environments experienced by the UEs evaluated. An additional approach would be to further model several D2D pairs in the multiple cells of the model. This would test and develop further the capability of the power control algorithm, which will not only consider the D2D interference in one cell, but also from D2D pairs in the multiple clustered cells (i.e. a group of surrounding cells) in the network. Thus, the power control algorithm proposed would yield better performance in the network since more resource blocks are reused by the numerous D2D UEs of the different sites/cells while inherent interference is still mitigated by the algorithm.

One instance is the management of a D2D pair geographically located in different cells/sectors. A detailed representation of such scenario is illustrated in Figure 6-3.

The DL interference scenario is illustrated for the example in the figure, in line with the implementation in this thesis: however, the uplink instance is just vice versa.

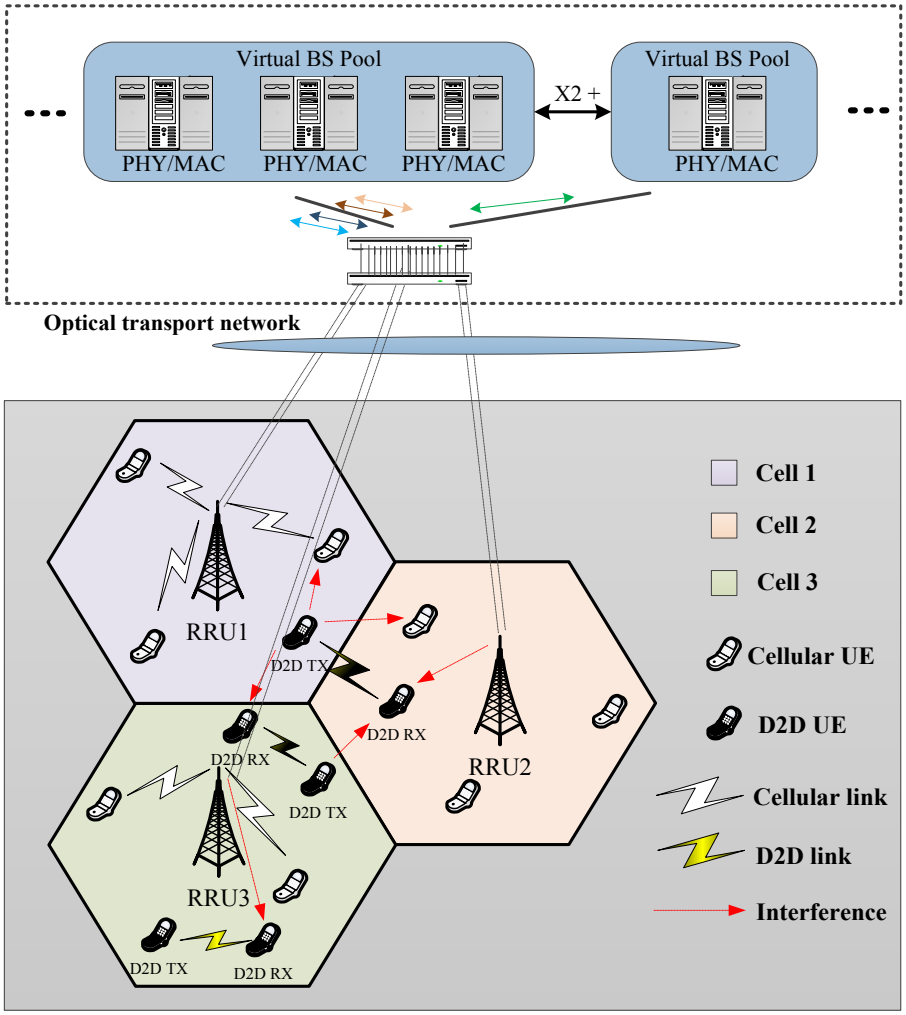

Figure 6-3 Illustration of interference in a multi-cell scenario with multiple D2D pairs supported by a CRAN architecture

As demonstrated in the figure, the D2D TX in cell 1 cause's interference to the D2D RX in cell 3 and also to the cellular UEs with close proximity in cell 1 and cell 2. The D2D RX in cell 2 gets interference from eNB 2 in addition to the interference it receives from the D2D TX in cell 3. Again, this would be an avenue to take advantage of the power control algorithm with requirement on control signal sharing between entities in the multiple cells simultaneously. One approach can be the consideration of

centralised processing using CRAN (described in the preceding subsection), so as to reduce overheads and delay in the implementation.

Figure 6-3 further extends the traditional CRAN implementation in Figure 6-2. Related to the algorithm implemented in this thesis, the SINR evaluation feedback from a cluster of eNBs will further consider interference from D2D transmission in neighbouring cells in this preposition. Thus, the proximity of the eNBs in the pool and fibre links interconnecting the RRUs would effectively reduce latencies/overhead and ensure fast exchange of control information in the hybrid network. An example of such control signals from the implementation in this thesis is the exchange of power reduction signals between the D2D TX and eNB in the power control algorithm.

Another possible direction in the adoption of the D2D communication technology is by combining it with other equally promising technologies. One likely example is the addition of CR to D2D communication. As stated earlier, a major motivation for investigating D2D communication in this thesis is due to its ability to simultaneously utilise the cellular resources (licensed spectrum), unlike similar technologies such as CR that only utilises idle UE resources. Although CR on its own has its limitations as mentioned earlier, the adoption of both technologies simultaneously could prove beneficial. Thus CR would improve the spectrum utilisation in the time and channel perspective, while D2D communication would further improve the space utilisation (as it achieves significant proximity gain) in the cellular networks. In some recent propositions [169], resource allocation for a CR inclusive network using D2D communication is equally discussed as a promising option for the future of the technologies. The secondary UEs in the network additionally form multiple clusters of

D2D groups (i.e. secondary UEs that can partake in D2D communication) as shown in Figure 6-4. In order to reduce the interference from the D2D transmission, the spectrum of primary UEs relatively far away from the individual D2D groups is selected for D2D communication (using spectrum sensing). Furthermore, secondary UEs intending to communicate using D2D communication from the different clusters can do so via the BS/eNB, instead of using a direct link.

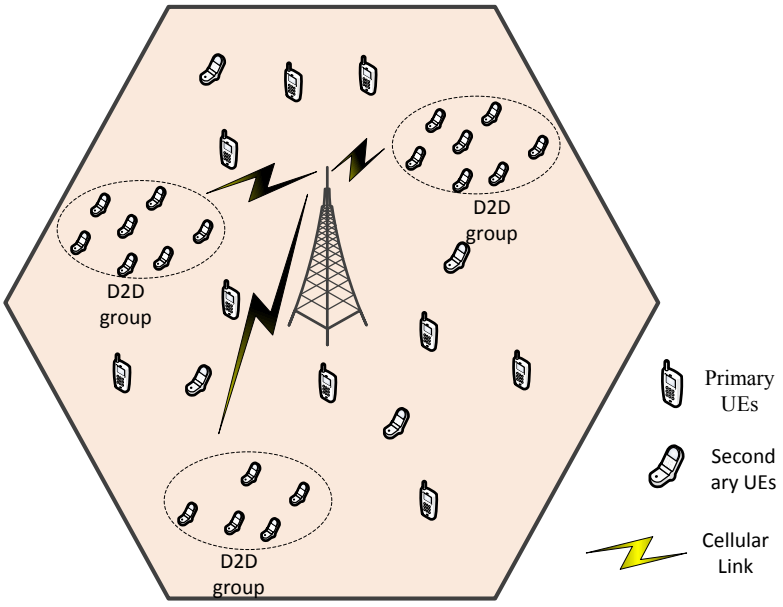

Figure 6-4 Illustration of CR network with D2D groups

One major achievement in this thesis is the illustration of enhanced D2D communication gain by including MH transmission. This investigation is quite significant because while most current research initiatives are focusing on interference mitigation between the cellular and D2D UEs in the network (which is highly relevant), this perspective (i.e. MH) provides other relevant directions in improving the performance gain of the technology. Simulation results show over 2 fold of UE goodput improvement for a D2D RX using MH transmission over SH transmission with the same distance between the D2D pair. However, a major factor in establishing MH transmission i.e. relay section, was assumed to be perfect in the performance

investigation. Traditionally, the sending node (D2D TX in this case) would require the CSI of all the potential relay nodes (i.e. idle UEs) within its part to the D2D RX [165]. This will however place enormous requirement on the D2D TX and equally add to the transmission time constraints of the network. One possible solution would be for the eNB to instantaneously convey the channel information of potential relays to the D2D TX, while acknowledging/replying the D2D communication set-up request during the D2D pairing. While this would overwhelm the D2D TX with additional information, it will however conserve energy of the TX as it does not require exchanging signalling information such as channel gain from all UEs in the path to its RX continuously.

Thus, it can be concluded from the above discussions and results presented in the thesis that MH transmission for D2D traffic can further improve the performance of D2D communication in future networks, and hence a key direction to further explore and improve. As mentioned earlier, features such as potential relay UEs (i.e. idle UEs) search, channel information amongst others should be achieved with minimum overhead to yield optimum gain of including MH transmission for D2D traffic. Additionally, similar technologies such as CR could be integrated (instead of being investigated as separate entities) with D2D communication to further maximise the resource utilisation in the networks. Thus, this could yield tremendous performance improvement as D2D communication would complement for the opportunistic transmission limitation of CR and take advantage of the spectrum sensing feature of CR to avoid interference in the network.

Furthermore, centralised processing could be a key solution to minimise the delay and overhead limitations in implementing key algorithms (such as power control and

inter-site/cell coordination) in the future cellular networks. Particularly, employing current networks such as CRAN could potentially prevail in achieving this objective. While this thesis focuses on the performance enhancement of the proposed D2D technology, a vital question raised afterwards is the security issues that would arise in conveying user data and information as the UE traffic hops or is conveyed between devices in the network?

REFERENCES

[1] M. Milosavljevic, M. P. Thakur, P. Kourtessis, J. E. Mitchell, and J. M. Senior, "Demonstration of Wireless Backhauling Over Long-Reach PONs," *Journal of Lightwave Technology,* vol. 30, pp. 811-817, 2012.

[2] R. Baldemair, E. Dahlman, S. Parkvall, Y. Selen, K. Balachandran, T. Irnich, G. Fodor, and H. Tullberg, "Future Wireless Communications," in *2013 IEEE 77th Vehicular Technology Conference (VTC Spring)* 2013, pp. 1-5.

[3] ITU. (2014). *ICT Facts and Figures*. Available: http://www.itu.int/en/ITU-D/Statistics/Documents/facts/ICTFactsFigures2014-e.pdf

[4] ERICSSON. (2012). *Voice and Video calling over LTE*. Available: http://www.ericsson.com/res/docs/whitepapers/WP-Voice-Video-Calling-LTE.pdf

[5] G. Fairhurst, A. Sathiaseelan, C. Baudoin, and E. Callejo, "Delivery of triple-play services over broadband satellite networks," *IET Communications,* vol. 4, pp. 1544-1555, 2010.

[6] ERICSSON. (2011). *Mobile Data Traffic Gowth*. Available: http://www.ericsson.com/news/1561267

[7] 3GPP. *3rd Generation Partnership Project*. Available: http://www.3gpp.org/

[8] IEEE. *Institute of Electrical and Electronics Engineers*. Available: http://www.ieee.org/index.html

[9] D. Astely, E. Dahlman, A. Furuskar, Y. Jading, M. Lindstrom, and S. Parkvall, "LTE: the evolution of mobile broadband," *IEEE Communications Magazine,* vol. 47, pp. 44-51, 2009.

[10] L. Kyunghan, L. Joohyun, Y. Yung, R. Injong, and C. Song, "Mobile Data Offloading: How Much Can WiFi Deliver?," *IEEE/ACM Transactions on Networking,* vol. 21, pp. 536-550, 2013.

[11] Metis-2020. (2012). *Laying the foundation for the year 2020 and beyond mobile wireless communications system*. Available: www.metis2020.com

[12] (2014, September). *5th Generation Non-Orthogonal Waveforms for Asynchronous Signalling*. Available: http://www.5gnow.eu/

[13] (2014, February). *The EU Framework Programme for Research and Innovation*. Available: http://ec.europa.eu/programmes/horizon2020/

[14] Combo. *Convergence of fixed and mobile broadband access/aggregation networks*. Available: http://www.ict-combo.eu/

[15] (2014, 01-09-14). *Beyond 2020 Heterogeneous Wireless Networks with Millimeter-Wave Small Cell Access and Backhauling*. Available: http://www.miwaves.eu/

[16] (2013). *Millimetre-Wave Evolution for Backhaul and Access*. Available: http://www.miweba.eu/

[17] T. Mshvidobadze, "Evolution mobile wireless communication and LTE networks," in *2012 6th International Conference on Application of Information and Communication Technologies (AICT)*, 2012, pp. 1-7.

[18] V. Krizanovic, D. Zagar, and G. Martinovic, "Mobile broadband access networks planning and evaluation using techno-economic criteria," in *Proceedings of the ITI 2012 34th International Conference on Information Technology Interfaces (ITI)*, 2012, pp. 281-286.

[19] M. Milosavljevic, P. Kourtessis, and J. M. Senior, "Transparent wireless transmission over the ACCORDANCE optical/wireless segment," in *2010 7th*

International Symposium on Communication Systems Networks and Digital Signal Processing (CSNDSP), 2010, pp. 138-142.

[20] J. Mietzner, R. Schober, L. Lampe, W. H. Gerstacker, and P. A. Hoeher, "Multiple-antenna techniques for wireless communications - a comprehensive literature survey," *IEEE Communications Surveys & Tutorials,* vol. 11, pp. 87-105, 2009.

[21] M. M. Rana, K. Jinsang, and C. Won-Kyung, "Performance analysis of sub-carrier mapping in LTE uplink systems," in *2010 9th International Conference on Optical Internet (COIN)*, 2010, pp. 1-3.

[22] L. Cheng-Chung, K. Sandrasegaran, Z. Xinning, and X. Zhuliang, "On the performance of capacity integrated CoMP handover algorithm in LTE-Advanced," in *Communications (APCC), 2012 18th Asia-Pacific Conference on*, 2012, pp. 871-876.

[23] V. 3GPP TR 36.913. (Dec, 2009) Requirements for further advancements for evolved Universal terrestrial Radio Access (E-UTRA) (LTE-Advanced).

[24] T. Watteyne, S. Lanzisera, A. Mehta, and K. S. J. Pister, "Mitigating Multipath Fading through Channel Hopping in Wireless Sensor Networks," in *2010 IEEE International Conference on Communications (ICC)*, 2010, pp. 1-5.

[25] (2014, 11-02-2014). *New GSA Evolution to LTE report: 2013 ends with 260 LTE networks in service*. Available: http://www.gsacom.com/index.php4

[26] B. Ayvazian. LTE Deployment Strategies: Network overlay vs. Single RAN [Online]. Available: http://whitepapers.lightreading.com/pdf_whitepapers/approved/1361377925_HR_Samsung_LTE_Strategies_WP_2-19-13.pdf

[27] D. Mavrakis. (2013, 2 Feb 2014). *Deploying LTE in Europe*. Available: http://www.telecoms.com/wp-content/blogs.dir/1/files/2013/02/Samsung-ITM-whitepaper-final-fp.pdf

[28] J. Gozalvez, "First LTE-Advanced Commercial Network Deployed [Mobile Radio]," *IEEE Vehicular Technology Magazine,* vol. 8, pp. 10-17, 2013.

[29] (2014, 13 Feb). *5G is coming, but what does it mean?* Available: http://nsn.com/news-events/insight-newsletter/articles/5g-is-coming-but-what-does-it-mean

[30] H. Tullberg. (2013, 28th Feb.). *The METIS view of 5G networks* [PDF]. Available: www.metis2020.com

[31] B. A. Bjerke, "LTE-advanced and the evolution of LTE deployments," *IEEE Wireless Communications,* vol. 18, pp. 4-5, 2011.

[32] A. B. MacKenzie, J. H. Reed, P. Athanas, C. W. Bostian, R. M. Buehrer, L. A. DaSilva, S. W. Ellingson, Y. T. Hou, M. Hsiao, P. Jung-Min, C. Patterson, S. Raman, and C. da Silva, "Cognitive Radio and Networking Research at Virginia Tech," *Proceedings of the IEEE,* vol. 97, pp. 660-688, 2009.

[33] S. Yong Sheng, T. Q. S. Quek, M. Kountouris, and S. Hyundong, "Energy Efficient Heterogeneous Cellular Networks," *IEEE Journal on Selected Areas in Communications,* vol. 31, pp. 840-850, 2013.

[34] A. Dementyev, S. Hodges, S. Taylor, and J. Smith, "Power consumption analysis of Bluetooth Low Energy, ZigBee and ANT sensor nodes in a cyclic sleep scenario," in *2013 IEEE International Wireless Symposium (IWS)*, 2013, pp. 1-4.

[35] M. R. Dzulkifli, M. R. Kamarudin, and T. A. Rahman, "Spectrum occupancy of Malaysia radio environment for cognitive radio application," in *IET*

International Conference on Wireless Communications and Applications (ICWCA 2012), 2012, pp. 1-6.

[36] C. Kai, M. Jia, H. Xianghui, Y. Xiao, D. Yan, Z. Long, and F. Zhiyong, "Spectrum survey for TV band in Beijing," in *2014 21st International Conference on Telecommunications (ICT)*, 2014, pp. 267-271.

[37] M. N. Tehrani, M. Uysal, and H. Yanikomeroglu, "Device-to-device communication in 5G cellular networks: challenges, solutions, and future directions," *IEEE Communications Magazine,* vol. 52, pp. 86-92, 2014.

[38] K. Doppler, M. Rinne, C. Wijting, C. B. Ribeiro, and K. Hugl, "Device-to-device communication as an underlay to LTE-advanced networks," *IEEE Communications Magazine,* vol. 47, pp. 42-49, 2009.

[39] A. Kumar;, D. Y. Liu;, D. J. Sengupta;, and Divya, "Evolution of Mobile Wireless Communication Networks: 1G to 4G," *International Journal of Electronics & Communication Technology,* vol. 1, pp. 68-72, 1-Dec. 2010.

[40] L. Kugler;. (2014, April 16, 2014.) The Next Generation of Mobile. *Communication of the ACM* [Magazine]. Available: http://cacm.acm.org/news/173908-the-next-generation-of-mobile/fulltext

[41] F. Hillebrand, "The creation of standards for global mobile communication: GSM and UMTS standardization from 1982 to 2000," *IEEE Wireless Communications,* vol. 20, pp. 24-33, 2013.

[42] B. Walke, "The roots of GPRS: the first system for mobile packet-based global internet access," *IEEE Wireless Communications,* vol. 20, pp. 12-23, 2013.

[43] G. Feng, G. Zehua, W. Liu, Z. Bing, T. Di, and H. Dahsiung, "A Research on Key Performance Indicator of Measurable QoE of EDGE Network," in

International Conference on Information Engineering and Computer Science (ICIECS 2009). , 2009, pp. 1-4.

[44] V. P. Etcharte and E. R. Vale, "The Integration of the Satellite Communications with the Terrestrial Mobile Network (UMTS)," *IEEE (Revista IEEE America Latina) Latin America Transactions,* vol. 10, pp. 1175-1179, 2012.

[45] M. Maternia, M. Januszewski, K. Ranta-Aho, J. Wigard, A. Bohdanowicz, M. Marzynski, and M. Wcislo, "On performance of long term HSPA evolution: Towards meeting IMT-Advanced requirements," in *2012 IEEE International Conference on Communications (ICC)*, 2012, pp. 6040-6044.

[46] C. Wen-Tzu and L. Jyun-Ting, "Analysis of the Impacts of Uplink Co-Channel Interference on Cell Coverage in an IEEE 802.16m System," *IEEE Transactions on Vehicular Technology,* vol. 63, pp. 2208-2215, 2014.

[47] O. Bejarano, E. W. Knightly, and P. Minyoung, "IEEE 802.11ac: from channelization to multi-user MIMO," *IEEE Communications Magazine,* vol. 51, pp. 84-90, 2013.

[48] E. Almeida, A. M. Cavalcante, R. C. D. Paiva, F. S. Chaves, F. M. Abinader, R. D. Vieira, S. Choudhury, E. Tuomaala, and K. Doppler, "Enabling LTE/WiFi coexistence by LTE blank subframe allocation," in *2013 IEEE International Conference on Communications (ICC)* 2013, pp. 5083-5088.

[49] RSAVY. (2012). *Constituent of 4G Americas, responsible for providing information for 3GPP family technologies* Available: http://www.4gamericas.org/documents/4G%20Americas%20Mobile%20Broadband%20Explosion%20August%2020121.pdf

[50] (2009, Nov. 2013). *WiMAX, HSPA+, and LTE: A Comparative Analysis*. Available: http://resources.wimaxforum.org/sites/wimaxforum.org/files/document_library/wimax_hspa+and_lte_111809_final.pdf

[51] K. Sung-won and K. Kun-yong, "Physical layer verification for 3GPP LTE (FDD)," in *2009 11th International Conference on Advanced Communication Technology (ICACT 2009)*, 2009, pp. 1095-1100.

[52] P. E. Mogensen, T. Koivisto, K. I. Pedersen, I. Z. Kovacs, B. Raaf, K. Pajukoski, and M. J. Rinne, "LTE-Advanced: The path towards gigabit/s in wireless mobile communications," in *2009 1st International Conference on Wireless Communication, Vehicular Technology, Information Theory and Aerospace & Electronic Systems Technology (Wireless VITAE 2009)* 2009, pp. 147-151.

[53] (2012, 04 February). *LTE-Advanced*. Available: http://www.4gamericas.org/index.cfm?fuseaction=page&sectionid=352

[54] M. Sawahashi, Y. Kishiyama, A. Morimoto, D. Nishikawa, and M. Tanno, "Coordinated multipoint transmission/reception techniques for LTE-advanced [Coordinated and Distributed MIMO]," *IEEE Wireless Communications,* vol. 17, pp. 26-34, 2010.

[55] L. Shiyuan, C. Qimei, W. Chao, and T. Xiaofeng, "Coordinated Cell Threshold user pairing criteria for uplink CoMP MU-MIMO," in *2011 International Conference on Computer Science and Network Technology (ICCSNT)*, 2011, pp. 1740-1744.

[56] S. Huan, F. Wei, L. Jianguo, and M. Yan, "Performance evaluation of CS/CB for coordinated multipoint transmission in LTE-A downlink," in *2012 IEEE*

23rd International Symposium on Personal Indoor and Mobile Radio Communications (PIMRC), 2012, pp. 1061-1065.

[57] W. Binbin, L. Bingbing, and L. Mingqian, "A Novel Precoding Method for Joint Processing in CoMP," in *2011 International Conference on Network Computing and Information Security (NCIS)*, 2011, pp. 126-129.

[58] L. Bhebhe and O. Zhonghong, "Impact of packet forwarding during Inter-eNodeB handover via X2 interface," in *2011 IEEE GLOBECOM Workshops (GC Wkshps)*, 2011, pp. 615-619.

[59] D.-H. Tuan, D.-N. Chau, N. Tuan Le-Hoang, and T.-H. Ha, "Wideband beamforming for reducing co-channel interference in broadband wireless communication systems," in *2010 International Conference on Advanced Technologies for Communications (ATC)*, 2010, pp. 225-230.

[60] Z. Yulong, Y. Yu-Dong, and Z. Baoyu, "Cognitive Transmissions with Multiple Relays in Cognitive Radio Networks," *IEEE Transactions on Wireless Communications,* vol. 10, pp. 648-659, 2011.

[61] Z. Yonghong and L. Ying-Chang, "Eigenvalue-based spectrum sensing algorithms for cognitive radio," *IEEE Transactions on Communications,* vol. 57, pp. 1784-1793, 2009.

[62] A. Galindo-Serrano and L. Giupponi, "Distributed Q-Learning for Aggregated Interference Control in Cognitive Radio Networks," *IEEE Transactions on Vehicular Technology,* vol. 59, pp. 1823-1834, 2010.

[63] R. Garello and Y. Jia, "Comparison of spectrum sensing methods for cognitive radio under low SNR," in *2011 IEEE-APS Topical Conference on Antennas and Propagation in Wireless Communications (APWC)*, 2011, pp. 886-889.

[64] S. Singh, P. D. Teal, P. A. Dmochowski, and A. J. Coulson, "Interference Management in Cognitive Radio Systems With Feasibility Detection," *IEEE Transactions on Vehicular Technology,* vol. 62, pp. 3711-3720, 2013.

[65] G. Fodor, E. Dahlman, G. Mildh, S. Parkvall, N. Reider, Miklo, x, G. s, Tura, and Z. nyi, "Design aspects of network assisted device-to-device communications," *IEEE Communications Magazine,* vol. 50, pp. 170-177, 2012.

[66] K. Doppler, Y. Chia-Hao, C. B. Ribeiro, and P. Janis, "Mode Selection for Device-To-Device Communication Underlaying an LTE-Advanced Network," in *2010 IEEE Wireless Communications and Networking Conference (WCNC)*, 2010, pp. 1-6.

[67] Y. Chia-Hao, O. Tirkkonen, K. Doppler, and C. Ribeiro, "On the Performance of Device-to-Device Underlay Communication with Simple Power Control," in *IEEE 69th Vehicular Technology Conference (VTC Spring 2009)*, 2009, pp. 1-5.

[68] A. Ran, S. Jun, Z. Su, and S. Shixiang, "Resource allocation scheme for device-to-device communication underlying LTE downlink network," in *2012 International Conference on Wireless Communications & Signal Processing (WCSP)*, 2012, pp. 1-5.

[69] C. Hyang Sin, G. Jaheon, C. Bum-Gon, and C. Min, "Radio resource allocation scheme for device-to-device communication in cellular networks using fractional frequency reuse," in *2011 17th Asia-Pacific Conference on Communications (APCC)*, 2011, pp. 58-62.

[70] L. Dong Heon, C. Kae Won, J. Wha Sook, and J. Dong Geun, "Resource allocation scheme for device-to-device communication for maximizing spatial

reuse," in *2013 IEEE Wireless Communications and Networking Conference (WCNC)*, 2013, pp. 112-117.

[71] X. Hongnian and S. Hakola, "The investigation of power control schemes for a device-to-device communication integrated into OFDMA cellular system," in *2010 IEEE 21st International Symposium on Personal Indoor and Mobile Radio Communications (PIMRC)*, 2010, pp. 1775-1780.

[72] M. G. da S Rego, T. F. Maciel, H. de H M Barros, F. R. P. Cavalcanti, and G. Fodor, "Performance analysis of power control for device-to-device communication in cellular MIMO systems," in *2012 International Symposium on Wireless Communication Systems (ISWCS)*, 2012, pp. 336-340.

[73] S. Wonjae, J. KyungHun, and C. Hyun-Ho, "Device-to-device communication assisted interference mitigation for next generation cellular networks," in *2013 IEEE International Conference on Consumer Electronics (ICCE)*, 2013, pp. 623-624.

[74] L. Long and E. Hossain, "Multihop Cellular Networks: Potential Gains, Research Challenges, and a Resource Allocation Framework," *IEEE Communications Magazine,* vol. 45, pp. 66-73, 2007.

[75] L. Yang-wen and R. Schober, "Cooperative Amplify-and-Forward Beamforming with Multiple Multi-Antenna Relays," *IEEE Transactions on Communications,* vol. 59, pp. 2605-2615, 2011.

[76] W. Guiying and F. Gang, "Energy-efficient relay deployment in next generation cellular networks," in *2012 IEEE International Conference on Communications (ICC)*, 2012, pp. 5757-5761.

[77] H. Zhang, P. Hong, and K. Xue, "Mobile-based relay selection schemes for multi-hop cellular networks," *Journal of Communications and Networks,* vol. 15, pp. 45-53, 2013.

[78] C. Yiyi, F. Zhiyong, X. Ding, and L. Yang, "Optimal power allocation and relay selection in dual-hop and multi-hop cognitive networks," in *2012 IEEE International Conference on Communications (ICC)*, 2012, pp. 1641-1645.

[79] G. Huang, W. Yue, and J. Coon, "Performance of multihop decode-and-forward and amplify-and-forward relay networks with channel estimation," in *2011 IEEE Pacific Rim Conference on Communications, Computers and Signal Processing (PacRim)*, 2011, pp. 352-357.

[80] H. Adam, C. Bettstetter, and S. M. Senouci, "Adaptive relay selection in cooperative wireless networks," in *2008 IEEE 19th International Symposium on Personal, Indoor and Mobile Radio Communications (PIMRC 2008)*, 2008, pp. 1-5.

[81] S. Devar, K. S. Karthik, B. Ramamurthi, and R. D. Koilpillai, "Downlink Throughput Enhancement of a Cellular Network using Two-Hop User-Deployable Indoor Relays," *IEEE Journal on Selected Areas in Communications,* vol. 31, pp. 1607-1617, 2013.

[82] L. Wen, M. Zhangchao, S. Shanshan, L. Jianyu, and Z. Hui, "Feasibility study of relay in 3GPP LTE-advanced from a coexistence perspective," in *IET International Conference on Communication Technology and Application (ICCTA 2011)*, 2011, pp. 357-361.

[83] C. Hyun-Ho, S. Eui-Seung, P. Eun-Kyoung, and L. Jung-Ryun, "Joint scheduling and power control for inter-hop interference mitigation in wireless

multihop networks," in *2012 Fourth International Conference on Ubiquitous and Future Networks (ICUFN)*, 2012, pp. 80-85.

[84] M. A. Manna, C. Gaojie, and J. A. Chambers, "Outage probability analysis of cognitive relay network with four relay selection and end-to-end performance with modified quasi-orthogonal spacetime coding," *IET Communications,* vol. 8, pp. 233-241, 2014.

[85] 5G-NOW. (2012). *5th Generation Non-orthogonal Waveforms for Asynchronous Signalling*. Available: http://www.5gnow.eu/

[86] A. Osseiran, F. Boccardi, V. Braun, K. Kusume, P. Marsch, M. Maternia, O. Queseth, M. Schellmann, H. Schotten, H. Taoka, H. Tullberg, M. A. Uusitalo, B. Timus, and M. Fallgren, "Scenarios for 5G mobile and wireless communications: the vision of the METIS project," *IEEE Communications Magazine,* vol. 52, pp. 26-35, 2014.

[87] N. Wooseok, B. Dongwoon, L. Jungwon, and K. Inyup, "Advanced interference management for 5G cellular networks," *IEEE Communications Magazine,* vol. 52, pp. 52-60, 2014.

[88] B. Bangerter, S. Talwar, R. Arefi, and K. Stewart, "Networks and devices for the 5G era," *IEEE Communications Magazine,* vol. 52, pp. 90-96, 2014.

[89] W. Cheng-Xiang, F. Haider, G. Xiqi, Y. Xiao-Hu, Y. Yang, Y. Dongfeng, H. Aggoune, H. Haas, S. Fletcher, and E. Hepsaydir, "Cellular architecture and key technologies for 5G wireless communication networks," *IEEE Communications Magazine,* vol. 52, pp. 122-130, 2014.

[90] A. Tudzarov; and T. Janevski;, "Functional Architecture for 5G Mobile Networks," *International Journal of Advanced Science and Technology,* vol. 32, pp. 65-78, July 2011.

[91] T. Shuminoski and T. Janevski, "Radio network aggregation for 5G mobile terminals in heterogeneous wireless networks," in *2013 11th International Conference on Telecommunication in Modern Satellite, Cable and Broadcasting Services (TELSIKS)*, 2013, pp. 225-228.

[92] M. Milosavljevic, S. Sofianos, P. Kourtessis, and J. M. Senior, "Self-organized cooperative 5G RANs with intelligent optical backhauls for mobile cloud computing," in *2013 IEEE International Conference on Communications Workshops (ICC)*, 2013, pp. 900-904.

[93] N. Saha, R. K. Mondal, and J. Yeong Min, "Opportunistic channel reuse for a self-organized visible light communication personal area network," in *2013 Fifth International Conference on Ubiquitous and Future Networks (ICUFN)*, 2013, pp. 131-134.

[94] D. B. Drajic, "60 Years of Shannon Information Theory," in *2007 8th International Conference on Telecommunications in Modern Satellite, Cable and Broadcasting Services (TELSIKS 2007)*, 2007, pp. 109-116.

[95] J. Hoydis, S. ten Brink, and M. Debbah, "Massive MIMO in the UL/DL of Cellular Networks: How Many Antennas Do We Need?," *IEEE Journal on Selected Areas in Communications,* vol. 31, pp. 160-171, 2013.

[96] H. Zhaojun, S. Shihai, S. Ying, Q. Chaojin, and T. Youxi, "Performance Analysis of RF Self-Interference Cancellation in Full-Duplex Wireless Communications," *IEEE Wireless Communications Letters,* vol. 3, pp. 405-408, 2014.

[97] S. Hong, J. Brand, C. Jung, M. Jain, J. Mehlman, S. Katti, and P. Levis, "Applications of self-interference cancellation in 5G and beyond," *IEEE Communications Magazine,* vol. 52, pp. 114-121, 2014.

[98] D. Choi and D. Park, "Effective self interference cancellation in full duplex relay systems," *Electronics Letters,* vol. 48, pp. 129-130, 2012.

[99] M. Wrulich, W. Weiler, and M. Rupp, "HSDPA Performance in a Mixed Traffic Network," in *2008 IEEE Vehicular Technology Conference (VTC Spring 2008)*, 2008, pp. 2056-2060.

[100] M. Wrulich, S. Eder, I. Viering, and M. Rupp, "Efficient Link-to-System Level Model for MIMO HSDPA," in *2008 IEEE GLOBECOM Workshops*, 2008, pp. 1-6.

[101] C. Li, C. Wenwen, W. Bin, Z. Xin, C. Hongyang, and Y. Dacheng, "System-level simulation methodology and platform for mobile cellular systems," *IEEE Communications Magazine,* vol. 49, pp. 148-155, 2011.

[102] P. Munoz, I. De La Bandera, R. Barco, F. Ruiz, M. Toril, and R. Luna, S.;, "Estimation of link-layer quality parameters in a system-level LTE simulator," in *2010 Fifth International Conference on Broadband and Biomedical Communications (IB2Com)*, 2010, pp. 1-5.

[103] J. C. Ikuno, "System Level Modeling and Optimization of the LTE Downlink," Doctor of philosophy Research, Vienna University of technology, Vienna, 2012.

[104] J. C. Ikuno, M. Wrulich, and M. Rupp, "System Level Simulation of LTE Networks," in *2010 IEEE 71st Vehicular Technology Conference (VTC 2010-Spring)*, 2010, pp. 1-5.

[105] J. Ikuno. LTE system level simulator [Online]. Available: http://www.nt.tuwien.ac.at/ltesimulator

[106] M. T. Kawser;, N. I. B. Hamid;, M. N. Hasan;, M. S. Alam;, and M. M. Rahman;, "Downlink SNR to CQI Mapping for Different Multiple Antenna

Techniques in LTE," *International Journal of information and Electronics Engineering,* vol. 2, p. 4, 2012 2012.

[107] G. Hui, L. Tiejun, Z. Shengli, Y. Chau, and Y. Shaoshi, "Zero-Forcing Based MIMO Two-Way Relay with Relay Antenna Selection: Transmission Scheme and Diversity Analysis," *IEEE Transactions on Wireless Communications,* vol. 11, pp. 4426-4437, 2012.

[108] W. Cheng, E. K. S. Au, R. D. Murch, M. Wai Ho, R. S. Cheng, and V. Lau, "On the Performance of the MIMO Zero-Forcing Receiver in the Presence of Channel Estimation Error," *IEEE Transactions on Wireless Communications,* vol. 6, pp. 805-810, 2007.

[109] 3GPP, "Technical Specification Group Radio Access Network for Evolved Universal Terrestrial Radio Access (E-UTRA)," Valbonne, France, Technical specification 2012.

[110] J. Turkka and A. Lobinger, "Non-regular layout for cellular network system simulations," in *2010 IEEE 21st International Symposium on Personal Indoor and Mobile Radio Communications (PIMRC)*, 2010, pp. 1929-1933.

[111] F. Khan;, *LTE for 4G Mobile Broadband: Air Interface Technologies and Performance* First ed. Cambridge: Cambridge University Press, 2009.

[112] 3GPP, "ETSI TR 136 942 V8.2.0 LTE; Evolved Universal Terrestrial Radio Access (E-UTRA); Radio Frequency (RF) system scenarios," 2009.

[113] ITU. M.1225: Guidelines for evaluation of radio transmission technologies for IMT-2000 [Online]. Available: www.itu.int/rec/R-REC-M.1225/en

[114] S. N. K. Marwat, "LTE Channel Modelling for System Level Simulations," Masters Mini-project, Communication Networks, University of Bremen, Bremen, 2011.

[115] L. C. Fernandes and A. M. Soares, "Simplified Characterization of the Urban Propagation Environment for Path Loss Calculation," *IEEE Antennas and Wireless Propagation Letters,* vol. 9, pp. 24-27, 2010.

[116] F. Darbari;, R. W. Stewart;, and I. A. Glover;. MIMO channel modelling [Online]. Available: http://cdn.intechopen.com/pdfs/9747/InTech-Mimo_channel_modelling.pdf

[117] C. Chia-Chin, F. Watanabe, H. Inamura, K. Kitao, and T. Imai, "Performance comparison of the 3GPP/3GPP2 SCM and ITU-R IMT-Advanced MIMO channel models," in *2009 IEEE 20th International Symposium on Personal, Indoor and Mobile Radio Communications*, 2009, pp. 890-894.

[118] M. S. Hossain;, R. Adhikary;, and N. Yesmin;, "Performance Evaluation of WINNER-II Channel Model for Long Term Evolution (LTE)," *International Journal of Scientific & Engineering Research,* vol. 4, 5th, May 2013.

[119] P. Kyösti;, J. Meinilä;, L. Hentilä;, X. Zhao;, T. Jämsä;, C. Schneider;, M. Narandzić;, M. Milojević;, A. Hong;, J. Ylitalo;, V.-M. Holappa;, M. Alatossava;, R. Bultitude;, Y. d. Jong;, and T. Rautiainen;. (2007, 18th, March). D1.1.2 V1.0 WINNER II Channel Models. Available: http://www.signal.uu.se/Publications/WINNER/WIN2D112.pdf

[120] H. M. A. B. Farid; and M. S. Hasan;, "Performance Analysis for Different Multiple Antenna Techniques in LTE," *International Journal of Emerging Technology and Advanced Engineering,* vol. 3, p. 6, 2013.

[121] B. Schulz. LTE Transmission Modes and Beamforming [Online]. Available: http://cdn.rohdeschwarz.com/dl_downloads/dl_application/application_notes/1ma186/1MA186_0e_LTE_transmission_modes_and_beamforming.pdf

[122] G. Klang and B. Ottersten, "Interference robustness aspects of space-time block code-based transmit diversity," *IEEE Transactions on Signal Processing,* vol. 53, pp. 1299-1309, 2005.

[123] L. Miguel, "MIMO Sace-Time Block Coding (STBC): Simulations and Results," ed. Georgia Tech, 2009, p. 8.

[124] B. Vucetic; and J. Yuan;, *Space-Time Coding*, First ed. West Sussex: John Wiley and sons, 2003.

[125] M. Rupp;, S. Caban;, C. Mehlführer;, and M. Wrulich;, *Evaluation of HSDPA and LTE: From Testbed Measurements to System Level Performance* John Wiley & Sons, 2011.

[126] 3GPP. (2010). *LTE: Evolved Universal Terrestrial Radio Access (E-UTRA): Physical channels and modulation (3GPP TS 36.211 version 8.9.0 Release 8)*. Available: http://www.etsi.org/deliver/etsi_ts/136200_136299/136211/08.09.00_60/ts_136211v080900p.pdf

[127] ROKE. (2009-2014). *LTE eNodeB MAC Scheduler Introduction*. Available: http://www.roke.co.uk/resources/datasheets/112-lte-mac-scheduler-intro.pdf

[128] S. Schwarz, C. Mehlfuhrer, and M. Rupp, "Low complexity approximate maximum throughput scheduling for LTE," in *2010 Conference Record of the Forty Fourth Asilomar Conference on Signals, Systems and Computers (ASILOMAR)*, 2010, pp. 1563-1569.

[129] M. T. Kawser;, H. M. A. B. Farid;, A. R. Hasin;, A. M. J. Sadik;, and I. K. Razu;, "Performance Comparison between Round Robin and Performance Comparison between Round Robin and," *International Journal of Information and Electronics Engineering,* vol. 2, p. 4, September 2012.

[130] M. H. HABAEBI;, J. CHEBIL;, A. G. AL-SAKKAF;, and T. H. DAHAWI;, "Comparison between scheduling techniques in long term evolution," *IIUM Engineering Journal,* vol. 14, p. 9, 2013.

[131] Y. Barayan; and I. Kostanic;, "Performance Evaluation of Proportional Fairness Scheduling in LTE," in *Proceedings of the World Congress on Engineering and Computer Science*, 2013, p. 6.

[132] A. Haider and R. Harris, "A Novel Proportional Fair Scheduling Algorithm for HSDPA in UMTS Networks," in *The 2nd International Conference on Wireless Broadband and Ultra Wideband Communications, (AusWireless)* 2007, pp. 43-43.

[133] R. Bendlin, H. Yih-Fang, M. T. Ivrlac, and J. A. Nossek, "Cost-constrained transmit processing in wireless cellular networks with universal frequency reuse," in *2010 44th Annual Conference on Information Sciences and Systems (CISS)*, 2010, pp. 1-6.

[134] M. Sawahashi, Y. Kishiyama, H. Taoka, M. Tanno, and T. Nakamura, "Broadband radio access: LTE and LTE-advanced," in *2009 International Symposium on Intelligent Signal Processing and Communication Systems (ISPACS 2009)*, 2009, pp. 224-227.

[135] Y. Yoon;, L. Duan;, F. Khaleghi;, and A. Soong;. Basic operation of the wrap-around technique for system-level simulation [Online]. Available: ftp://ftp.3gpp2.org/TSGC/Working/2002/TSG-C-0207/TSG-C-2002-07-SanDiego/WG3/c30-20020708-030%20ericy%20wrap%20around%20proposal.pdf

[136] F. Sallabi, A. Lakas, K. Shuaib, and M. Boulmalf, "WCDMA downlink simulator with efficient wrap-around technique," in *2005 Second IFIP*

International Conference on Wireless and Optical Communications Networks (WOCN), 2005, pp. 472-476.

[137] SYMENA. (2002, 09). Available: http://www.symena.com

[138] (June, 2012). *Automatic cell planning tool*. Available: http://www.remopt.com/capesso.php

[139] L. Qiang, W. Zhe, and M. Fuying, "Inter-cell interference coordination research for LTE," in *2011 IEEE 4th International Symposium on Microwave, Antenna, Propagation, and EMC Technologies for Wireless Communications (MAPE)*, 2011, pp. 695-700.

[140] G. Piro, L. A. Grieco, G. Boggia, F. Capozzi, and P. Camarda, "Simulating LTE Cellular Systems: An Open-Source Framework," *IEEE Transactions on Vehicular Technology,* vol. 60, pp. 498-513, 2011.

[141] A. Amate, S. Sofianos, M. Milosavljevic, P. Kourtessis, and J. M. Senior, "An efficient inter-site interference model for 4G wireless networks," in *2013 IEEE International Conference on Communications (ICC)*, 2013, pp. 5355-5359.

[142] 3GPP, "Evolved Universal Terrestrial Radio Access (E-UTRA): Radio Frequency (RF) system scenarios; version 10.3.0 (Release 10), 3GPP TR 36.942," ed. France, 2012.

[143] S. Ross, *First Course in Probability*, 8th ed.: Prentice Hall, 2009.

[144] G. Alexandridis, G. Siolas, and A. Stafylopatis, "A biased random walk recommender based on Rejection Sampling," in *2013 IEEE/ACM International Conference on Advances in Social Networks Analysis and Mining (ASONAM)*, 2013, pp. 648-652.

[145] Q. Li, Y. Yang, S. Fang, and G. Wu, "Coordinated beamforming in downlink CoMP transmission system," in *2010 5th International ICST Conference on Communications and Networking in China (CHINACOM)*, 2010, pp. 1-5.

[146] X. Zhengzheng, T. Meixia, and W. Xiaodong, "Coordinated Multicast Beamforming in Multicell Networks," *IEEE Transactions on Wireless Communications,* vol. 12, pp. 12-21, 2013.

[147] S. Bin, F. Roemer, and M. Haardt, "Flexible Coordinated Beamforming (FlexCoBF) algorithm for the downlink of multi-user MIMO systems," in *2010 International ITG Workshop on Smart Antennas (WSA)*, 2010, pp. 414-420.

[148] E. Aryafar, M. A. Khojastepour, K. Sundaresan, S. Rangarajan, and E. Knightly, "ADAM: An Adaptive Beamforming System for Multicasting in Wireless LANs," *IEEE/ACM Transactions on Networking,* vol. 21, pp. 1595-1608, 2013.

[149] N. Seifi, M. Matthaiou, and M. Viberg, "Coordinated user scheduling in the multi-cell MIMO downlink," in *2011 IEEE International Conference on Acoustics, Speech and Signal Processing (ICASSP)*, 2011, pp. 2840-2843.

[150] J. Uk, L. Kang Yong, C. Kee Seong, and R. Won, "Transmit Beamforming Based Inter-Cell Interference Alignment and User Selection with CoMP," in *2010 IEEE 72nd Vehicular Technology Conference Fall (VTC Fall)*, 2010, pp. 1-5.

[151] W. Qi, J. Shi, S. Qiang, L. Xiao, H. Yongming, and G. Xiqi, "On downlink coordinated scheduling for inter-cell interference alleviation with inter-BS cooperation," in *2012 IEEE Globecom Workshops (GC Wkshps)*, 2012, pp. 1178-1182.

[152] N. Patwari, J. N. Ash, S. Kyperountas, A. O. Hero, R. L. Moses, and N. S. Correal, "Locating the nodes: cooperative localization in wireless sensor networks," *IEEE Signal Processing Magazine,* vol. 22, pp. 54-69, 2005.

[153] H. Wymeersch, J. Lien, and M. Z. Win, "Cooperative Localization in Wireless Networks," *Proceedings of the IEEE,* vol. 97, pp. 427-450, 2009.

[154] T. B. Lavate, V. K. Kokate, and A. M. Sapkal, "Performance Analysis of MUSIC and ESPRIT DOA Estimation Algorithms for Adaptive Array Smart Antenna in Mobile Communication," in *2010 Second International Conference on Computer and Network Technology (ICCNT)*, 2010, pp. 308-311.

[155] P. Phunchongharn, E. Hossain, and D. I. Kim, "Resource allocation for device-to-device communications underlaying LTE-advanced networks," *IEEE Wireless Communications,* vol. 20, pp. 91-100, 2013.

[156] L. Jianguo, W. Dongyao, W. Jun, L. Jing, P. Jiyong, S. Gang, J. Qi, S. Huan, and M. Yan, "Uplink power control and interference coordination for heterogeneous network," in *2012 IEEE 23rd International Symposium on Personal Indoor and Mobile Radio Communications (PIMRC)*, 2012, pp. 519-523.

[157] F. Daquan, L. Lu, Y.-W. Yi, G. Y. Li, F. Gang, and L. Shaoqian, "Device-to-Device Communications Underlaying Cellular Networks," *IEEE Transactions on Communications,* vol. 61, pp. 3541-3551, 2013.

[158] P. Nguyen and B. Rao, "Throughput improvements for cellular systems with device-to-device communications," in *2013 Asilomar Conference on Signals, Systems and Computers*, 2013, pp. 1973-1977.

[159] Y. Chia-Hao, K. Doppler, C. B. Ribeiro, and O. Tirkkonen, "Resource Sharing Optimization for Device-to-Device Communication Underlaying Cellular Networks," *IEEE Transactions on Wireless Communications,* vol. 10, pp. 2752-2763, 2011.

[160] X. Shaoyi, W. Haiming, and C. Tao, "Effective Interference Cancellation Mechanisms for D2D Communication in Multi-Cell Cellular Networks," in *2012 IEEE 75th Vehicular Technology Conference (VTC Spring)*, 2012, pp. 1-5.

[161] T. Yu, S. Jun, and S. Shixiang, "Radio resource allocation based on greedy algorithm and successive interference cancellation in Device-to-Device (D2D) communication," in *IET International Conference on Information and Communications Technologies (IETICT 2013)*, 2013, pp. 452-458.

[162] N. Young-Han, Y. Akimoto, K. Younsun, L. Moon-il, K. Bhattad, and A. Ekpenyong, "Evolution of reference signals for LTE-advanced systems," *IEEE Communications Magazine,* vol. 50, pp. 132-138, 2012.

[163] HUAWEI. (2013). *5G A technology vision*. Available: http://www.huawei.com/5Gwhitepaper/

[164] H. Monowar; and H. Ekra;, "Resource Allocation for Network-Integrated Device-to-Device Communications Using Smart Relays," presented at the International Workshop on Device-to-Device (D2D) Communication With and Without Infrastructure (GC13 WS - D2D) in conjunction with IEEE Globecom'13 Atlanta, USA, 2013.

[165] X. Weicheng, S. Shixiang, and S. Jun, "Relay selection strategy for Device to Device communication," in *IET International Conference on Information and Communications Technologies (IETICT)*, 2013, pp. 318-323.

[166] N. Obaid and A. Czylwik, "The impact of deploying pico base stations on capacity and energy efficiency of heterogeneous cellular networks," in *2013 IEEE 24th International Symposium on Personal Indoor and Mobile Radio Communications (PIMRC)*, 2013, pp. 1904-1908.

[167] H. Yuan, N. Zheng, Y. Yan, and P. Skov, "Performance evaluation of coordinated multipoint reception in CRAN under LTE-Advanced uplink," in *2012 7th International ICST Conference on Communications and Networking in China (CHINACOM)*, 2012, pp. 778-783.

[168] M. Hadzialic, B. Dosenovic, M. Dzaferagic, and J. Musovic, "Cloud-RAN: Innovative radio access network architecture," in *2013 55th International Symposium ELMAR*, 2013, pp. 115-120.

[169] C. Peng, D. Lei, Y. Hui, X. Youyun, and W. Hailong, "Resource allocation for cognitive networks with D2D communication: An evolutionary approach," in *2012 IEEE Wireless Communications and Networking Conference (WCNC)*, 2012, pp. 2671-2676.

Appendix A

In this appendix, further details are provided for the contents in Chapter 3 of the thesis. These include a detailed description of the antenna azimuth for the cell layout in the developed SLS model (shown in Figure A-1 and Figure A-2). It also includes an illustration of the pixels enclosed on the ROI map. Furthermore, a summary of the different CQIs and their corresponding coding rate and efficiency (data bits per symbol), with precoding codebook of different antenna ports are equally provided in this section.

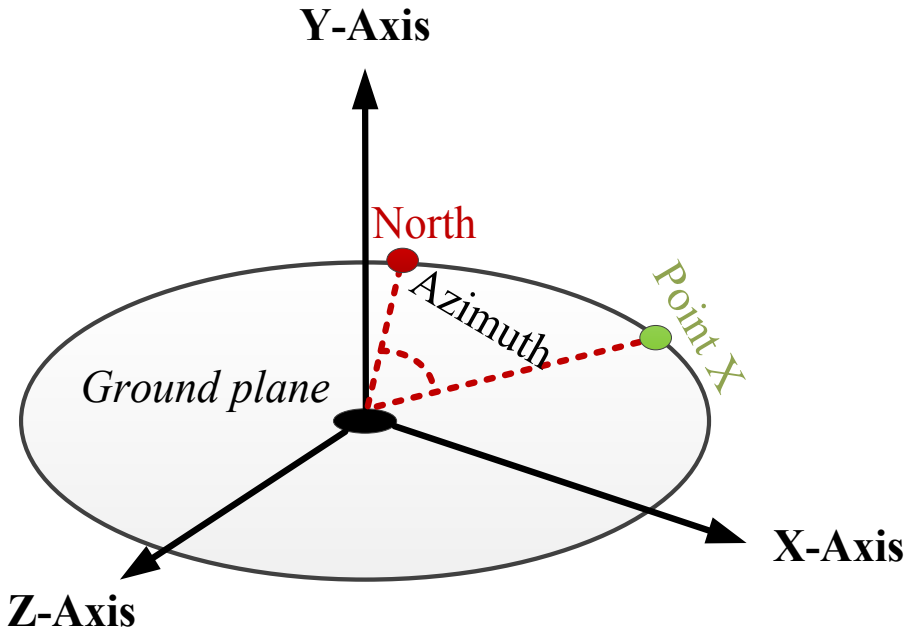

Figure A-1 Description of Azimuth angle on a ground plane

As shown in Figure A-1, the azimuth angle in general refers to the angle between the true North and another random point X on the ground plane (horizontal): this differs from the elevation angle, which is the angle from the ground plane to a vertical point Y. Figure A-2 then describes the azimuth of the sectored antennas in the SLS model developed in Chapter 3. Thus, the eNB is placed in the middle, and 120 degrees

separated antennas cover the 3 different sectors S1, S2, S3 with azimuths of 30 degrees, 150 degrees, and 270 degrees respectively as shown in the figure (Figure A-2).

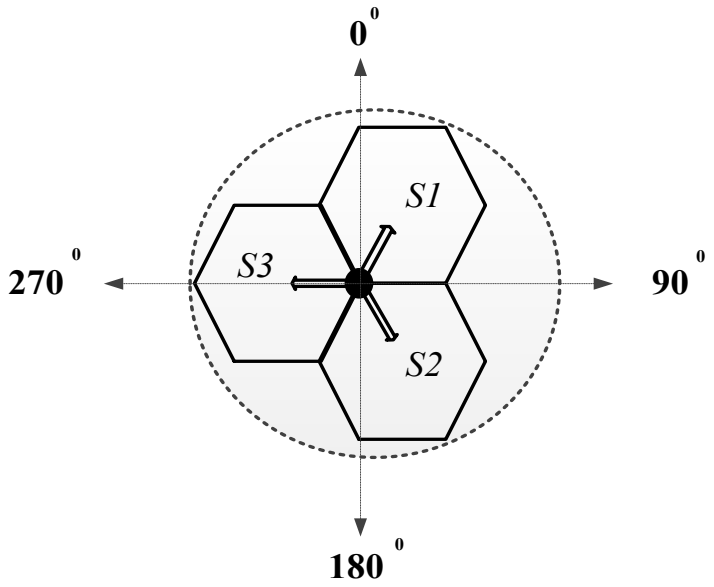

Figure A-2 Azimuth angle for the different sectors belonging to an eNB site

Figure A-3 illustrates pixels that cover the surface area on the ROI map. Every pixel on the maps surface area has an x and y coordinate and also pathloss and shadow fading values (in dB). The UEs are then distributed randomly on the pixels and they obtain the pre-calculated pathloss values from the pixels they are dropped on.

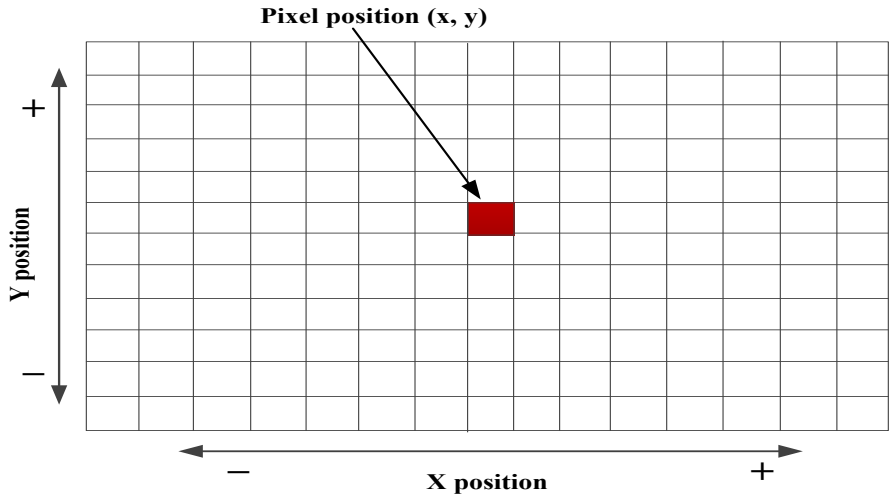

Figure A-3 A portion on the ROI map showing pixel positions

Table A-1 provides an overview of the LTE CQI index used in the simulator with their corresponding values.

Table A-1 Overview of CQI index and corresponding values [106]

CQI index	Modulation	Coding rate	Efficiency[b/s/Hz]
0	Out of range (No transmission)		
1	QPSK	78	0.1523
2	QPSK	120	0.2344
3	QPSK	193	0.3770
4	QPSK	308	0.6016
5	QPSK	449	0.8770
6	QPSK	602	1.1758
7	16 QAM	378	1.4766
8	16 QAM	490	1.9141
9	16 QAM	616	2.4063
10	64 QAM	466	2.7305
11	64 QAM	567	3.3223
12	64 QAM	666	3.9023
13	64 QAM	772	4.5234
14	64 QAM	873	5.1152
15	64 QAM	948	5.5547

Table A-2 and Table A-3 show the U and D_i matrices and codebook precoding matric respectively for the different antenna ports in the network.

Table A-2 U and D_i matrices for different number of antennas [126]

Number of layers	U	$D(i)$
2	$\frac{1}{\sqrt{2}}\begin{bmatrix}1 & 1\\ 1 & e^{-j2\pi/2}\end{bmatrix}$	$\begin{bmatrix}1 & 0\\ 0 & e^{-j2\pi i/2}\end{bmatrix}$
3	$\frac{1}{\sqrt{3}}\begin{bmatrix}1 & 1 & 1\\ 1 & e^{-j2\pi/3} & e^{-j4\pi/3}\\ 1 & e^{-j4\pi/3} & e^{-j8\pi/3}\end{bmatrix}$	$\begin{bmatrix}1 & 0 & 0\\ 0 & e^{-j2\pi i/3} & 0\\ 0 & 0 & e^{-j4\pi i/3}\end{bmatrix}$
4	$\frac{1}{\sqrt{2}}\begin{bmatrix}1 & 1 & 1 & 1\\ 1 & e^{-j2\pi/4} & e^{-j4\pi/4} & e^{-j6\pi/4}\\ 1 & e^{-j4\pi/4} & e^{-j8\pi/4} & e^{-j12\pi/4}\\ 1 & e^{-j6\pi/4} & e^{-j12\pi/4} & e^{-j18\pi/4}\end{bmatrix}$	$\begin{bmatrix}1 & 0 & 0 & 0\\ 0 & e^{-j2\pi i/4} & 0 & 0\\ 0 & 0 & e^{-j4\pi i/4} & 0\\ 0 & 0 & 0 & e^{-j6\pi i/4}\end{bmatrix}$

Table A-3 Codebook for precoding of different antenna ports [126]

Codebook index	Number of layers	
	1	2
0	$\frac{1}{\sqrt{2}}\begin{bmatrix}1\\ 1\end{bmatrix}$	$\frac{1}{\sqrt{2}}\begin{bmatrix}1 & 0\\ 0 & 1\end{bmatrix}$
1	$\frac{1}{\sqrt{2}}\begin{bmatrix}1\\ -1\end{bmatrix}$	$\frac{1}{\sqrt{2}}\begin{bmatrix}1 & 1\\ 1 & -1\end{bmatrix}$
2	$\frac{1}{\sqrt{2}}\begin{bmatrix}1\\ j\end{bmatrix}$	$\frac{1}{\sqrt{2}}\begin{bmatrix}1 & 1\\ j & -j\end{bmatrix}$
3	$\frac{1}{\sqrt{2}}\begin{bmatrix}1\\ -j\end{bmatrix}$	

Appendix B

In this appendix, the UE relocation algorithm included in the wrap-around interference modelling technique is described in details. As shown in Figure B-1, a one-tier cell layout is divided into 4 quasi-triangular quadrants within the ROI: the ROI encloses the pathloss map which provides real life attenuation of signals to UEs due to effects such as interference from neighbouring sites/sectors and fading. The UEs are constantly moving at a speed of 5 km/h each TTI. Hence, when they exit the border cells in one TTI, they are handed over directly to adjacent sites/sectors based on the wrap-around Implementation (as shown in Chapter 4). An example using the figure is that a UE exiting site 7 in one TTI will be relocated to site 2 in the following TTI. Thus all UEs are kept within the ROI, and handed over to transit cells accordingly to achieve realistic events and more accurate results in the simulator.

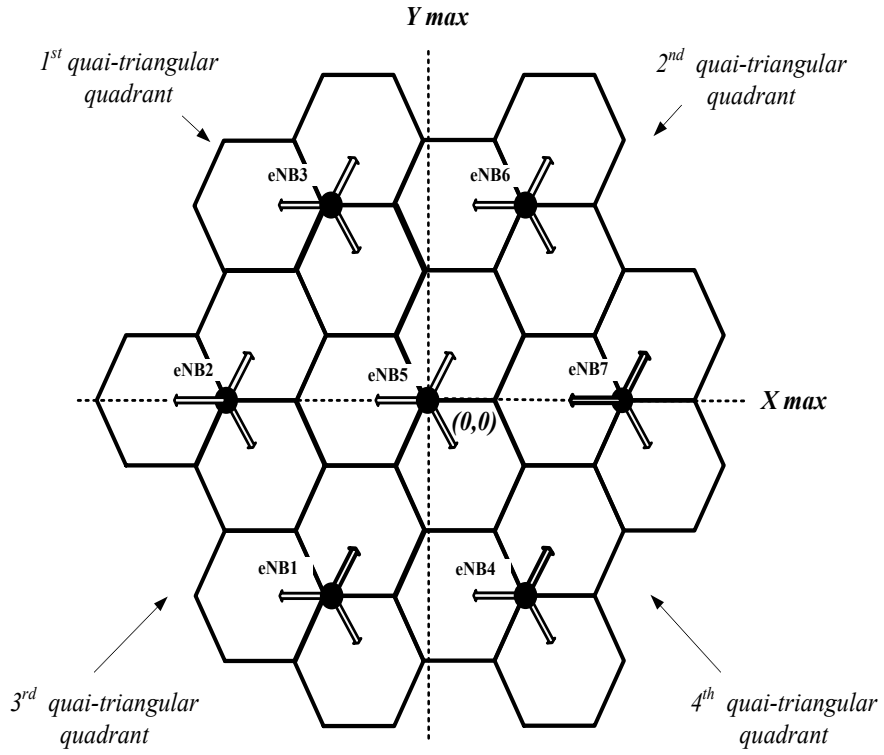

Figure B-1 Illustration of the cell layout highlighting the quadrants in the ROI

Figure B-2 presents a flow chat describing the processes for all the quadrants in the ROI.

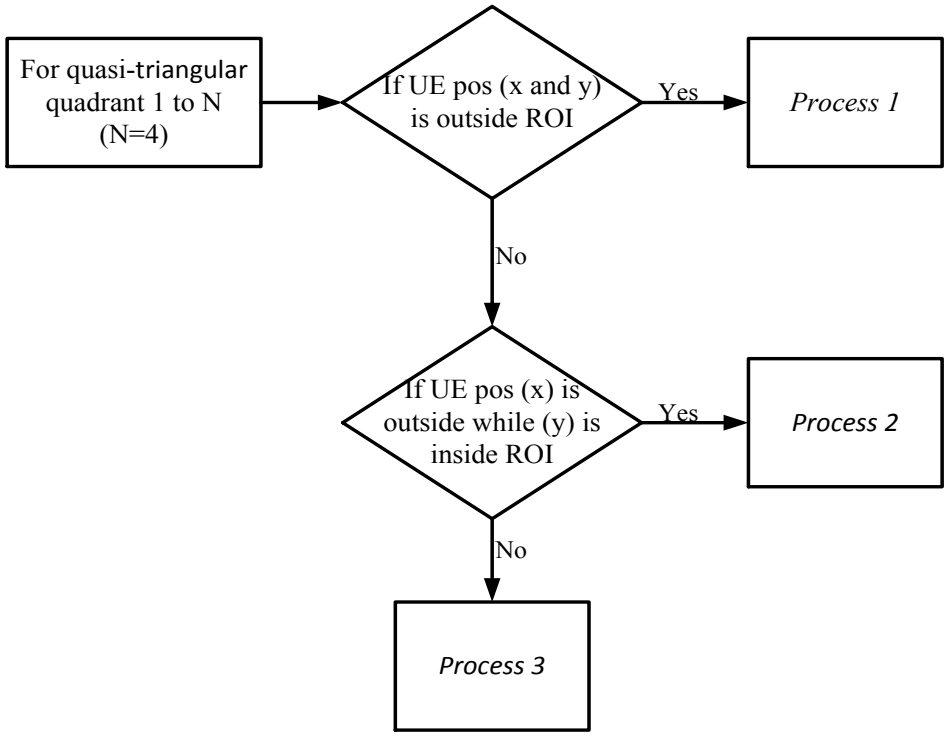

Figure B-2 Flow chart describing conditions for UE relocation algorithm in quasi quadrants of the ROI

1st Quasi-triangular quadrant

- *Process 1*

$$X_{new} = X_{old} - 2 \times X_{\max} \quad \text{(B.1)}$$

$$Y_{new} = Y_{old} - 2 \times Y_{\max} \quad \text{(B.2)}$$

- *Process 2*

$$X_{new} = X_{old} - 2 \times X_{\max} \quad \text{(B.3)}$$

$$Y_{new} = -Y_{old} \quad \text{(B.4)}$$

- *Process 3*

$$X_{new} = -X_{old} \quad \text{(B.5)}$$

$$Y_{new} = Y_{old} - 2 \times Y_{\max} \quad \text{(B.6)}$$

2nd Quasi-triangular quadrant

- *Process 1*

$$X_{new} = X_{old} + 2 \times X_{\max} \quad \text{(B.7)}$$

$$Y_{new} = -Y_{old} \quad \text{(B.8)}$$

- *Process 2*

$$X_{new} = -X_{old} \quad \text{(B.9)}$$

$$Y_{new} = Y_{old} - 2 \times Y_{\max} \quad \text{(B.10)}$$

- *Process 3*

$$X_{new} = X_{old} + 2 \times X_{\max} \quad \text{(B.11)}$$

$$Y_{new} = Y_{old} - 2 \times Y_{\max} \quad \text{(B.12)}$$

3rd Quasi-triangular quadrant

- *Process 1*

$$X_{new} = X_{old} + 2 \times X_{\max} \quad \text{(B.13)}$$

$$Y_{new} = Y_{old} + 2 \times Y_{\max} \quad \text{(B.14)}$$

- *Process 2*

$$X_{new} = X_{old} + 2 \times X_{\max} \quad \text{(B.15)}$$

$$Y_{new} = -Y_{old} \quad \text{(B.16)}$$

- *Process 3*

$$X_{new} = -X_{old} \quad \text{(B.17)}$$

$$Y_{new} = Y_{old} + 2 \times Y_{\max} \quad \text{(B.18)}$$

4th Quasi-triangular quadrant

- *Process 1*

$$X_{new} = X_{old} - 2 \times X_{\max} \tag{B.19}$$

$$Y_{new} = Y_{old} + 2 \times Y_{\max} \tag{B.20}$$

- *Process 2*

$$X_{new} = X_{old} - 2 \times X_{\max} \tag{B.21}$$

$$Y_{new} = -Y_{old} \tag{B.22}$$

- *Process 3*

$$X_{new} = -X_{old} \tag{B.23}$$

$$Y_{new} = Y_{old} + 2 \times Y_{\max} \tag{B.24}$$